

2022

THE POTENTIAL IMPACT OF MACROALGAL GENERATED HYDROGEN PEROXIDE LEVELS ON CO-OCCURRING ORGANISM IN ROCK POOLS

Pattinasarany, Agapery Yoane

<http://hdl.handle.net/10026.1/19997>

<http://dx.doi.org/10.24382/877>

University of Plymouth

All content in PEARL is protected by copyright law. Author manuscripts are made available in accordance with publisher policies. Please cite only the published version using the details provided on the item record or document. In the absence of an open licence (e.g. Creative Commons), permissions for further reuse of content should be sought from the publisher or author.

This copy of the thesis has been supplied on condition that anyone who consults is understood to recognise that its copyright rests with its author and that no quotation from the thesis and no information derived from it may be published without the author's prior consent.



**UNIVERSITY OF
PLYMOUTH**

**THE POTENTIAL IMPACT OF MACROALGAL GENERATED HYDROGEN
PEROXIDE LEVELS ON CO-OCCURRING ORGANISM IN ROCK POOLS**

by

AGAPERY YOANE PATTINASARANY

**A thesis submitted to University of Plymouth
in partial fulfilment for the degree of**

DOCTOR OF PHILOSOPHY

School of Biological and Marine Sciences

November 2022

Acknowledgements

First of all, I would like to express my profound gratitude to my Lord Jesus Christ that finally I could finish this thesis even though tears and sweat occurred during the process. Without His grace, I believe I would not have been able to complete all this work.

Likewise, I take this opportunity to thank the Directorate General of Higher Education, Ministry of Research, Technology and Higher Education of the Republic of Indonesia who have given me the opportunity and funding to pursue my doctoral degree at the School of Biological and Marine Sciences of the University of Plymouth, UK.

My sincere gratitude is also given to Dr John Moody (Director of Studies) who has really provided me with great-great support during this study beginning with study theme and experimental design. He has provided valuable criticism, comments, and suggestions on each chapter of this dissertation to enhance the sensitivity of the analysis biologically or statistically. He was also available anytime whenever I knocked on his door for consultation and discussion, even after he had retired. My sincere gratitude is also given to Dr Murray Brown (supervisor) for his constructive suggestions and criticism during my study and in the writing up of this thesis. I have learnt so many things during the period working with him, and he has made me understand about the detail in writing a scientific report. I have had great pleasure in working with him. I would also like to thank Dr Mick Hanley (supervisor and become my DoS) for his great comments and criticism into parts of this thesis to help improve it. His presence when I need help with my study extension was greatly appreciated.

Special thanks are also given to Andy Atfield and Nicholas Crocker at the School of Biological and Marine Sciences the University of Plymouth, who have helped me in providing technical skills in the lab and field work.

A very special thanks to my wife Verra for supporting me during my last year of study mentally and financially, particularly her prayers and her patience to accompany me in my up and down situations. She is my angel. For my daughter Joane and son Christo who always support me with their lovely attitude and motivate me with their talents; I should also be proud and thank you for them.

Last, but not least, all members of Plymouth and Devonport Methodist circuit especially Stoke and Woodford Methodist Church who always bring my work in their prayers. May God bless you all.

Author's Declaration

At no time during the registration for the degree of Doctor of Philosophy has the author been registered for any other University award without prior agreement of the Doctoral College Quality Sub-Committee.


Work submitted for this research degree at the University of Plymouth has not formed part of any other degree either at the University of Plymouth or at another establishment

Publication:

Agapery Pattinasarany, Murray T. Brown, Mick E. Hanley and A. John Moody

Novel application of a portable luminometer for the measurement of hydrogen peroxide levels in rock pools. Limnology and Oceanography Methods. (Publication in preparation)

Word count of main body of thesis: 29774

Signed:  Date: 18 November 2022

THE POTENTIAL IMPACT OF MACROALGAL GENERATED HYDROGEN PEROXIDE LEVELS ON CO-OCCURRING ORGANISM IN ROCK POOLS

by

AGAPERY YOANE PATTINASARANY

Abstract

Macroalgae have been identified as a potential source of ROS (e.g., hydrogen peroxide) in some rock pools and enclosed habitats; the accumulation of ROS may be harmful to other organisms. Although some studies have found vulnerability to these ROS, there has been little research on the potential impact of photosynthesis-induced oxidative stress on organisms living in rock pools. The aims of this study were to investigate the levels of hydrogen peroxide produced by macroalgae and to assess the effect of similar levels of H₂O₂ on a rock-pool resident, the snakelocks anemone. The objective of the first experimental chapter was to assess the physicochemical parameters in rock pools during a tidal cycle, including hydrogen peroxide levels. During this work, two methods for measuring H₂O₂ levels were used. A fluorescence method, which is commonly used in laboratories, was developed further by examining whether the reaction product was sufficiently stable to carry out the fluorogenic reaction in the field and then measure the fluorescence back in the lab, whereas the luminescence method involved a novel application of a low-cost portable luminometer designed for measuring environmental ATP using firefly bioluminescence. According to this study, the ‘weediest’ pools had the highest H₂O₂ levels. Temperature, pH, PAR, and salinity were also measured at low tide to see how much the conditions changed hourly depending on the presence or absence of macroalgae (weediness). Photosynthetic activity was detected in the pools as evidenced by an increase in pH and dissolved oxygen, which was greater in weedy pools than in non-weedy pools. Furthermore, the influence of abiotic stress, i.e., different physicochemical circumstances, on the steady state hydrogen peroxide production (Chapter 2) of three species of intertidal macroalgae, a green alga (*Ulva lactuca*), a brown alga (*Fucus serratus*), and a red alga (*Chondrus crispus*), was investigated in the laboratory. All three species reached steady-state levels of hydrogen peroxide after 4 h of exposure at various temperatures, pH levels, salinities, and light intensities. The highest level of H₂O₂ was found with *F. serratus* (4.6 μM), while the lowest was with *C. crispus* (1 μM). H₂O₂ production was doubled when macroalgae were desiccated, but it was reduced when *C. crispus* was present. The fluorescence of chlorophyll *a* was also measured to investigate the effect of abiotic stress on photosynthesis in the macroalgae. The raw fluorescence of the macroalgae showed the typical polyphasic O-J-I-P increase.

Even under stress, photosynthetic units are active, and there was an effect on the downregulation of the photochemical machinery, which manifested as dynamic photoinhibition; however, it was only an increase in light intensity that had a substantial impact on photosynthesis. The goal of the final experimental chapter was to investigate the effect of ambient H₂O₂ on two morphs of the snakelocks anemone (*Anemonia viridis*). Following tissue extraction, total glutathione and TBARS levels were measured, as well as superoxide dismutase and catalase activity, measured using spectrophotometry. Furthermore, zooxanthellae counts were performed. Notably, no other physiological indicators were altered in the anemone, including total glutathione, implying that the pool of reduced glutathione (GSH) remained stable. Furthermore, despite the fact that superoxide dismutase (SOD) activity increased as H₂O₂ concentration increased, there was no significant difference between treatments. Catalase (CAT) activity, on the other hand, increased dramatically at the highest H₂O₂ concentration used. This suggests that H₂O₂ alone was unlikely to have changed zooxanthellae density in this study.

Table of Contents

Author's Declaration	3
Acknowledgements	4
Abstract	5
Chapter 1 Introduction.....	14
1.1 The intertidal	15
1.2 Rocky intertidal	16
1.2.1 Species distribution	16
1.2.2 Species interactions.....	17
1.3 Rock pools	19
1.3.1 Variation of physicochemical parameters in rock pools	20
1.3.2 Rockpool biophysical interactions	20
1.4 Production of reactive oxygen species (ROS).....	22
1.4.1 Potential effects of abiotic factors on ROS accumulation in rock pools...	27
1.5 Aims and objectives	29
Chapter 2 Development and application of modified fluorometric and chemiluminescence methods for the measurement of hydrogen peroxide in rock pools..	31
2.1 Introduction	32
2.2 Materials and Methods	35
2.2.1 Standardisation of hydrogen peroxide (H ₂ O ₂) solutions.....	35
2.2.2 Fluorescence (FL) method for measurement of H ₂ O ₂	35
2.2.3 Chemiluminescence (CL) method for H ₂ O ₂ measurement	36
2.2.4 Field studies	38
2.2.5 Statistical analysis	41
2.3 Results	42
2.3.1 Standardisation of H ₂ O ₂ concentrations.....	42
2.3.2 Detection of hydrogen peroxide using the fluorescence method	42
2.3.3 Detection of hydrogen peroxide using the chemiluminescence (CL) method	47
2.3.4 The physicochemical parameters and levels of H ₂ O ₂ in rock pools	51

2.4	Discussion.....	57
2.4.1	Fluorometric and chemiluminescence methods for measuring hydrogen peroxide levels	57
2.4.2	Studies on hydrogen peroxide levels in the field	59
Chapter 3	Production of hydrogen peroxide and physiological responses to environmental factors by three different macroalgae	63
3.1	Introduction	64
3.2	Materials and Methods	67
3.2.1	Plant material and sample preparation	67
3.2.2	Measurement of hydrogen peroxide levels in response to exposure of macroalgae to various environmental conditions.....	67
3.2.3	Chlorophyll fluorescence measurements	68
3.2.4	Statistical analyses	71
3.3	Results	72
3.3.1	Levels of extracellular H ₂ O ₂ produced by macroalgae	72
3.3.2	Effects of abiotic stressors on H ₂ O ₂ steady state levels produced by macroalgae	73
3.3.3	Effects of abiotic stress on chlorophyll <i>a</i> fluorescence.....	78
3.4	Discussion.....	85
Chapter 4	Effects of hydrogen peroxide on the snakelocks anemone (<i>Anemonia viridis</i>)	89
4.1	Introduction	90
4.2	Materials and Methods	93
4.2.1	Sample collection and maintenance	93
4.2.2	Exposure of <i>A. viridis</i> to H ₂ O ₂	93
4.2.3	Quantification of zooxanthellae density.....	94
4.2.4	Thiobarbituric acid reactive substances assay.....	95
4.2.5	Measurement of total glutathione content.....	95
4.2.6	Measurement of superoxide dismutase activity	97
4.2.7	Measurement of catalase activity	98
4.2.8	Measurement of total protein	98
4.2.9	Statistical analysis	100

4.3	Results	101
4.3.1	Changes in zooxanthellae density	101
4.3.2	Lipid peroxidation.....	101
4.3.3	Changes in non-enzymatic and enzymatic antioxidant content and activities 103	
4.4	Discussion.....	106
Chapter 5	General Discussion	112
References	119

List of Tables

Table 1.1 The generation of ROS from molecular oxygen	23
Table 1.2 Levels of H ₂ O ₂ measured in natural waters.....	25
Table 1.3 Enzymatic antioxidants and their locations	27
Table 2.1 Characteristics of the fourteen rock pools monitored.....	40
Table 2.2 Pearson correlation coefficients for physicochemical parameters	53

List of Figures

Figure 1.1 Schematic of H ₂ O ₂ production and removal mechanisms in plants.....	25
Figure 1.2 The ascorbate-glutathione (Asc-GSH - Halliwell-Asada) pathway.....	26
Figure 2.1 Reaction of luminol with H ₂ O ₂ leading to chemiluminescence.....	37
Figure 2.2 The apparent UV spectrum of hydrogen peroxide in Hepes buffer.....	42
Figure 2.3 Calibration curve for H ₂ O ₂ produced using the fluorescence method.....	43
Figure 2.4 Time courses for the formation of the fluorescent product.....	44
Figure 2.5 The stability of the fluorescent product.....	45
Figure 2.6 The effects of catalase on fluorescence.....	46
Figure 2.7 (A) the effect of pH on calibration curves produced using the luminol/HRP chemiluminescence method, and (B) the same data plotted as log ₁₀ (RLU).....	48
Figure 2.8 (A) an example of the use of two internal standards to determine the concentration of H ₂ O ₂ by the chemiluminescence method.....	49
Figure 2.9 The correlation between FL and CL methods.....	53
Figure 2.10 Mean values of pH within three rockpool types.....	51
Figure 2.11 Mean temperatures within three rockpool types.....	52
Figure 2.12 Mean salinity within three rockpool types.....	53
Figure 2.13 Mean dissolved oxygen values within three rockpool types.....	54
Figure 2.14 Mean levels of H ₂ O ₂ within three rockpool types.....	55
Figure 2.15 Mean levels of H ₂ O ₂ within two rockpools at Plymouth Hoe.....	56
Figure 3.1 Example of changes in the fluorescence of chlorophyll <i>a</i> over time.....	69
Figure 3.2 Time courses of H ₂ O ₂ excretion from <i>F. serratus</i> , <i>U. lactuca</i> and <i>C. crispus</i>	72
Figure 3.3 The effects of pH on the level H ₂ O ₂ in seawater.....	73
Figure 3.4 Effects of light intensity on levels of H ₂ O ₂	74
Figure 3.5 Effects of temperature on levels of H ₂ O ₂	75
Figure 3.6 Effects of salinity on levels of H ₂ O ₂	76
Figure 3.7 Effect of desiccation on levels of H ₂ O ₂	77
Figure 3.8 Levels of H ₂ O ₂ in seawater surrounding combinations of macroalgae.....	78
Figure 3.9 The maximum quantum yield (F _v /F _m) of three species of macroalgae.....	79

Figure 3.10 Performance index (PI) of <i>Chondrus crispus</i> exposed to three abiotic stressors	81
Figure 3.11 Performance index (PI) of <i>Fucus serratus</i> exposed to four abiotic stressors	82
Figure 3.12 Performance index (PI) of <i>Ulva lactuca</i> exposed to four abiotic stressors....	83
Figure 3.13 Four flux ratios derived from OJIP analysis for three species of macroalga.	84
Figure 4.1 The H ₂ O ₂ concentration profile in seawater over 4 h	94
Figure 4.2 Calibration graph of MDA standards	95
Figure 4.3 Example time courses for the glutathione assay	96
Figure 4.4 Example time courses for the SOD assay	98
Figure 4.5 Calibration graph of protein using BCA assay at 562 nm	99
Figure 4.6 Zooxanthellae densities of <i>A. viridis</i> (tentacle tissue).....	101
Figure 4.7 Effects of hydrogen peroxide on malondialdehyde content in tentacle extracts	102
Figure 4.8 Total glutathione levels of <i>A. viridis</i> (tentacle tissue)1034	
Figure 4.9 Effects of hydrogen peroxide on superoxide dismutase (SOD) activity in tentacle extracts	107
Figure 4.10 Effects of hydrogen peroxide on catalase (CAT) activity in tentacle extracts	105

List of Abbreviations

Abbreviation	Meaning
APX	ascorbate peroxidase
ASW	artificial seawater
CAT	catalase
Chl <i>a</i>	chlorophyll <i>a</i>
CL	chemiluminescence
DHA	dehydroascorbate
DO	dissolved oxygen
FL	fluorescence
F_v/F_m	maximum photochemical quantum yield of PSII
GPX	glutathione peroxidase
GR	glutathione reductase
GSH	reduced glutathione
GSSG	glutathione disulphide
LPX	lipid peroxidation
MDHA	monodehydroascorbate
MDHAR	monodehydroascorbate reductase
NADH	nicotinamide adenine dinucleotide, reduced form
NSW	natural seawater
ROS	Reactive Oxygen Species
SOD	superoxide dismutase
TBARS	thiobarbituric acid reactive substances

Chapter 1

Introduction

1.1 The intertidal

The intertidal is the meeting zone of the sea and the land, the lowest of low tide and the highest of high tide. It receives input from the seawater during regular high tide as well as by wave splash. This area can be a narrow lane or a huge area of shoreline where high tidal excursion interacts with shallow beach slope. The intertidal zone is divided into three sections, generally referred to as littoral, sublittoral, and supralittoral. However, because these zones are all functionally intertidal and are strongly influenced by tides and waves on longer time scales, they can also be referred to as the littoral fringe (high shore), the eulittoral zone (middle shore), and the sublittoral fringe (low shore) (Dugan et al, 2013). The high shore is regularly flooded during the peaks of daily high tides only and generally spends more time exposed to the air than submerged. The mid shore which regularly exposed to air and submerged by average tides for approximately about 6 h per tidal cycle or twice a day. The low shore is fundamentally underwater and infrequently exposed for just a few hours at low tide (Dugan et al, 2013; Chappuis et al., 2014). The rise and fall of the tides is the most important factor influencing life in the intertidal zone.

As part of coastal marine systems, the intertidal zone provides many key ecosystem services that are among the most ecologically and socio-economically vital on the planet (Barbier et al. 2011). This zone's diversity of habitats, high productivity, and accessibility attract a diverse range of resource users who utilize the area in a variety of ways. It has been estimated that marine habitats from the intertidal zone out to the continental shelf (excluding coral reef and wetland) provide over 79,000 US\$/ha/year worth of ecosystem goods (e.g., food and raw materials) and services (e.g., disturbance regulation and nutrient cycling) (de Groot et al., 2012; Costanza et al., 2014). The intertidal zone has a high density of plant and animal communities. Because of the abundance of nutrients, the distribution of many species is constrained by competition for space with other species. The intertidal zone is home to a diverse range of habitats, including mangroves, seagrass meadows, sandy beaches, and rocky shores.

1.2 Rocky intertidal

The intertidal rocky shore is one of conspicuous biological zonation relative to two other zones in the marine intertidal, sandy beaches and mudflats. Each species on the rocky intertidal has an upper and lower distributional limit along the vertical intertidal gradient (Ellis, 2003), while others have a lack of attached intertidal plan. Hence rocky shores have been the subject of numerous marine ecological studies during the last 60 years (see Conhell, 1961; Lewis, 1964; Hawkins and Jones, 1992; Little and Kitching, 1996; Raffaelli and Hawkins, 1996; Underwood, 2000; and Bertness et al., 2001, for reviews). In comparison to many other marine ecosystems, rocky shore habitats are often easy to access and influenced by events that occur both at sea and on land, and they are extremely vulnerable to human activities. They have a lot of environmental gradients packed into a small space, and many of the existing species are sessile or slow moving, making them easy to identify, respond quickly, and manageable for experimental manipulations.

In addition, rocky shores have the greatest biodiversity - their diversity rivals that of tropical rainforests - because they provide many ecological niches in any coastal habitat (Denny and Gaines, 2007; Smith, 2013). They have secure and complex surfaces that create numerous microhabitats sheltered for living things to attach to and to live in. Such microhabitats are widely created from the low to the upper shore and even the type of rock that makes up the shoreline varies, which in turn influences the type of animals and plants that inhabit the region and prevents any single species from occupying the entire coast (Ellis, 2003). With abundance and variety of food, the rocky shore supports many different species, such as grazing and filter feeding and sessile animals in large numbers, where a lot of food is transported to them by the water movement (Raffaelli & Hawkins, 2012; Smith, 2013). Widely changing abiotic environments in a dynamic environment, subject to intense water currents and wave motion, along with the creatures that live there, also form the shoreline.

1.2.1 Species distribution

The distribution of organisms in the rocky intertidal has been studied throughout the world and general features of zonation along the vertical have been described (see Stephenson and Stephenson, 1949; Lewis, 1964; Connell, 1972; Ellis, 2003). Patterns of vertical distribution vary from place to place, and the potential causes of these patterns have been the subject of numerous studies. At the upper limits of the intertidal zone, the

tide creates distinct physical patterns in relation to abiotic factors such as temperature and ice exposure, waves, wind and desiccation (Hawkins and Hartnoll, 1985; Kiirikki, 1996, Reichert et al., 2008). At the lower limits, biological interactions play the most important part such as competition, grazing and predation (Underwood and Jernakoff, 1981; Hawkins and Hartnoll, 1985; Thomas, 1994; Bulleri et al., 2002; Erlandsson et al., 2011; Burrows et al., 2009; Mangialajo et al., 2012) in addition to the combination of abiotic and biotic factors (Underwood and Jernakoff, 1981). The horizontal distribution is determined by the effects of differences in water movement along a shore (Connell, 1972; Schoch et al., 2006; Tuya and Haroun, 2006). For instance, the distribution of organisms and their assembly along the beach at various scales, from small to large (Burrows et al., 2009; Cruz-Motta et al., 2010; Veiga et al., 2013).

Plants and animals living in coastal areas are bathed in a nutritional broth that comes from the land and the decay of plants or algae that are more or less in constant concentration, and light is not limited to those shallow depths where photosynthetic organisms are flourishing. This condition makes the rocky shore more productive than the open ocean (Poremba et al., 1999, Raffaelli & Hawkins, 2012). However, the rocky shore environment is regulated by submergence and aerial exposure to the tidal cycle. This condition produces a strong environmental stress gradient that occurs perpendicular to the shoreline and exhibits its most extreme values towards the upper boundary of the zones (Widdows and Brinsley, 2002 (Martínez et al., 2012; Tomanek and Helmuth, 2002). At increasingly higher levels on the shore, marine organisms are stressed by experiencing increasingly longer periods of time spent in open air. Temperatures fluctuate as much as 10 to 20 °C over the course of a single low tide compared to those in the sea (Raffaelli & Hawkins, 2012). The most important stress, however, in temperate and tropical areas is greater desiccation due to the combined effects of heat and low relative humidity.

1.2.2 Species interactions

The relationship between environmental stress and species interactions also drives the zonation and community dynamics in general (Menge and Sutherland, 1987; Bertness and Callaway, 1994; Travis et al., 2004), and macroalgae are known to influence community structure (Wright et al., 2014). Macroalgae can improve extreme physical conditions in their environment by forming a small-scale canopy that modifies local hydrodynamics, stabilising sediments and providing space free from competition and predation (Bertness et al., 1999; Wright et al., 2014). *Corinactis californica* densities are

up to 4-fold greater under canopies of the stipitate kelp, *Eisenia arborea*, than in areas just outside the canopy. Temperature may have a major in-direct effect on community structure. The role of the macroalgae also may differ based on the algae itself, their density, and the baseline conditions of the environment. For example, benthic diatoms are found to increase with the density and complexity of macroalgal cover (Umanzor et al., 2017). Different macroalgal morphologies can redirect particles differently, which in turn affects the abundance and distribution of subtidal passive suspension feeders (Morrow & Carpenter, 2008).

However, macroalgae are exposed during emersion at low tide, resulting in stress in algal cells. This may result in a decrease in photosynthesis rate leading to alteration in a series of physiological processes (Burritt et al., 2002; Heber et al., 2010; Gao et al., 2011). For example, effects of heat and low humidity at the low tide as a result of desiccation cause interruption of the electron flow between photosystem (PS) I and II together with the accumulation of reactive oxygen species (ROS) (Collén and Davison, 1999a, 1999b; Contreras et al., 2005, 2009; Kumar et al., 2010, Bischof & Rautenberger, 2012). This may lead to an oxidative stress condition if not buffered.

These studies demonstrate that the distribution of species and assemblages along horizontal and vertical axes is complex, and they have been thoroughly studied in order to gain insight into intertidal rocky shore ecology. However, most of the work mentioned above has been conducted on open freely draining rock whereas rock pools as a part of intertidal rocky shore have been much less extensively studied. Even though they are both regulated by the tidal cycle and are equally affected by seawater and have similar physicochemical factors, and support the diversity of rocky shore, because the rock pools are immersed during low tide, they are considered to be different to intertidal habitats (Underwood, 1981). Yet, rock pools are normally more diversified and have stronger interactions between physicochemical parameters and biological processes, than draining rock habitats (Metaxas and Scheibling, 1993; Benedetti-Cecchi et al., 2000).

1.3 Rock pools

Rock pools are natural aquaria that are commonly situated in the rocky intertidal zone of richly structured rocky shores (Metaxas and Scheibling, 1993). They act as refuges for many intertidal organisms in the trapped water at low tide and create productive microhabitats that contain a diverse range of plants, invertebrates and fish (Metaxas and Scheibling, 1993; Underwood and Jernakoff, 1984; Zander et al. 1999). Those who live in rock pools, on the other hand, are not constantly submerged in the same volume of water and form a closed water system during low tide. They are isolated from sea and hence there is no effect of waves and current flow during low tide and are subjected to large thermal and chemical changes as well as variation in the duration and quantity of light exposure depending on the tide.

Because of the random nature of their formation, the environment of rock pools varies according to factors such as shape, size, volume, surface area, depth, internal topography, sediment content and type, wave exposure and flushing rate, degree of shading and sun exposure, and the presence or absence of freshwater runoff. As a result, no two pools exhibit identical physiochemical conditions and exhibit significant spatial variation in community structure, even between pools at the same shore height (Metaxas and Scheibling, 1993; Martins et al., 2007; Firth et al., 2013), despite the fact that pool diameter experiments on the assemblage of organisms using a set of standard diameters revealed no significant difference in community structure (Underwood and Skilleter, 1996) These conditions offer a unique natural laboratory to study the habitat preferences, physiological boundaries and adaptations of intertidal pool organisms. For example, the influence of tidal height on the pattern of organisms (e.g., Dethier, 1982; Wolfe and Harlin, 1988; Kooistra et al., 1989; Metaxas and Scheibling, 1993; Griffiths et al., 2003), on physical factors (Astles 1993; Griffiths et al., 2006) and water chemistry and volume (Kemp 2009; Tsering et al. 2012) which experience continuous and rapid change in temperature, salinity, pH and dissolved oxygen content (Griffith, 2003). These conditions can be influenced more for inhabitants by physical factors, such as pool depth and volume of water (Underwood and Skilleter, 1996; Macieira and Joyeux, 2011) combined with biological factors such the availability of shelter (Gibson, 1982), presence of preferred food resources (Gibson, 1974), presence of predators including herbivores (Paine, 1974), and quantity of algal covering (Jones, 1984).

1.3.1 Variation of physicochemical parameters in rock pools

Studies on the physicochemistry of rock pools have shown high diurnal and seasonal fluctuations. The greatest diurnal variation is in oxygen saturation with higher values recorded by the late afternoon due to photosynthetic activity in pools and the lowest values just before dawn when respiration dominates biological processes (Morris and Taylor, 1983; Huggett and Griffiths, 1986), and pool water stratification has also occurred (Daniel and Boyden, 1975). Some rock pool studies have found that the temperature can increase by up to 15 °C during exposure on a day in the spring tide, of clear sunshine in summer and decreasing at night (Klugh, 1924; Daniel and Boyden, 1975; Metaxas and Scheibling, 1993). Fluctuations in salinity can be large, the water becoming increasingly hypersaline because of evaporation and also becoming hyposaline rapidly in the rain (Pyefinch, 1943), thus, the stratification can change due to evaporation, rainfall, and freezing. (Naylor and Slinn, 1958; Ganning, 1971; Morris and Taylor, 1983). Oxygen concentrations change diurnally and, as consequence, the metabolic activities of the organisms living within (Pyefinch, 1943; Daniel and Boyden, 1975; Morris and Taylor, 1983). The height of the pool on the coast affects temperature, salinity, oxygen, and total carbon dioxide concentrations (Metaxas and Scheibling, 1993). pH also shows seasonal variations in the magnitude of their daily fluctuation (Ganning, 1971; Monis and Taylor, 1983). With the incoming tide, changes in the physicochemical factors occur rapidly. Changes in the direction and magnitude will depend on the time of the day. In the case of daytime immersion, oxygen saturation will decrease, and overall carbon dioxide will rise, but with a significantly lower range. Night-time exposure will lead to opposite changes (Morris and Taylor, 1983).

1.3.2 Rockpool biophysical interactions

Plants and animals that live in rockpools are more protected from desiccation than those that live in open water during low tide (Newell, 1979). However, the configuration and composition of rock pool assemblies are further controlled by biological factors within the pool, such as the availability of shelter (Gibson, 1982); presence of preferred food resources (Gibson, 1974); presence of predators (Paine, 1974); and quantity of algal turf versus algal plants (Jones, 1984), combined with physical factors, such as pool depth, volume and vertical position on the rocky shore (Macieira & Joyeux, 2011). With significant variation in the biological and physical environment factors throughout the tidal cycle (Huggett and Griffiths, 1986; Horn et al., 1999), the relationship between these parameters clarified the distribution of species and the abundance mechanism

(Underwood and Jernakoff, 1984; Benedetti-Cecchi et al., 2000). For example, there are differences in species abundance between rock pools at the same height (Sze, 1981; Wolfe and Harlin, 1988; Arrontes and Underwood, 1991); these differences are associated with the degree of wave exposure and species interactions, such as herbivory, predation and competition difference (Sze, 1981; Metaxas and Scheibling, 1993). Legrand et al. (2017) found that photosynthesis increased oxygen concentration and pH during the daytime of emersion but decreased nutrient concentrations. The increase of pH in rock pools provides an alkaline environment which is advantageous to coralline algal in the calcification process. Rock pools, on the other hand, exhibit a significant reduction in oxygen content and pH at night, owing to the high rate of community respiration as a result increasing the dissolution in coralline algae in upper shore rock pools (Legrand et al., 2017). Furthermore, in comparison to rock pools that have a barren substratum, rock pools supporting algal cover have greater species diversity and abundance of individuals (Marsh et al. 1978; Bennett & Griffiths 1984). The high productivity observed in rock pool habitats is mostly explained by the diversity of macroalgae (Araujo et al., 2006) and which develop in rock pools (Firth et al., 2014).

As mentioned above, rock pools containing algae have been shown to support higher numbers of species and individuals. This is in part because macroalgae serve as a source of food (Hay, 1991; Cyr and Pace, 1993). They found that herbivores normally consume 50-100% of macroalgae production. This is higher in the tropical than temperate habitats (Paul et al., 2001). In addition, in the water column, the fronds of algal plants establish floating cover and are most commonly used by midwater and pelagic species (Davis, 2000). They also increase oxygen content in pools containing dense stands of algae which can reach 26.2 mg l⁻¹ during the day and 1.2 mg l⁻¹ at night compared to values for the open sea in the same area of about 8.7 mg l⁻¹ (Stephenson et al., 1934). Like oxygen, pH in rock pools also fluctuate diurnally dependent upon biological processes in rock pools (Pyefinch, 1943; McGregor, 1965; Ganning, 1971; Green, 1971; Daniel and Boyden, 1975; Morris and Taylor, 1983).

The composition of rock pool communities is expected to have a large impact on the physicochemical environment, particularly during the summer when rock pools are occupied by dense canopy-forming algae. According to several studies, the dominance of macroalgal assemblages varies with tide height (Femino and Mathieson, 1980; Wolfe and Harlin, 1988a; Kooistra et al., 1989). Important macroalgae were discovered in Nova Scotia, Canada, to exhibit significant heterogeneity among macroalgae communities in

pools located at the same height but a few meters apart from the beach. Recruitment heterogeneity and/or changes in physical pool characteristics have been proposed as possible explanations for the variability in macroalgae percent cover (Metaxas et al., 1994). Pool size and depth, as well as tidal height and wave exposure, have all been identified as important determinants of macroalgal abundance (Sze, 1982; Wolfe and Harlin, 1988b; Metaxas et al., 1994). Underwood and Skilleter (1996), on the other hand, discovered that the diameter of the pool had no effect on the structure of rock pool assemblages.

The rock pool environment can also be quite erratic, with abrupt changes when the tide returns to reconnect a pool to the sea (Johnson and Skutch, 1928; Naylor and Slinn, 1958; Morris and Taylor, 1983; Huggelt and Griffiths, 1986). In addition, the long intervals between water renewals in relatively small pools suggested that toxic materials could accumulate (Sze, 1981). Under normal physiological conditions, ROS (e.g., hydrogen peroxide) molecules are less likely to cause any oxidative damage as their function is to sense and respond to fluctuating a signalling molecule at low level and steadily maintained at optimal level to prevent cells from damage (Martin and Sies, 2017). In rock pools, macroalgae experience considerable variation in the physicochemical environment, including salinity, temperature, light intensity levels and pH, can suppress photosynthesis by affecting the electron transport chain, photophosphorylation and CO₂ fixation. Inhibition of photosynthesis disrupts their fitness and survival because they induced the production of reactive oxygen species (ROS). High levels of ROS during environmental stresses can create a threat to cells. However, depending on their tolerance level, macroalgae show different responses to environmental stress (Dummermuth et al., 2002). Therefore, it is important to study the effects of physicochemical stresses on macroalgae in the rock pool environment as potential sources of ROS (e.g., hydrogen peroxide), and the accumulation of these may have detrimental effects on other organisms.

Environmental fluctuations, such as mentioned above, affect the metabolism and physiological responses of the organisms. One of the common responses to different environmental stresses is the accelerated rate of production of reactive oxygen species (ROS), which can cause extensive damage to cellular components, including proteins, lipids and DNA, all of which may eventually lead to cell death (Mittler, 2002).

1.4 Production of reactive oxygen species (ROS)

The mechanism by which solar photons are received and transformed into the energy storage molecules adenosine triphosphate (ATP) and nicotinamide adenine dinucleotide phosphate (NADPH) is critical for life on Earth. When exposed to environmental or biotic stress, absorbed light energy is frequently inefficiently utilized for photosynthesis. This can occur due to a disruption of CO₂ fixation, which leads to a blockage of electron transport as a result, the electron transport chain will stop running, and ATP will no longer be produced by chemiosmotic coupling (Foyer, 2018).

Reactive oxygen species (ROS) production, including singlet oxygen (¹O₂), superoxide (O₂^{•-}), hydrogen peroxide (H₂O₂) and the hydroxyl radical (•OH) (Fridovich, 1998; Gechev et al., 2006; Møller et al., 2007), mostly results by energy transfer or by the sequential monovalent reduction (electron transfer) of molecular oxygen found in cells as side-products of metabolic reactions (Table 1.1). If triplet oxygen absorbs sufficient energy to reverse the spin of one of its unpaired electrons, it will form the singlet oxygen (¹O₂). If a single electron is added to the ground state O₂ molecule, the product is the superoxide radical O₂^{•-}. The two-electron reduction product of oxygen in biological systems exists as hydrogen peroxide (H₂O₂), and the four-electron product is water (H₂O) (Halliwell, 2006; Tomanek, 2015).

Table 1.1 The generation of ROS from molecular oxygen (Bhattacharjee, 2012).

Nomenclature	Reaction
singlet oxygen	$^3Chl + O_2 \longrightarrow ^1O_2$
superoxide	$O_2 + e^- \longrightarrow O_2^{\bullet-}$
hydrogen peroxide	$O_2^{\bullet-} + e^- + 2 H^+ \longrightarrow H_2O_2$
hydroxyl radical	$H_2O_2 + e^- + H^+ \longrightarrow H_2O + OH^{\bullet}$
water	$OH^{\bullet} + e^- + H^+ \longrightarrow H_2O$

The generation of ROS is a routine physiological event for aerobic organisms under normal conditions through various reactions in photosynthetic and respiratory metabolism (Foyer and Shigeoka, 2011). For example, generation of ATP in the oxidative phosphorylation process in mitochondria generates superoxide. ROS serve as important signalling molecules that are involved in the control of growth and development as well as being stress signalling molecules (Laloi et al., 2006; Bartosz, 2009). However, under extreme conditions, ROS production can escalate rapidly beyond the ability of organisms to balance them. Therefore, an imbalance between ROS generation and removal occurs,

which is referred to oxidative stress.

Hydrogen peroxide (H_2O_2) is relatively stable and has a longer half-life of 1 ms than other ROS (Dynowski et al., 2008), allowing it to reach intracellular and extracellular locations relatively far from sites of production (Møller et al., 2007). H_2O_2 can diffuse across membranes via aquaporins, which catalyse H_2O_2 transmembrane movement as well as water (Henzler and Steudle, 2000), and it can also directly cross the hydrophobic lipid bilayer (Bienert et al., 2006). Strictly, H_2O_2 is not a radical, because it has no unpaired electrons, but it can lead to the production of the hydroxyl radical, $\bullet\text{OH}$, via the Fenton and Haber-Weiss reactions involving oxidation of transition metals such as Fe^{2+} and Cu^{2+} making the effects of H_2O_2 just as harmful (Halliwell, 2006).

As a common cellular metabolite in plants and macroalgae, H_2O_2 is produced through processes in chloroplasts, mitochondria and peroxisomes (Tripathy and Oelmüller, 2012), and via some enzymes such as peroxidases, amine oxidases, flavin-containing enzymes and glycolate oxidase (Fig. 1.1) (Niu and Liao, 2016). In chloroplasts, H_2O_2 is produced on the reducing side of photosystem I (PSI) via the reduction of O_2 to $\text{O}_2\bullet^-$ (Mehler reaction). Electron transport chain components in PSI such as Fe-S centres and reduced thioredoxin (TRX) are auto-oxidizable, i.e., they can reduce oxygen to $\text{O}_2\bullet^-$ (superoxide radical) (Dat et al., 2000; Sharma et al., 2012). Reduction of $\text{O}_2\bullet^-$ leads to the formation of H_2O_2 that occurs either via spontaneous dismutation or catalysed by superoxide dismutase. In peroxisomes, H_2O_2 is produced as a part of the process of the metabolic pathways of β -oxidation and photorespiration. Glycolate, as a product of ribulose-1,6-bisphosphate, via RuBisCO is transported from chloroplasts to peroxisomes where it is oxidised via glycolate oxidase to form H_2O_2 (Neill et al., 2002; Foyer and Noctor, 2003). H_2O_2 is also generated in mitochondria during aerobic respiration when $\text{O}_2\bullet^-$ is produced by complexes I and III of the electron transport chain (Fig. 1.1), and then rapidly converted to H_2O_2 catalysed via the enzyme superoxide dismutase. The mitochondria seem to be the main H_2O_2 producers for plants growing in the dark (Foyer and Noctor, 2003; Niu and Liao, 2016), but the generation of H_2O_2 in chloroplasts and peroxisomes is up to a hundred times faster than in mitochondria (Bhattacharjee, 2012).

Table 1.2 Levels of H₂O₂ measured in natural waters

Levels of H ₂ O ₂ (nM)	Source of H ₂ O ₂	Generated via	Reference
21000	rainwater	gas-phase photochemical reactions	Hanson et al. (2001)
4910	freshwater	photochemical reactions	Richard et al. (2007)
100	seawater	light absorbing organic materials	Miller and Kester (1994)
1-3	deep seawater	organism in dark production	Palenik and Morel (1988)

Production of H₂O₂ has been reported from intact organisms such as green microalgae (*Chlamydomonas* and *Chlorogonium spp.*: Zepp et al., 1987), green macroalgae (Collén et al., 1995), red macroalgae (Collén, 1994). H₂O₂ has also been found in natural waters with the concentration ranging from 1 nM to 21 μM (Table 1.2), the majority being generated via photochemical reactions.

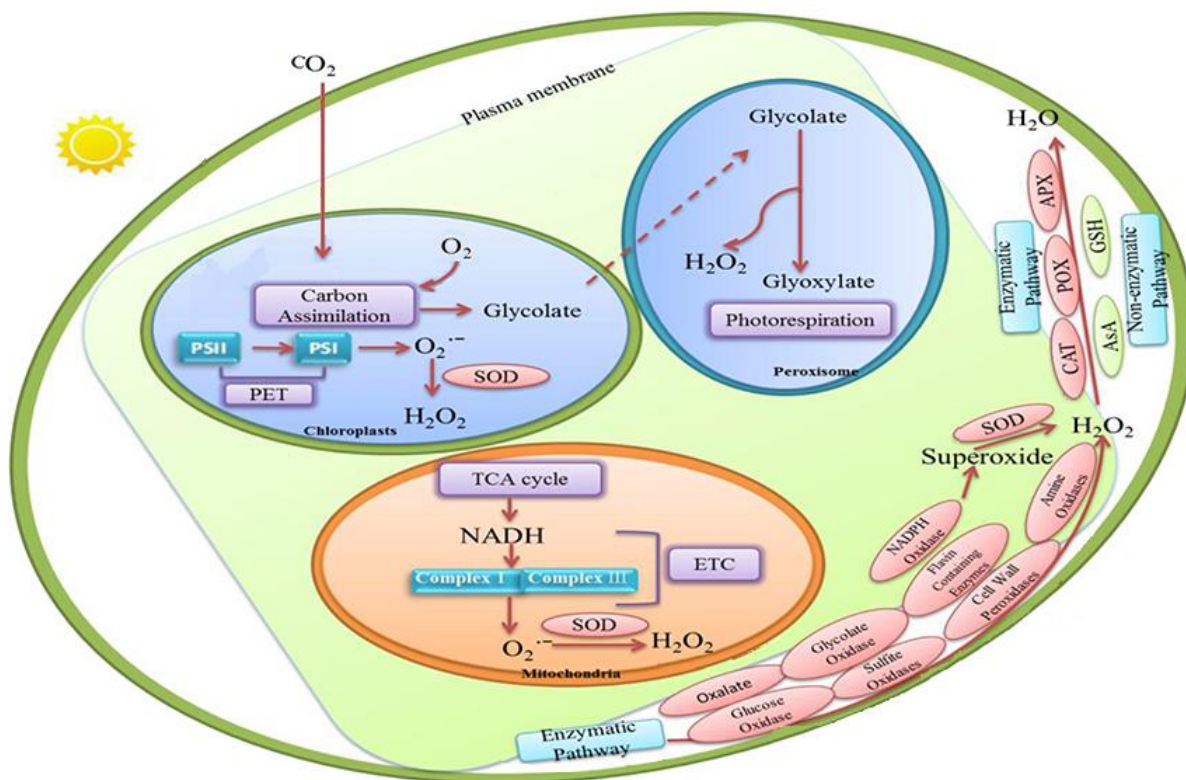


Figure 1.1 Schematic of H₂O₂ production and removal mechanisms in plants (from Niu and Liao, 2016).

To minimise H_2O_2 effects, plants employ two types of scavenging. These are enzymatic (Table 1.3) and non-enzymatic antioxidants, which are present in cells as protective agents against the damage associated with H_2O_2 . Three major enzymatic defence systems that collectively work to minimize the overall level of ROS including H_2O_2 namely superoxide dismutase (SOD), peroxidases and catalases (Sampath-Wiley et al., 2008; Asada, 1999). SODs are classified based on their metal cofactors and localisation: the copper/zinc form (Cu/ZnSOD) is found in the cytosolic fractions and also in apoplasts, while the manganese form (Mn-SOD) is found in the mitochondria and peroxisomes (Sampath-Wiley et al., 2008). The iron (Fe-SOD) form is found in the chloroplast compartment, which is the most ancient SOD group (Alscher et al., 2002; Mittler, 2002). SODs catalyse the conversion of superoxide radicals into hydrogen peroxide and oxygen; the hydrogen peroxide then metabolised to oxygen and water by catalase or to water by glutathione peroxidase (GPX). As plants have no scavenger for the very destructive hydroxyl, $\bullet OH$, the activation of SOD and catalase/peroxidase is essential to limiting the formation of both the H_2O_2 and $O_2\bullet^-$.

Ascorbate peroxidase (APX) is a substrate-specific, haem-containing enzyme that scavenges H_2O_2 and utilises ascorbate (Asc) as a cofactor, which is regenerated from two oxidised forms; monodehydroascorbate (MDHA) and dehydroascorbate (DHA), in the Asc-glutathione cycle

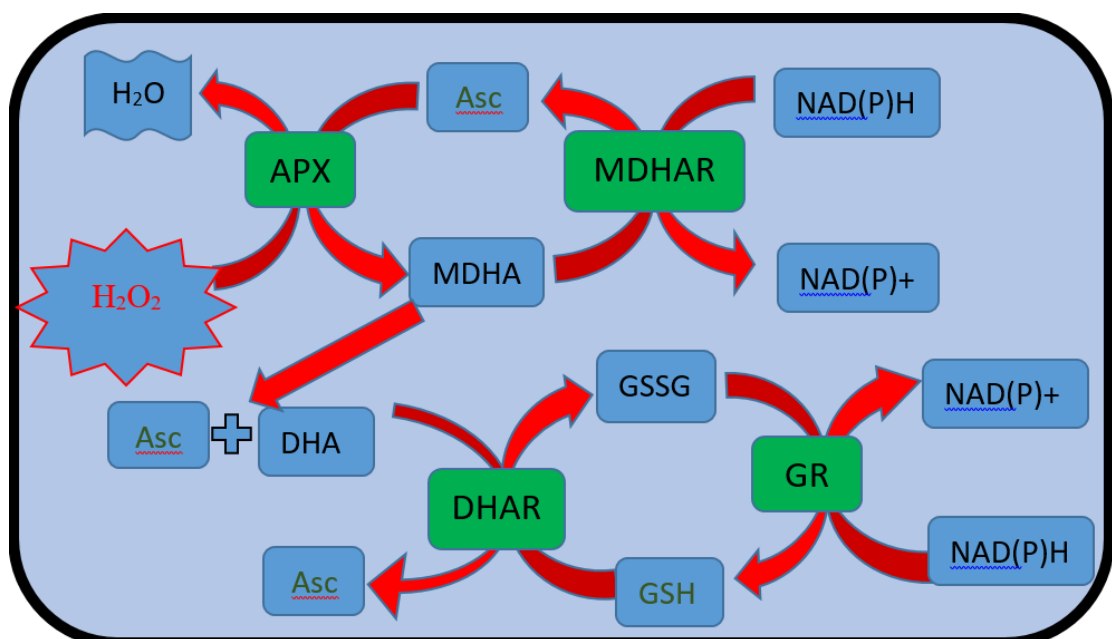


Figure 1.2 The ascorbate-glutathione (Asc-GSH - Halliwell-Asada) pathway [ascorbate, Asc; ascorbate peroxidase, APX; monodehydroascorbate, MDHA; monodehydroascorbate reductase, MDHAR; dehydroascorbate, DHA; dehydroascorbate reductase, DHAR; glutathione, GSH; oxidized glutathione, GSSG; glutathione reductase, GR; nicotinamide adenine dinucleotide

phosphate (reduced form), NAD(P)H; nicotinamide adenine dinucleotide phosphate (oxidized form), NAD(P)⁺].

also called Halliwell-Asada pathway. To regenerate hydrogen peroxide via ascorbate peroxidase, enzymes such as glutathione reductase (GR), monodehydroascorbate reductase (MDHAR), and dehydroascorbate reductase (DHAR), as well as glutathione, are involved. (Bischof and Rautenberger, 2012; Shigeoka et al., 2002). Catalase scavenges H₂O₂ in peroxisomes generated by photorespiration and the β-oxidation of fatty acids and is thought to play a significant role in the protection of aerobic organisms from the toxic effects of H₂O₂ (Gill and Tuteja, 2010).

Table 1.3 Enzymatic antioxidants and their locations (adapted from Mittler, 2002)

Enzyme	Reaction	Location
Superoxide dismutase (SOD)	$O_2^{\bullet-} + O_2^{\bullet-} + 2 H^+ \rightarrow 2 H_2O_2 + O_2$	Chl, Cyt, Mit, Per, Apo
Ascorbate peroxidase (APX)	$H_2O_2 + AA \rightarrow 2 H_2O + DHA$	Chl, Cyt, Mit, Per, Apo
Catalase (CAT)	$2 H_2O_2 \rightarrow H_2O + O_2$	Per
Glutathione peroxidase (GPX)	$H_2O_2 + GSH \rightarrow H_2O + GSSG$	Cyt
Glutathione reductase (GR)	$GSSG + NAD(P)H \rightarrow$ $2 GSH + NAD(P)^+$	Chl, Cyt, Mit, Per, Apo

Key Chl: chloroplasts, Cyt; cytosol; Mit, mitochondria; Per, peroxisomes; Apo, apoplast

1.4.1 Potential effects of abiotic factors on ROS accumulation in rock pools

Living in rock pools is harsh as in addition to exposure to endogenous H₂O₂, organisms may have to cope with stress from exogenous ROS. Macroalgae living in rock pools are exposed to large fluctuations in irradiance levels. At low tide on sunny days the water is still for many hours, with extreme changes in temperature, salinity and pH that may accelerate endogenous cellular H₂O₂ production (Emamverdian et al., 2015; Lewis et al., 1998; Mamboya et al., 2009). For example, any limitation on CO₂ fixation will reduce NADP⁺ regeneration through the Calvin cycle, and hence cause an over reduction of the photosynthetic electron transport chain leading to greater leakage of electrons to O₂ during photosynthesis generating O₂^{•-} that then dismutates to H₂O₂. In macroalgae and aquatic plants, H₂O₂ can diffuse through biological membranes and cell walls into the surrounding water (Abele et al., 1998; Ross and Alstyne, 2007). For example, it has been demonstrated by Collén and co-workers (Collén and Pedersén, 1996; Collén et al., 1995)

that H₂O₂ produced endogenously in the green seaweed *Ulva rigida* and released from the thallus can reach concentrations of up to 4 μM in the surrounding seawater. Additional sources of H₂O₂ in rock pools can come from the activity of the microphytobenthos, increasing H₂O₂ concentrations in the water even further (Palenik et al., 1987; Zika et al., 1985a; Johnson et al., 1989; Arakaki et al., 2007). In some areas, such as the intertidal surface waters of the North-Sea Wadden coast, off Germany, H₂O₂ production driven by UV exceeds the biological and chemical decomposition resulting in accumulation on micromolar concentration (Abele et al., 1998). Moreover, a study by Yocis et al. (2000) on the photoproduction of H₂O₂ at the sea surface in Antarctic waters suggests that it could increase significantly due to intensified solar irradiation following the depletion of stratospheric ozone, while in the Antarctic intertidal pool water during the warm season, levels of H₂O₂ can reach 2 μM and micromolar concentrations in surface water (Abele et al., 1998). This condition may affect the redox process lead to effects on biochemistry and the physiology of the organisms inhabiting rock pools (Moffett and Zafiriou, 1990). For example, when the shrimp, *Crangon crangon*, was exposed to increased hydrogen peroxide levels, the metabolic rate decreased by an average of 26% in intact animals and by up to 60% in isolated tail muscle (Abele et al., 1998).

Rain events can also be responsible for increases in H₂O₂ in the marine environment, as discovered by Cooper et al. (1987) in the Gulf of Mexico, where concentrations increased tenfold during heavy rains. They found that with the low level of nitric oxide (NO) and sulphuric dioxide in the marine air, which reacts rapidly with HO₂• and hydrogen peroxide, respectively, the level of H₂O₂ in rainwater can reach 82 μM. Such conditions make exogenous H₂O₂ increase and potentially make hydrogen peroxide a problematic pollutant. At 4 °C, H₂O₂ exposure generated physiological alterations in the Antarctic intertidal limpet *Concinna nacella*, including decreased O₂ consumption and increased lysosome damage, respectively (Abele et al., 1998)

Fluctuations of the physicochemical properties in rock pools can also exacerbate the presence of H₂O₂ in seawater. For example, the production of H₂O₂ by seaweed and other microalgae is increased at high pH. In the work of Collén and Pedersén (1996), they found that H₂O₂ production in seawater at pH 9 was fivefold higher than in normal seawater (pH 8.2). At low tide, values of pH 10 can be reached in rock pools (Truchot and Duhamel-Jouve, 1980). Salinity might cause problems for macroalgae, as under moderate hypo and hyper-salinity, thiobarbituric acid reactive substance (TBARS) and peroxide contents correlate with increased absorption of H₂O₂ by thalli of *Ulva fasciata* compared

to surrounding seawater (Lu et al., 2006). High temperature and emersion-induced physiological stress have been thoroughly established in the red algal *Mastocarpus stellatus* (Collén and Davison, 1999; Smirnoff, 1995). The rise in temperatures in the summertime is accompanied with the elevated H₂O₂ content in *Hypnea musciformis* and reversed when temperature decreased (Maharana et al., 2012). The intertidal brown macroalgae *Fucus vesiculosus* has been reported to increase reactive oxygen production at higher temperatures of 20 °C compared to 0 °C under laboratory conditions (Collén and Davison, 2001).

Symbiotic algae that live in the rock pool organisms such as anemones, might also be impacted. Like in corals, photosynthesis and ascorbate content decrease resulting in accumulation of H₂O₂ leading oxidative damage. Downs et al. (2002) suggested that oxidative damage has occurred by failure of the quenching enzymes in coral cytosol to prevent the formation of hydroxyl radical, when H₂O₂ in surrounding seawater and diffused from symbiont or zooxanthellae, into the coral cytoplasm, resulting in coral bleaching (Levy et al., 2006; Higuchi et al., 2009). They concluded that H₂O₂ from surrounding seawater increase stress in coral and decrease photosynthesis in coral. Other studies of coral also found that symbiotic algae also release H₂O₂ to the water make corals susceptible to be bleached in stagnant water. Hence, it is suggested that strong currents are needed to enable rapid H₂O₂ removal and prevention of oxidative damage (Nakamura, 2010).

1.5 Aims and objectives

The presence of macroalgae in some rock pools is a potential source of ROS and, in particular, of hydrogen peroxide. The physicochemical conditions in rock pools at low tides could exacerbate endogenous ROS production by organisms living in them and is likely to increase the steady-state concentration of hydrogen peroxide of their surroundings. It is hypothesised that when released into the surrounding seawater this production may affect other co-occurring organisms and that the level of susceptibility will be related to the degree of tolerance of these organisms to this environmental stress. The main aim of the work described in this thesis was to investigate whether hydrogen peroxide levels are reached that could impact on a species that may be especially vulnerable to increased hydrogen peroxide levels in rock pools such as snakelocks anemones (*Anemone viridis*) due to the presence of zooxanthellae.

The objective of the work described in Chapter 2 was to evaluate and describe the physicochemical environment of rock pools and algal cover over a tidal cycle in a range of rock pools. The parameters measured were temperature, salinity, dissolved oxygen, irradiance and hydrogen peroxide. For the latter, two methods used for determining H₂O₂ concentrations in seawater were developed. A portable luminometer, designed to measure environmental ATP in a field biomedical context, was used for measuring H₂O₂ *in situ* via horseradish peroxidase catalysed luminol-dependent chemiluminescence, as well as a laboratory-based fluorescence method that used horseradish peroxidase to catalyse the oxidation of homovanillic acid (HVA) by H₂O₂.

The work in Chapter 3 provides a physiological evaluation of abiotic stress in three different classes of macroalgae that are commonly found in rock pools: green macroalgae represented by *Ulva lactuca*, brown by *Fucus serratus* and red by *Chondrus crispus*. Macroalgae were collected and exposed to higher physicochemical conditions for four hours, and the hydrogen peroxide was measured as well as the chlorophyll fluorescence. The objectives of this chapter were to compare the steady-state level of hydrogen peroxide produced by red, brown and green algae exposed to different abiotic stress and their physiological responses after the exposure to the stress condition.

The focus of the work in Chapter 4 was on the effects of hydrogen peroxide on a co-occurring rockpool organism, specifically two morphs of the anemone *Anemonia viridis*. Anemones were exposed to various levels of hydrogen peroxide for four hours, and biochemical assays were performed on the samples, allowing total glutathione, malondialdehyde and superoxide dismutase content of the extracts to be measured by spectrophotometry; also, zooxanthellae counts were also performed.

Chapter 2
Development and application of modified fluorometric and chemiluminescence methods for the measurement of hydrogen peroxide in rock pools

2.1 Introduction

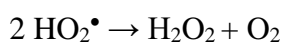
Research on rock pools dates to a key paper by Klugh (1924) who described this habitat and the factors such as substrate, volume of seawater, wave action etc., that affect it. Since then, there have been numerous studies reporting on the marked changes in physicochemical environmental conditions such as temperature, pH, salinity, dissolved oxygen and carbon dioxide over diurnal and seasonal time scales (Morris & Taylor, 1983; Bridges, 1983; Huggett and Griffiths, 1986; Legrand et al., 2017). It is now well established that, rock pools provide productive microhabitats for many aquatic species, including a diverse range of photosynthetic organisms, invertebrate and fish (Martins et al., 2007; Firth et al., 2013). For example, some animals use them for foraging (Benedetti-Cecchi et al., 1998), as refuges (Underwood & Jernakoff, 1984; Zander et al., 1999), for breeding (Bonner et al., 1997; Peterson & Boulton, 1999), while others live there permanently (Schneider & Frost, 1996; Therriault & Kolasa, 2001).

Compared to creatures living in emergent substrata, those in intertidal rock pools have a greater capacity for adaptation as they are protected from desiccation (Newell, 1979). Also, the interactions can be stronger because some taxa are more abundant in pools (e.g., algae) and they generally have greater diversity than the adjacent areas of draining rock (Metaxas & Scheibling, 1993). They do, however, experience considerable variations in the physicochemical factors than those of the open ocean (Morris & Taylor, 1983) and therefore at the timing of low tide, organisms such as seaweeds are more challenged with exposure to stressful environmental conditions including high UV radiation, salinity, high temperature, pH fluctuations and high dissolved oxygen when it occurs in the middle of the day (Huggett and Griffiths, 1986).

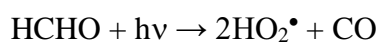
During oxygenic photosynthesis, seaweeds use water as a reductant and steadily release molecular oxygen, which can be accumulated and easily chemically converted to potentially damaging reactive oxygen species (e.g., H_2O_2). With drastic changes in physicochemical conditions, studies have shown that these conditions may accelerate the cellular H_2O_2 production (Collén and Davison 1999a, b; Burritt et al., 2002; Lu et al., 2006; Pereira et al., 2009; Wu et al., 2009) which can subsequently be diffused into the surrounding water (Collén & Pedersén, 1996).

The occurrence of H_2O_2 in seawater was first reported by van Baalen and Marler in 1966. It was suggested that the source of hydrogen peroxide follows three pathways:

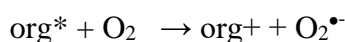
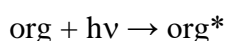
photochemically in the atmosphere and in seawater catalysed by dissolved pigments or metabolic activity of microorganisms; in the atmosphere, where gaseous H₂O₂ is formed from the dismutation of hydroperoxyl radicals (Davide et. al., 2003),



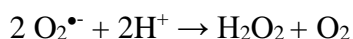
where the production of HO₂[•] is from the photolysis of formaldehyde;



and in seawater, where dissolved organic pigments (org) act as light receptors that become excited leading to the production of O₂^{•-}.



A precursor such as superoxide (O₂^{•-}) of H₂O₂ and O₂ could be catalysed by superoxide dismutase (SOD) or a reduced metal ion such as copper (Cu) and iron (Fe) (Cooper et al., 1987; Cooper and Zika, 1983; Petasne and Zika, 1987; von Sonntag and Schuchmann, 1991) that rapidly disproportionates O₂^{•-} according to the equation:



Now it is known that hydrogen peroxide (H₂O₂) is an unavoidable toxic by-product of normal aerobic metabolism in both animals and plants, and, in general, its production increases under stress conditions (Dat et al., 2000; Mittler, 2002; Lushchak, 2011). Elevated levels of H₂O₂ are also indicative of higher photochemical activity in water (Cooper and Zika, 1983; Moore et al., 1993). In surface ocean, H₂O₂ concentrations are reported to be 20-420 nM (Price et al., 1998; Gerinnga et al., 2004) while in the open sea at depths of more than 1000 m H₂O₂ concentrations of 0.5-2.9 nM have been measured (Hopwood et al., 2017). Although H₂O₂ is potentially a powerful oxidant its reaction rates with many biomolecules are slow and it appears unable to directly oxidize DNA and lipids, while in proteins it can only oxidize cysteine and methionine residues (Halliwell and Gutteridge, 2007). However, the danger of H₂O₂ largely comes from its conversion to the highly reactive hydroxyl radical (OH[•]) either by exposure to ultraviolet light or through the Fenton and the Haber-Weiss reactions (Halliwell et al., 2000). Decomposition of H₂O₂ can occur both biologically (Cooper and Zepp, 1990) and photochemically (Moffett and Zafiriou, 1993), giving rise to the steady state levels seen in natural waters,

i.e., daytime surface concentrations typically in the range 10^{-7} - 10^{-6} M (see Kieber et al. (2003) for a review).

In contrast to the many methods used to determine levels of hydrogen peroxide in open seawater, there is little information specifically related to rock pools. Burns et al. (2012) listed more than 30 analytical measurements for the determination of hydrogen peroxide, but of these, they considered only ten to have a sufficiently low limit of detection for the study of H_2O_2 in natural waters. Methods used for H_2O_2 determination in sea-water fall into three categories: chemiluminescence (CL), e.g., using luminol chemiluminescence (Kok et al., 1978; Xiao et al., 2002); colorimetry (Bader et al., 1988); and fluorescence (FL), either by fluorescence-bleaching e.g., using scopoletin (Abele-Oeschger et al., 1997; van Baalen and Marler, 1966; Zika et al., 1985b), or by fluorescence-induction using a hydroxyphenyl carboxylic acid such as *p*-hydroxyphenyl acetic acid (Hwang and Dasgupta, 1986; Kok et al., 1978; Miller and Kester, 1988). FL and CL methods are preferred because they generally offer the highest sensitivity (Miller et al., 2005). In all cases, improved specificity for peroxides (H_2O_2 and organic hydroperoxides), is obtained by using horseradish peroxidase (HRP) to catalyse the reaction between H_2O_2 and the detection reagent (Burns et al., 2012). Controls are included, in which samples are pre-treated with catalase to remove H_2O_2 .

In the present study, a CL method was compared to an FL method for measuring concentrations of H_2O_2 in rock pools *in situ*. The latter method used homovanillic acid (HVA) as the detection reagent which, unlike scopoletin and *p*-hydroxyphenyl acetic acid, has been used for measuring H_2O_2 production by cells or sub-cellular fractions, e.g., mitochondria. The application of HVA in this study was based on its high fluorescence coefficient and stability when dimerized (HVA dimer) (Paździuch-Czochra and Wideńska, 2002). The CL method used the reaction of luminol with H_2O_2 in the presence of HRP to produce a luminol radical that emits luminescence as it decays to the ground state. This type of CL-based method has been widely used with natural water samples because it is less susceptible to interference than FL-based (and spectrophotometric) methods, but it normally requires rather specialized instrumentation that are typically laboratory based and relatively expensive. As the aim of this study was to determine concentrations *in situ*, luminescence was detected using a portable, low-cost luminometer designed for measuring ATP in a field biomedical context, e.g., for the detection of microbial contamination of surfaces, using the firefly bioluminescence system. The aim was also to describe the relative role of algal assemblages on the physicochemical

environment and H₂O₂.

2.2 Materials and Methods

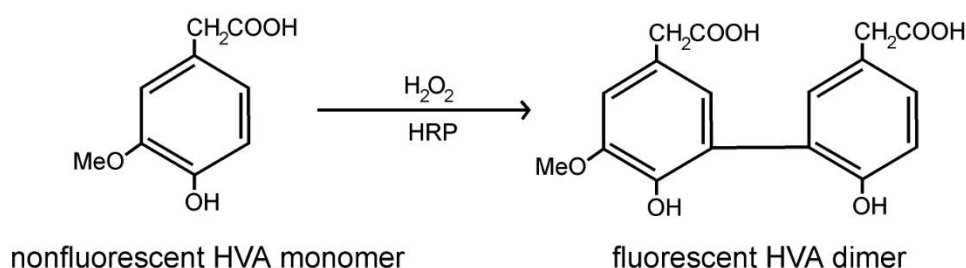
All reagents were obtained from Sigma-Aldrich (Poole, UK) unless otherwise stated.

2.2.1 Standardisation of hydrogen peroxide (H₂O₂) solutions

H₂O₂ solutions were prepared from a nominal 30% by weight stock solution (Sigma H1009, 29.0-32.0% (w/w) containing stabiliser). This stock solution (approximately 8.8 M) was tested at intervals by dilution of 1 µl to 1 ml of distilled water or 50 mM HEPES buffer, pH 7.5, in a UV-transparent cuvette (made of UV-transparent plastic or quartz; see Results) followed by measurement of the absorbance at 240 nm. Newly purchased stock solution diluted in this way gave A₂₄₀ values consistent with an extinction coefficient at 240 nm of 43.6 M⁻¹ cm⁻¹ (Hildebrandt and Roots, 1975), and with the value 38.3 ± 1.1 M⁻¹ cm⁻¹ (mean ± 95% confidence limits), reported by Morgan et al. (1988). The value of 43.6 M⁻¹ cm⁻¹ is commonly used, and so this was used in the current work. Over a period of months, some decrease in A₂₄₀ was noted, so concentrations of standard solutions prepared from the stock were adjusted accordingly. At 189.3 M⁻¹ cm⁻¹, the extinction coefficient for H₂O₂ is much higher at 200 nm (Morgan et al., 1988), but the problems associated with reliably measuring absorbance in the far UV, i.e., low light intensity coupled with high basal absorbance from plastic cuvettes and/or buffer substances, precluded routine measurement of A₂₀₀.

2.2.2 Fluorescence (FL) method for measurement of H₂O₂

The FL method was based on that of Staniek and Nohl (1999), which was originally used for measuring H₂O₂ production by isolated mitochondria. In this method homovanillic acid (HVA) is oxidised by H₂O₂ in a reaction catalysed by horseradish peroxidase (HRP) yielding a dimeric product that is fluorescent.



In the version of the method used here, 1.5 ml of standard H₂O₂ solution or of H₂O₂-

containing natural waters were mixed with 1.5 ml of buffered HRP solution, prepared by dissolving 2.5 U/ml of HRP (Sigma, P8125) in 50 mM sodium HEPES buffer, pH 7.5, containing 1 mM sodium EDTA. Standard H₂O₂ solutions were either prepared in fresh distilled water or artificial seawater as appropriate. This was either carried out in plastic fluorescence cuvettes in the laboratory or in 15 ml Falcon tubes in the field. The reaction was started by the addition of 30 µl of 10 mM HVA dissolved in the same buffer. With the concentration of HRP used here the endpoint to produce the fluorescent product was reached in < 10 min at room temperature (20 °C). In the field the vials were stored in the dark in a cool box with ice packs before transportation to the laboratory, approximately 4-5 h later, where they were stored at -20 °C for a few days before measurement of fluorescence. After thawing and equilibration at room temperature, the fluorescence was measured in an LS50B fluorimeter (Perkin-Elmer, Buckinghamshire, UK) using an excitation wavelength of 312 nm and an emission wavelength of 420 nm).

In the field, individual water samples were split into three parts, one used for the reaction as described above; the second as the +catalase control and treated with catalase (2 µl of 100-fold diluted Sigma C-100 catalase) for at least 5 min before addition of the HVA and HRP, as described above; and the third part as the +internal standard, spiked with 3 µl of a 0.88 mM standard H₂O₂ solution to a final concentration of 0.88 µM H₂O₂. The standard H₂O₂ solution was produced using two, 100-fold dilutions of the stock solution.

2.2.3 Chemiluminescence (CL) method for H₂O₂ measurement

The CL method is based on the luminol-dependent chemiluminescence method of Collén et al. (1995). The assay involves the oxidation of luminol (3-aminophthalhydrazide) by H₂O₂, catalysed by horseradish peroxidase (HRP), in a complex series of reactions (Fig. 2.1). One outcome of these oxidations is the formation of an excited form of 3-aminophthalate, which when returning to its ground state releases light with a λ_{max} of 428 nm (Yue and Liu, 2020).

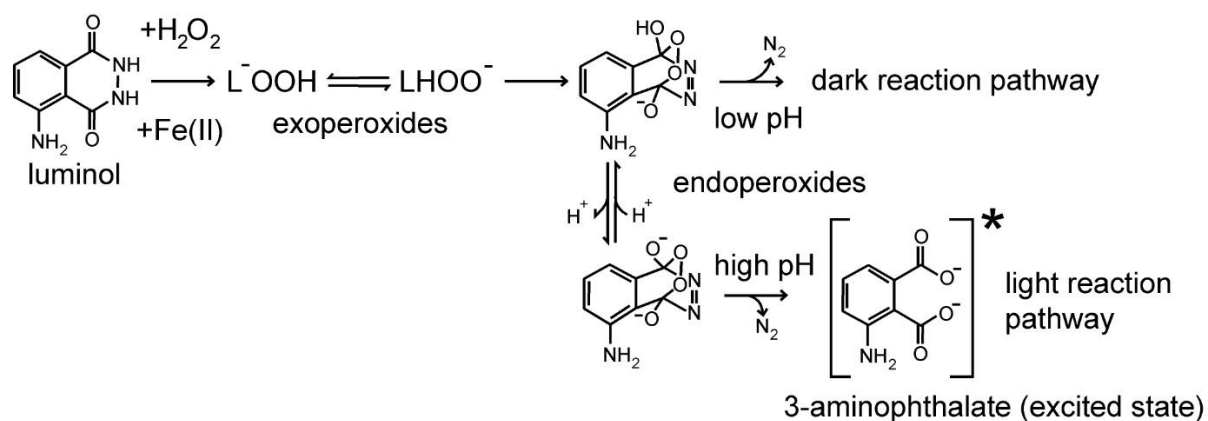


Figure 2.1 Reaction of luminol with H_2O_2 leading to chemiluminescence (based on Yue and Liu, 2020). Horseradish peroxidase acts as a catalyst, similar to Fe(II) in this scheme. The decay of the excited form of 3-aminophthalate back to its ground state releases light (chemiluminescence).

Emitted light was detected using a low-cost portable luminometer (Hygiena Pi-102), designed for the measurement of ATP using the firefly bioluminescence system. It should be noted that the peak emission wavelength (575 nm) for the *Photinus pyralis* luciferase with ATP (Steghens et al., 1998), is much higher than that for HRP-catalysed luminol chemiluminescence; however, the Hygiena luminometer was found to be capable of detecting light at 428 nm.

A 5 mM luminol stock solution was prepared by dissolving 8.8 mg luminol (5-amino-2,3-dihydro-1,4-phthalazinedione) in 1 ml of 1 M NaOH followed by the addition of 9 ml of 0.4 M MOPS buffer, pH 7.0. Horseradish peroxidase (Sigma, P8125) was dissolved in 50 mM Tris-chloride buffer, pH 9.0, at 660 U ml^{-1} . In the laboratory both solutions were kept on ice during use, while in the field they were stored in the dark in a cool box with ice packs. Chemiluminescence measurements were carried out by mixing 1 ml of sample (standard H_2O_2 solution or of H_2O_2 -containing natural waters) with $12 \mu\text{l}$ of 5 mM luminol and $12 \mu\text{l}$ of buffered HRP in 3 ml translucent polystyrene tubes. Note that the purpose of the high concentration of buffer used in the preparation of the HRP solution was to increase the light output by raising the pH of the mixture close to 9. After mixing (4-6 s), the tubes were immediately transferred to the luminometer, and the light output measured (integration time = 5 s). It is important to measure the light output as soon as possible after mixing as the output rapidly declines.

In the field, individual water samples were split into at least four parts. One part was used for the reaction as described above, while a second part, the +catalase control, was treated with catalase ($2 \mu\text{l}$ of 100-fold diluted Sigma C-100 catalase) for at least 5 min before

addition of the HRP and luminol as described above. At least two other parts were used for internal standards and were spiked with known concentrations of H₂O₂ by adding small volumes of 0.88 mM H₂O₂, before measuring the chemiluminescence as described above. In addition, a calibration curve for 0-8.8 μM H₂O₂ was produced using external standards prepared by diluting H₂O₂ in artificial seawater.

To estimate H₂O₂ concentrations in samples using external standards the luminescence data (relative luminescence units, RLU) were first log₁₀ transformed and the log₁₀(RLU) of the reagent blank subtracted before plotting the calibration curve. The curve was then fitted with a single rectangular hyperbola (2 parameter; Equation 1) using SigmaPlot 13.0 (Systat Software, Inc.).

$$y = \frac{a \times x}{b + x} \quad \text{Equation 1}$$

The H₂O₂ concentration corresponding to the log₁₀(RLU) for each unknown sample was then obtained using Equation 2.

$$x = \frac{b \times y}{a - y} \quad \text{Equation 2}$$

To estimate the H₂O₂ concentrations in samples using internal standards the luminescence data for each sample, including the data obtained after spiking with H₂O₂, were log₁₀ transformed. The log₁₀(RLU) for the +catalase control was then subtracted from the log₁₀(RLU) values obtained for each sample before and after spiking with H₂O₂, after which they were fitted with a single rectangular hyperbola (3 parameter; Equation 3), where x_0 is an offset on the x axis equivalent to the unknown concentration of H₂O₂ in the sample. This is referred to as the extrapolation method.

$$y = \frac{a \times (x + x_0)}{b + (x + x_0)} \quad \text{Equation 3}$$

For this to be valid the minimum number of spike concentrations used was two, 0.88 and 2.64 μM, in which case the value of b was constrained during the curve fitting to match that obtained from the calibration curve obtained with external standards.

2.2.4 Field studies

Field studies were carried out between June and August 2016 at Wembury Point in the South Hams, Devon, UK (50.3167° N, 4.1086° W; Grid Ref. SX503487) and in June 2018 at Plymouth Hoe (50.3639° N, 4.1492° W; Grid. Ref. SX478539). Rock pools are

common over the whole vertical extent of the rocky shore at Wembury Point.

2.2.4.1 Rock pool characteristics

Twelve rock pools were monitored at Wembury Point during low tides under fair weather conditions. Selected rock pools were distributed at different vertical heights above chart datum in the mid intertidal zone and were colonized commonly by green algae such as *Ulva* spp. and brown algae such as *Sargassum muticum* in lower pools (see Metaxas and Scheibling, 1993). The majority of the selected rock pools were replenished with seawater at high tide and isolated from the sea at low tide. With a measuring tape, the following rock pool characteristics were measured: length (l), the maximum linear distance across the surface of the rock pool; width (w), the distance perpendicular to the length axis at the midpoint of the rock pool; radius (r), the length of the rock pool divided by two; and depth (d), measurement of the deepest point within the rock pool. Using the formula $V = r^2d$, these measurements were used to estimate pool volume.

2.2.4.2 Physicochemical and H₂O₂ measurements on the rock pools

The experimental work was carried out to examine the potential relationships between physicochemical parameters, the presence of seaweed and levels of H₂O₂ regardless of the seaweed species present. Selected rock pools presented different volumes, depths and percent (%) cover of seaweed. The latter was determined using netting with a mesh size of 10 × 10 cm. The netting was placed over the rock pool contoured to the rock pool shape, and % cover gained from number of mesh squares with seaweed present divided by the total number of netting squares. Greater than 40% cover of seaweed was categorised as high 'weediness' (HW), between 10 and 40% was categorised as middle 'weediness' (MW) and less than 10% as low 'weediness' (LW), when assessing relationships of algal community to the physicochemistry and H₂O₂ concentrations of the pools. In addition, most of the pools also had encrusting algae. Measurements of temperature, dissolved oxygen concentration (DOC), pH and salinity were performed in each of the rock pools, using an YSI 556 MPS (Yellow Springs, OH 45387 USA).. Measurements for H₂O₂ were taken at different points in the pools such as in the middle and at the edge of each rock pool, and seawater was stirred around the sampling point to homogeneity prior to each measurement. Seawater samples were taken for measuring levels of hydrogen peroxide in the field and laboratory using the two methods described in Sections 2.2.2 and 2.2.3 above.

Table 2.1 Characteristics of the fourteen rock pools monitored at Wembury Point (1-12) and Plymouth Hoe (13 and 14). Surface area is the surface of the rock pools measured at low tide.

Pool	'weediness' (H, high; M, medium; and L, low)	estimated surface area (m ²)	estimated volume (m ³)	description
1	HW	1.42	0.265	Single alga (<i>Ulva intestinalis</i>) to one side of the pool on the upper shore; gravel substrate
2	HW	0.99	0.042	Green algae dominant (<i>Ulva lactuca</i> and <i>U. intestinalis</i>)
3	HW	0.89	0.059	Mixed algae in the middle dominated by brown algae (<i>Fucus serratus</i> , <i>Sargassum muticum</i>); encrusting algae on rock substrate
4	MW	0.82	0.049	Mixed algae dominated by green and brown algae with few coralline algae
5	LW	1.71	0.114	No macroalgae present with encrusting algae on the bottom of the substrate
6	MW	4.53	1.511	Mixed algae dominated by green algae
7	MW	0.68	0.072	Upper shore pool with single alga (<i>Ulva intestinalis</i>)
8	HW	0.42	0.068	Mixed brown and red algae (mainly <i>Corralina officinalis</i>)
9	MW	1.49	0.249	Mixed algae dominant by brown algae (<i>Sargassum muticum</i>) with small boulders substrate
10	LW	0.48	0.068	A few brown algae present, with a hard crust of algae on the substrate
11	LW	1.35	0.280	Few mixed algae at the edges of the pool
12	LW	0.39	0.068	Few algae at the sides with encrusting algae on the substrate
13	HW	4.64	1.392	Dominated by <i>Ulva lactuca</i> with rocky substrate
14	MW	0.66	0.035	Few <i>Ulva lactuca</i> in at the side with few <i>Fucus serratus</i> thalli falling in the pool

2.2.5 Statistical analysis

All statistical analyses were carried out using SPSS (IBM SPSS, version 24), unless specified otherwise. Comparisons between means were determined using one-way analysis of variance (ANOVA). A post hoc Tukey/LSD Multiple Comparison procedure, with probability of $P \leq 0.05$, was used to identify significant differences between individual means.

2.3 Results

2.3.1 Standardisation of H₂O₂ concentrations

When the H₂O₂ spectrum was measured using UV plastic cuvette (disposable PMMA UV grade, Fisher), there was an apparent peak (λ_{\max}) at 220 nm in the UV. As subsequent investigation was done using catalase, to demonstrate that H₂O₂ was being detected with different buffers (Hepes and phosphate) and distilled water using plastic cuvette it was found (Fig. 2.2) that the peak absorbance decayed exponentially on addition of catalase. However, there was shift in the peak down towards 200 nm after every measurement. It was concluded that the peak was an artefact caused by the absorbance from the cuvette below 220 nm being too high for the instrument.

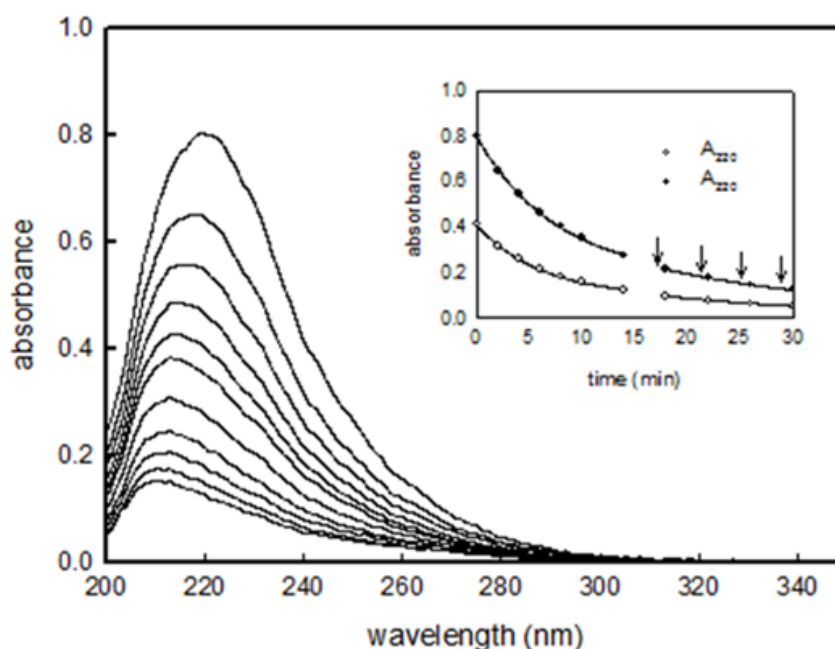


Figure 2.2 The apparent UV spectrum of hydrogen peroxide in Hepes buffer, pH 7.5 before and in a time series after addition of catalase (insert showing time course at a ' λ_{\max} ' and at 220 nm). Oxygen bubbles are especially prone to form during the breakdown of hydrogen peroxide. In the last four measurements (\downarrow), the mixture was stirred to disperse the bubbles in the cuvette.

2.3.2 Detection of hydrogen peroxide using the fluorescence method

The calibration curve for the fluorescence method is shown in Figure 2.3. It is based on the HRP-catalyzed oxidation of HVA by H₂O₂ (see Section 2.2.2), which is produced with H₂O₂ concentrations ranging from 0 to 6.2 μ M. Fluorescence intensity and concentration were linearly related ($R^2 = 0.999$). After reaction with hydrogen peroxide,

the maximum values of the excitation and emission spectra were determined (insert in Fig. 2.3). These spectra confirm that the fluorescent product was as expected. The emission wavelength was set to 500 nm for the excitation spectrum and the excitation peak was determined to be 312 nm, while the emission wavelength was set to 280 nm for the emission spectrum and the emission peak was determined to be 423 nm. These values are consistent with those found in earlier research (Staniek and Nohl, 1999, Barja 2002, Gomes et al., 2005).

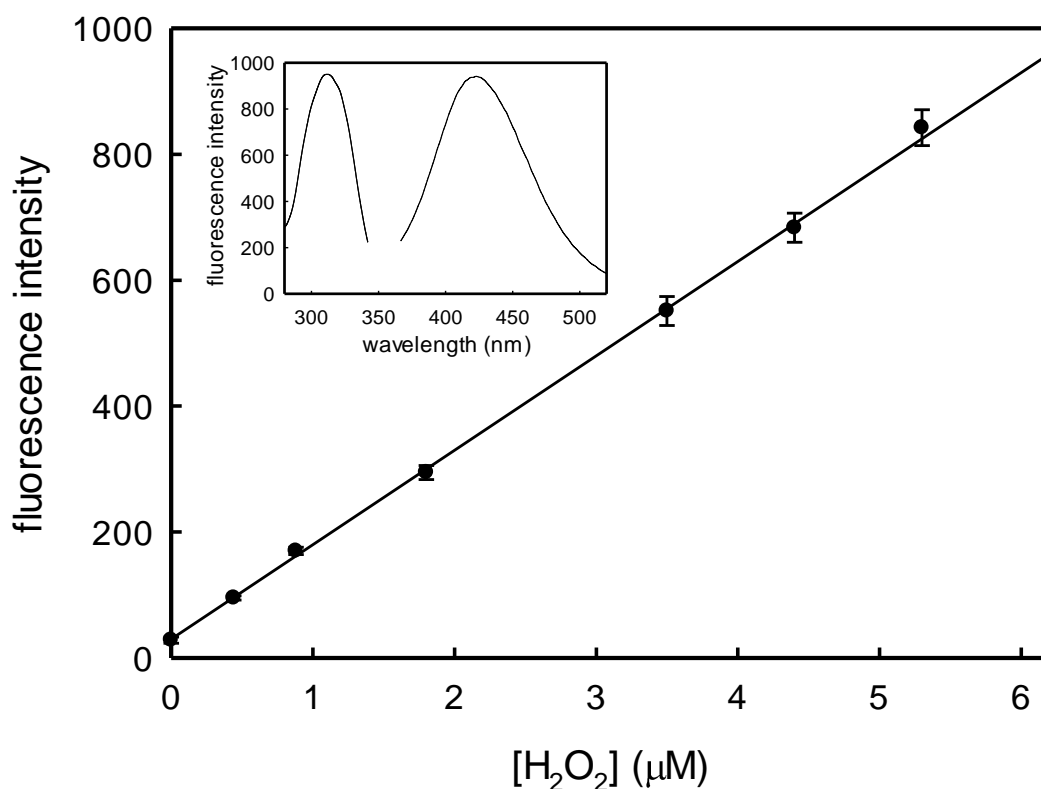


Figure 2.3 Calibration curve for H₂O₂ produced using the fluorescence method, based on the HRP-catalysed oxidation of homovanillic acid by H₂O₂ as described in Section 2.2.2. H₂O₂ standards were prepared in fresh artificial seawater. Data are means \pm SEM for three independent replicates; in each case the fluorescence was measured after 3 h incubation at room temperature. The insert shows the excitation and emission spectra for the fluorescent product.

To establish the time required to reach the end point of the reaction, the fluorescence intensity of the fluorescent product, from the reaction of hydrogen peroxide with HVA, was measured over 0 to 100 s. Figure 2.4 shows the increase in fluorescence increase with time in the presence of H₂O₂ concentrations between 1 and 2.5 μM. For all concentrations the end point for the fluorescent product was reached within 60 s.

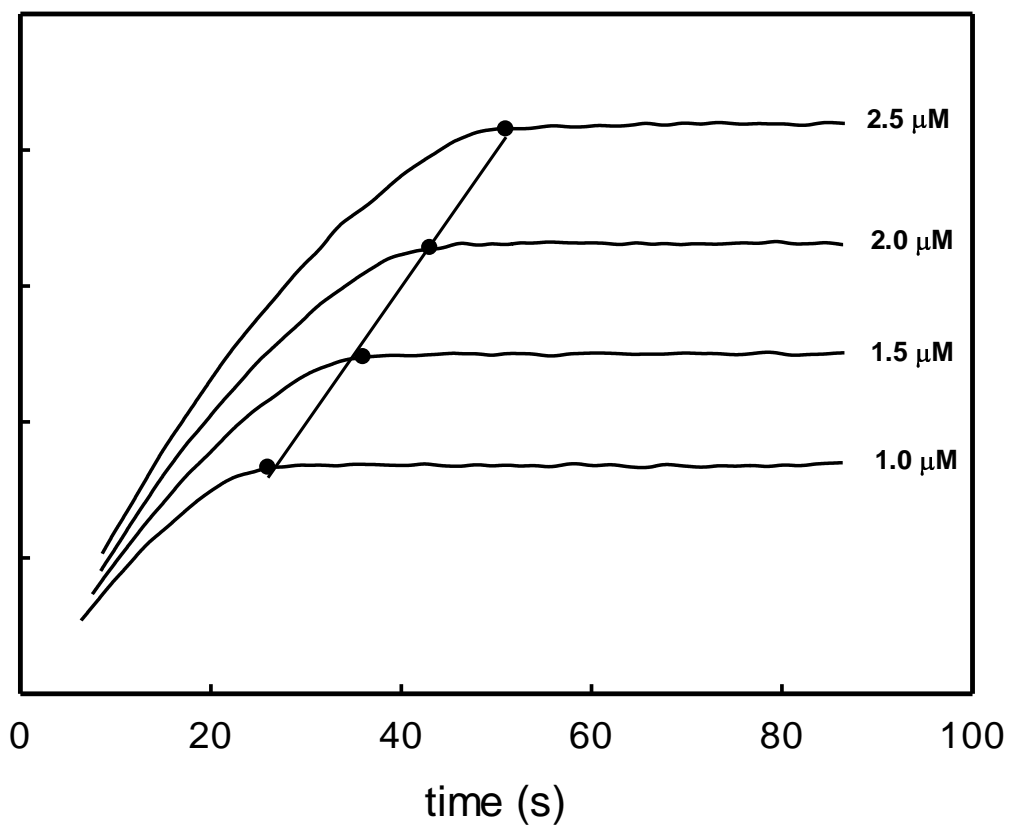


Figure 2.4 Time courses for the formation of the fluorescent product for the HRP-catalysed oxidation of homovanillic acid by H₂O₂. 0.88 mM H₂O₂ was added to the 3 ml standard method of 1.5 ml distilled water, 1.5 ml HRP and 30 μl HVA. The end point was reached within 60 s (●) and there was a linear relationship between the time taken to reach the end point and the concentration of H₂O₂.

The temporal stability of the HVA dimer produced using the reagent mixture with seawater samples in various concentrations of H₂O₂ revealed no significant increase in fluorescence over a 5 h period (Fig. 2.5). This gave confidence in the results of the field method, which required time for mobilization before being analysed in the lab.

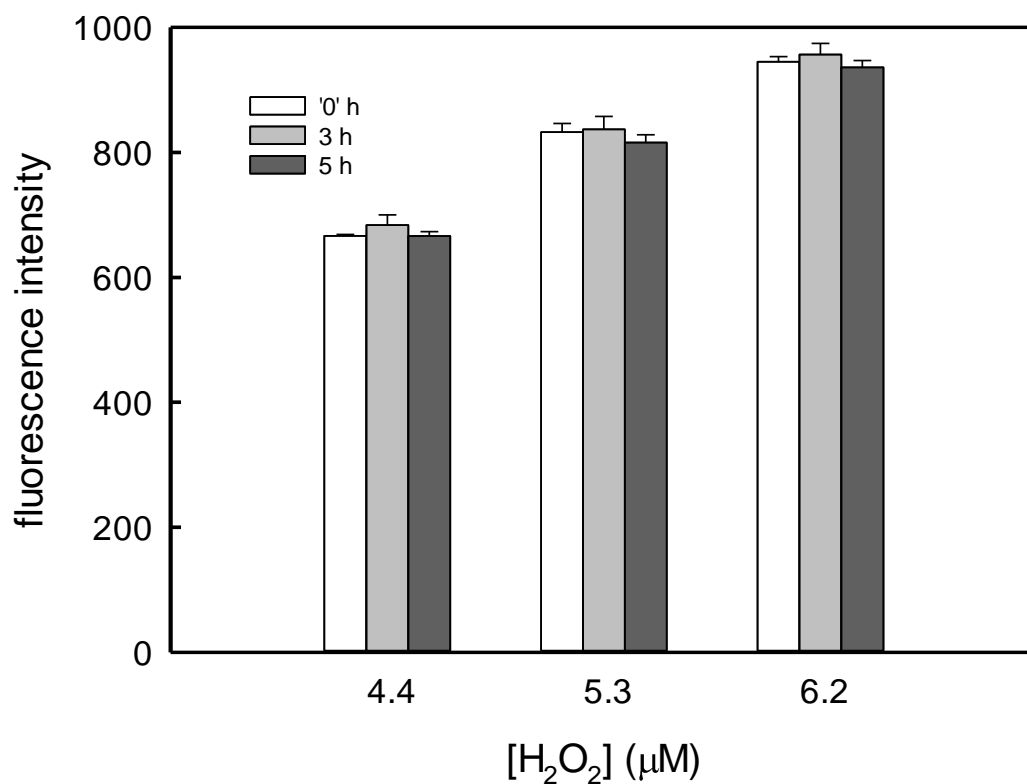


Figure 2.5 The stability of the fluorescent product produced in the HRP-catalysed oxidation of homovanillic acid by H₂O₂. H₂O₂ standards were prepared in fresh artificial seawater. Fluorescence was measured at 1 min, i.e., immediately after the end point had been reached ('0'), after 3 h and after 5 h. Data are means \pm SEM for four independent replicates. There was no significant difference between the fluorescence measured at each time point (ANOVA, P = 0.079).

Figure 2.6 shows the effect of the addition of catalase, in the presence and absence of HVA and HRP, on the fluorescence obtained with freshly distilled water (DW), filtered seawater (FSW) and freshly prepared artificial seawater (ASW-Instant Ocean).

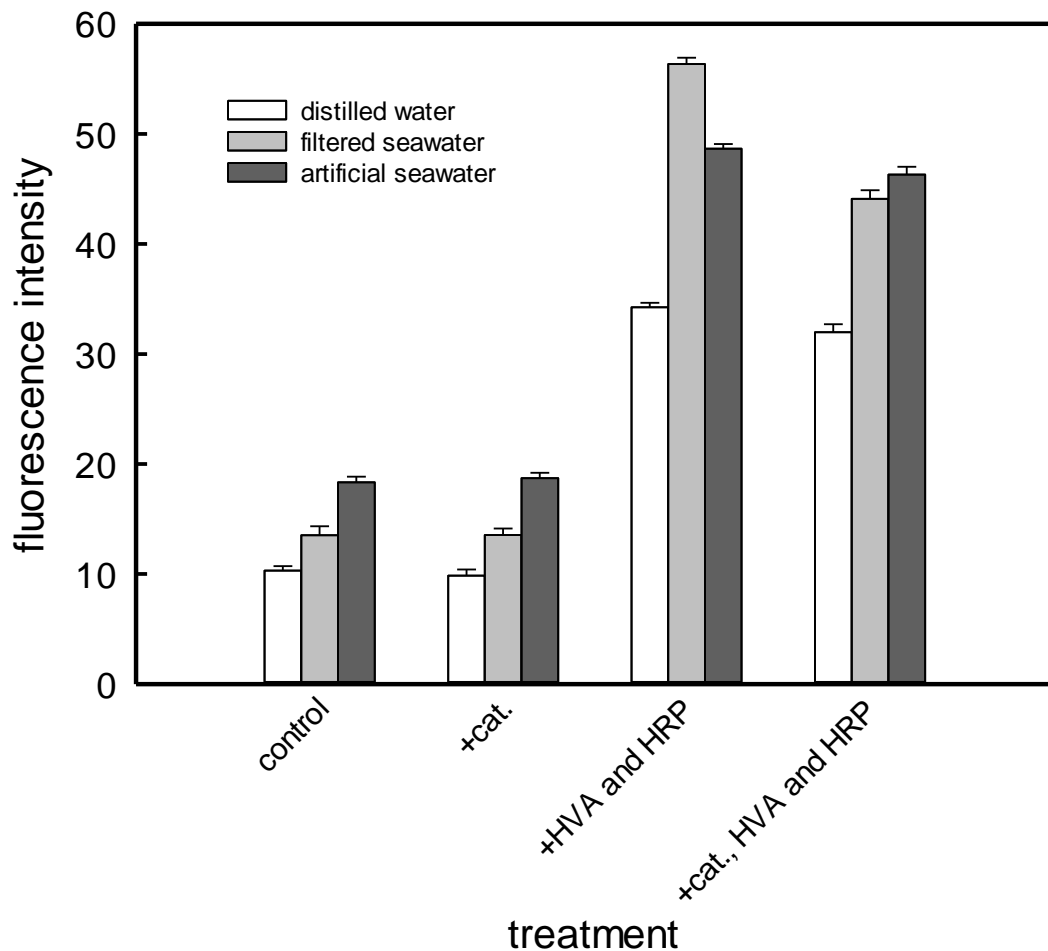


Figure 2.6 The effects of catalase on fluorescence in the presence and absence of HVA and HRP. All water types (AWT) were measured alone (control); AWT treated with catalase (+cat); AWT 1.5 ml with 30 μ l HVA and 1.5 ml HRP (+HVA and HRP); AWT was treated with catalase for 10 min before HVA and HRP were added (+cat., HVA and HRP).

There were significant effects of water type and treatment on fluorescence, as well as a significant interaction between water type and treatment (two-way ANOVA, $P < 0.00005$ in all cases). Basal fluorescence was highest in ASW, followed by FSW and then DW (Tukey's HSD, $P < 0.05$). In all three, the addition of HVA and HRP led to a significant increase in the fluorescence, which was highest in FSW, followed by ASW, and then DW. In the absence of HVA and HRP, catalase had no significant effect on the fluorescence, whereas, in the presence of HVA and HRP, catalase significantly reduced the fluorescence, although only by a small amount (7%) for both DW and ASW, consistent with H_2O_2 concentrations of 15 and 16 nM, respectively. Catalase pre-treatment caused a larger decrease in fluorescence in FSW, consistent with an H_2O_2 concentration of 82 nM in this water type. After pre-treatment with catalase the fluorescence found in the presence of HVA and HRP was not significantly different for FSW and ASW.

2.3.3 Detection of hydrogen peroxide using the chemiluminescence (CL) method

The effect of pH on calibration curves for the chemiluminescence method (Section 2.2.3) using H_2O_2 concentrations ranging from 0 to $8.8 \mu\text{M}$ is shown in Figure 2.7A. It can be seen that the sensitivity of the method increases with increasing pH in the range 8-9. The chemical reactions involved in the luminol-dependent chemiluminescence triggered by hydrogen peroxide are complex, but the increase in sensitivity with increasing pH is probably related to an increase in the deprotonation of an endoperoxide intermediate which is critical for the production of chemiluminescence (Fig. 2.1; Yue and Liu, 2020). At higher concentrations, an approximately linear relationship between chemiluminescence and $[\text{H}_2\text{O}_2]$ was observed, and there appeared to be a threshold below which H_2O_2 cannot be detected, which decreased with increasing pH. However, when the same data are plotted as $\log_{10}(\text{RLU})$ versus $[\text{H}_2\text{O}_2]$ (Fig. 2.7B), it is clear that the assay is more sensitive to changes at lower than at higher hydrogen peroxide concentrations.

At a pH of 8, the CL intensity achieves steady state within a few seconds, which is reflective of robust peroxidase activity. Despite this, the sensitivity is limited since the CL efficiency of luminol is low. On the other hand, when the pH is 9.0, sensitivity is high, but peroxidase activity is relatively low (Fig 2.7). It is vital to find a consensus between the ideal pH for highest CL intensity from luminol and the ideal pH for maximal peroxidase activity. The optimal solution is to work at a pH where steady state may be reached in about 30 seconds while maintaining sufficient sensitivity (Khan et al., 2014).

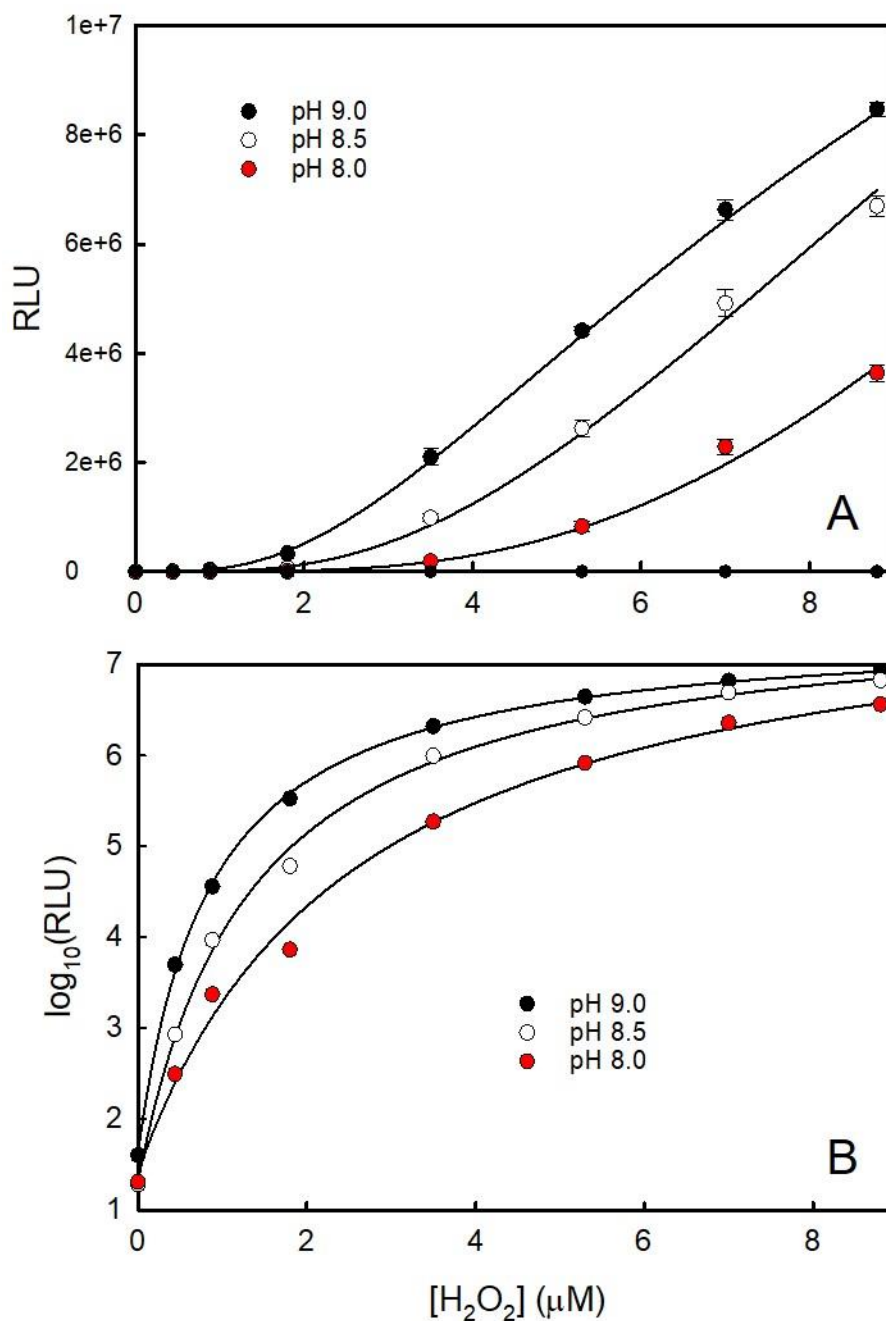


Figure 2.7 (A) the effect of pH on calibration curves produced using the luminol/HRP chemiluminescence method, and (B) the same data plotted as $\log_{10}(RLU)$. The data in B were fitted with rectangular hyperbolas (3 parameters), and these curves were then back-transformed to give the curves in A.

The non-linear relationship between $\log_{10}(RLU)$ and $[H_2O_2]$ is shown in Figure 2.6B. With a linear calibration relationship, it is possible to use a single internal standard (spike), but with a non-linear relationship like that shown in Figure 2.6 at least two internal standards (Spikes 1 and 2) are needed. After subtracting the $\log_{10}(RLU)$ value for the plus catalase control, the $\log_{10}(RLU)$ values for the sample, the sample plus Spike 1 (0.88 M), and the sample plus Spike 2 (2.64 M) can be fitted with a three-parameter

rectangular hyperbola (Equation 3) to determine the $[\text{H}_2\text{O}_2]$ in the sample (the extrapolation method, see Section 2.2.3 and Fig. 2.8A). Figure 2.8B illustrates the relationship between $[\text{H}_2\text{O}_2]$ estimated using this method and $[\text{H}_2\text{O}_2]$ estimated using external standards for a set of six H_2O_2 solutions that were tested blind. There was good agreement between the two methods up to around $1.5 \mu\text{M}$ hydrogen peroxide, but above this, there was increasing disagreement.

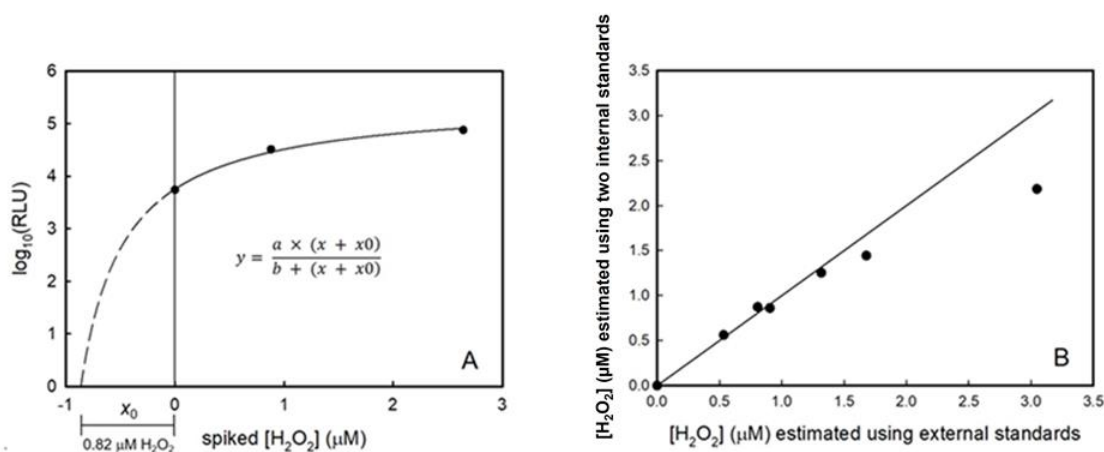


Figure 2.8 (A) an example of the use of two internal standards to determine the concentration of H_2O_2 by the chemiluminescence method. A solution nominally containing unknown $\mu\text{M H}_2\text{O}_2$ was split into four parts, one treated with catalase, one untreated and the remaining two spiked with 0.44 and $1.8 \mu\text{M H}_2\text{O}_2$, respectively, after which chemiluminescence was measured as described in Section 2.2.3. After plotting $\log_{10}(\text{RLU})$ minus the $\log_{10}(\text{RLU})$ for the +catalase control the data were fitted with the 3-parameter equation (rectangular hyperbola) shown, where x_0 is the $[\text{H}_2\text{O}_2]$ already in the sample before spiking. (B) a comparison between the $[\text{H}_2\text{O}_2]$ determined using two internal standards as in A versus the concentration of $[\text{H}_2\text{O}_2]$ determined using external standards as described in Section 2.2.3. Six solutions of H_2O_2 in the range 0 - $3.0 \mu\text{M}$ were prepared and tested blind using the chemiluminescence method.

Figure 2.9 shows the relationship between the concentrations of hydrogen peroxide measured using the FL and CL methods. For the measurements in the laboratory, which encompassed a greater range of concentration of H_2O_2 than those obtained in the field, there was a significant correlation between the two methods (Pearson's $R^2 = 0.966$, $P < 0.00001$). However, the FL method consistently gave lower values compared to the CL method particularly at low concentrations. There was no correlation between the two methods for the measurements carried out in the field, but the H_2O_2 concentrations in the field samples were low and the range was small and despite the lack of correlation they seem to follow the same relationship as that seen between the two methods in the laboratory.

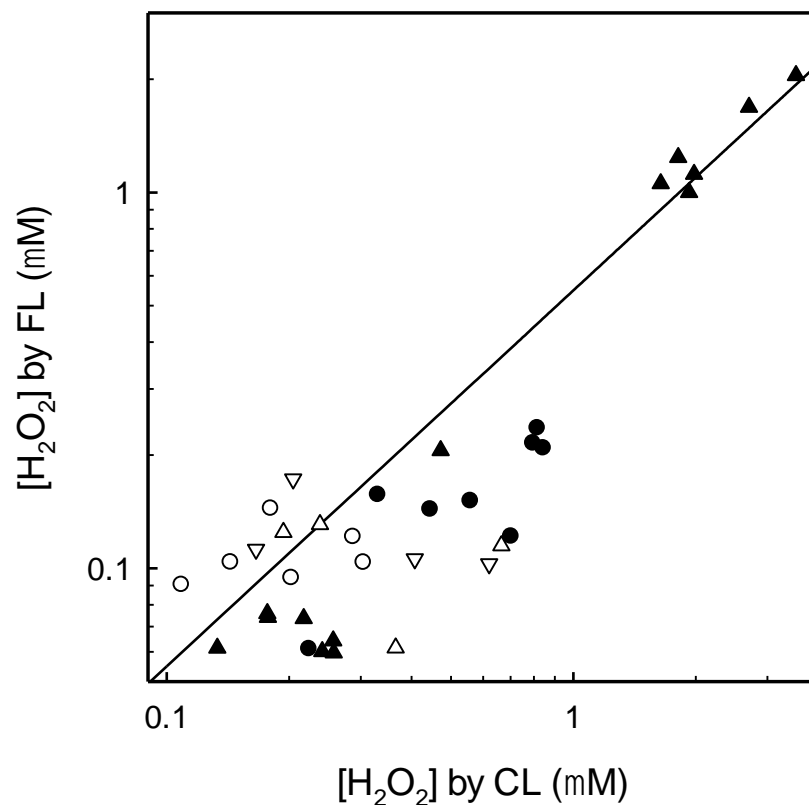


Figure 2.9 The correlation between FL and CL methods that were used in measuring $[\text{H}_2\text{O}_2]$ in the laboratory (filled symbols) and in the field (empty symbols). ●, *Fucus serratus*; ▼, *Ulva lactuca*; ▲, *Chondrus crispus*; ▽, pool with >75% coverage of seaweed; △ pool with about 50% coverage; ○, pool with <10% coverage (Table 2.1, pools 1-12).

2.3.4 The physicochemical parameters and levels of H₂O₂ in rock pools

The physicochemical parameters of seawater in the rock pools generally fluctuated during data collection. For all groups of pools that had different percent cover of seaweed, the mean pH of each pool group increased over time during the low water period, the pools becoming more alkaline. Mean pH increased after emersion between 8.27 ± 0.04 and a value of 9.13 ± 0.03 (means \pm SEM) over four hours. There was significant difference between the three types of pools ($F_{(2,93)} = 8.6$; $P < 0.05$) during 4 h sampling. The LW pools had the lowest pH and there were no significant differences between the MW and HW pools (Fig. 2.10).

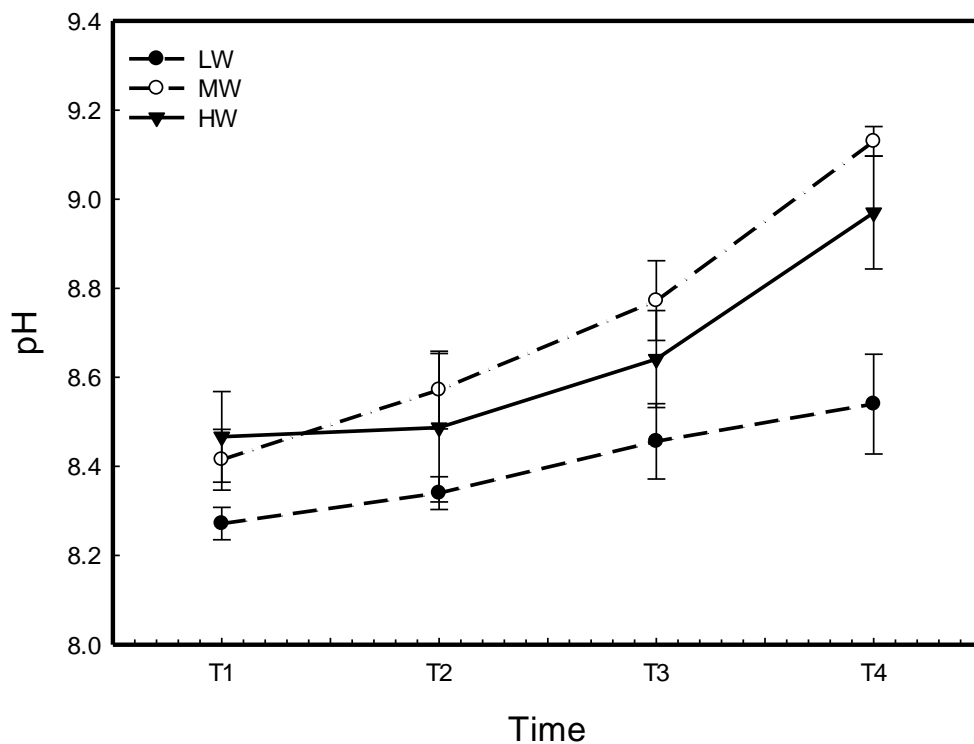


Figure 2.10 Mean values of pH within three rockpool types (LW = Low weediness, MW = Middle weediness and HW = High weediness). See Table 2.1, pools 1-12. Measurements were taken at roughly hourly intervals during emersion at four consecutive times. Error bars indicate \pm SEM, $n = 4$.

Temperature increased during emersion for all pools. Mean (\pm SEM) of the lowest temperature was 17.1 ± 0.1 °C when the first temperature sample collection had been taken and was 22.1 ± 0.7 °C by the end of the data collection period (Fig. 2.11). The temperature for HW rockpools was significantly lower than for other pools. The rockpools where seaweed was low attained the highest mean temperatures during data collection ($F_{(2,93)} = 7.5$; $P < 0.05$).

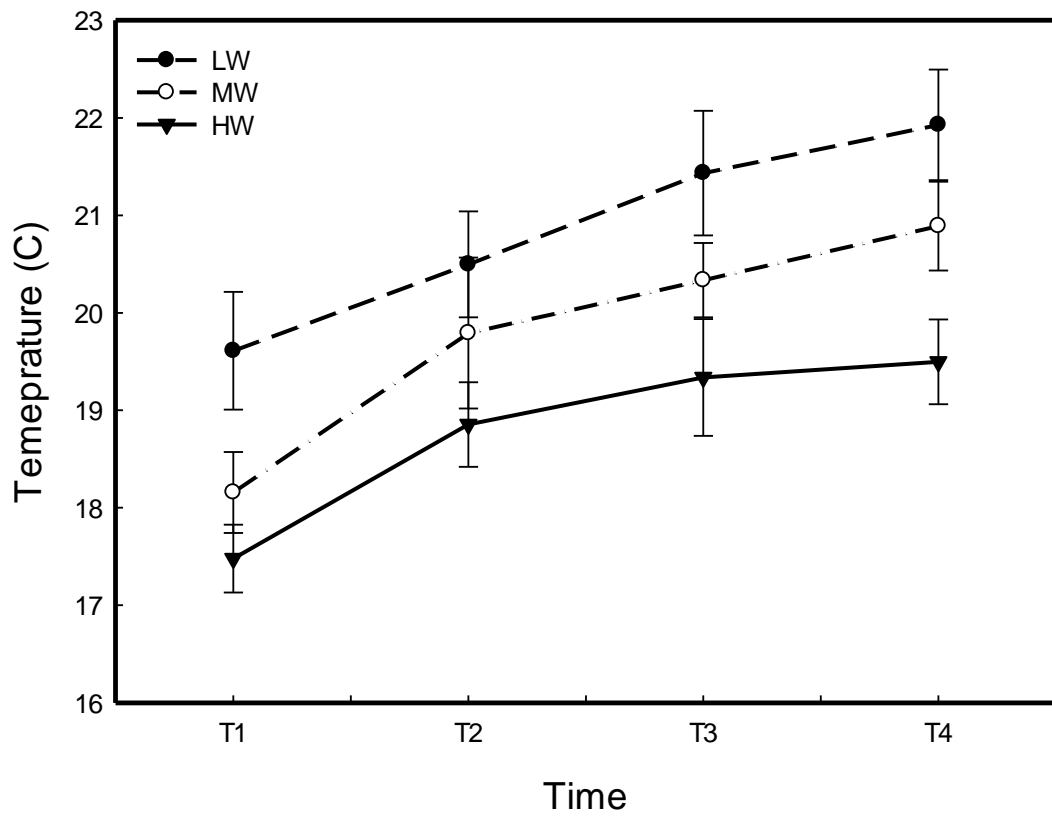


Figure 2.11 Mean temperatures within three rockpool types (LW = Low weediness, MW = Middle weediness and HW = High weediness). See Table 2.1, pools 1-12. Measurements were taken at roughly hourly intervals during emersion at four consecutive times. Error bars indicate \pm SEM, $n = 4$.

Salinity increased following a linear trend over the emersion time from 36.9 ± 0.1 to 37.5 ± 0.1 psu, averaged for all groups (Fig. 2.12). In addition, there was a positive correlation between salinity and temperature (Table 2.2).

Table 2.2 Pearson correlation coefficients for physicochemical parameters, temperature, pH, dissolved oxygen (DO) salinity and H₂O₂ concentration). asterisk: significant correlation coefficient ($P < 0.05$), $n = 109$.

	Temperature	pH	DO	Salinity
pH	0.049			
DO	-0.107	0.362*		
Salinity	0.191*	-0.155	0.110	
H ₂ O ₂	0.004	0.147	0.011	0.040

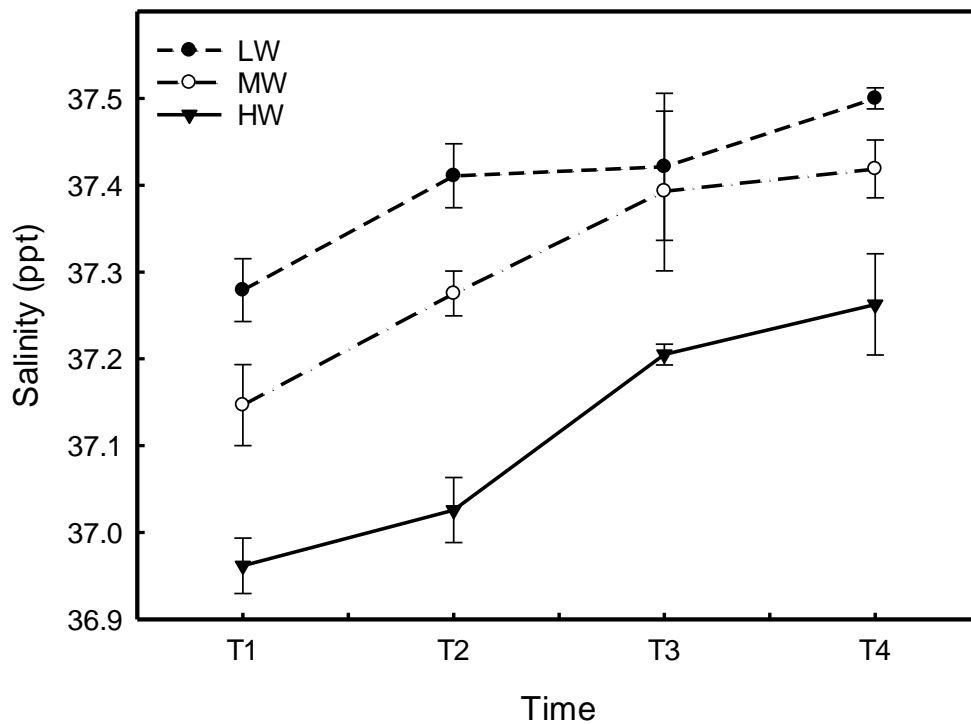


Figure 2.12 Mean salinity within three rockpool types (LW = Low weediness, MW = Middle weediness and HW = High weediness). See Table 2.1, pools 1-12. Measurements were taken at roughly hourly intervals during emersion at four consecutive times. Error bars indicate \pm SEM, $n = 4$.

Dissolved oxygen levels at the end of the four-hour period were greater in pools where seaweed cover was present (MW and HW). There were no significant differences between MW and HW due to the high levels of variability in the data (Fig. 2.12). The concentration and increase in DO in pools with low seaweed cover (LW) were significantly lower than the other pools according to Tukey's HSD ($F_{(2,93)} = 15.7, P < 0.05$). The oxygen level in all pool types remained steady or slightly declined by the end of measurement period. In addition, dissolved oxygen was positively correlated with pH (Table 2.2).

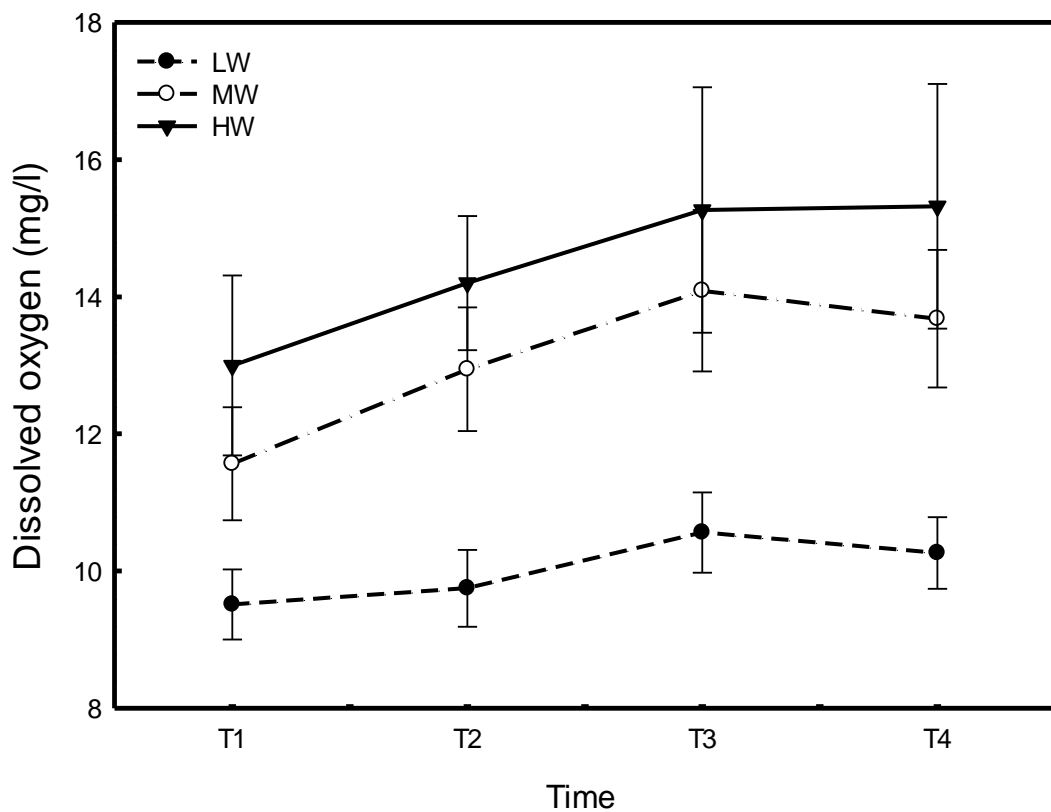


Figure 2.13 Mean dissolved oxygen values within three rockpool types (LW = Low weediness, MW = Middle weediness and HW = High weediness). See Table 2.1, pools 1-12. Measurements were taken at roughly hourly intervals during emersion at four consecutive times. Error bars indicate \pm SEM, $n = 4$.

The concentration of hydrogen peroxide (H_2O_2) found in the observed rockpools varied more than any other physicochemical factor (Fig. 2.14). The peroxide levels in all three groups of rockpools increased rapidly during the first hour, with the HW group showing the most variation. Both pool groups, LW and MW, continued to rise slightly before decreasing sharply, whereas H_2O_2 levels in the HW group fell steadily until the end of data collection. The concentration of H_2O_2 in the pool group types differed significantly between seaweed-containing and non-seaweed-containing pools ($F_{(2,93)} = 53.9$; $P < 0.01$) (Fig. 2.14).

To find out the potential sources of H_2O_2 within the pools, the local concentration of H_2O_2 measured in the middle of macroalgae assemblages against those taken outside. It is worth mentioning that there was a statistically significant difference when means were compared of H_2O_2 concentrations outside and inside the assemblages per hour measurement ($F_{(1,6)} = 6.218$; $P = 0.047$); the inside measurements tended to be higher, particularly during the second and third hour of sampling (Fig. 2.15).

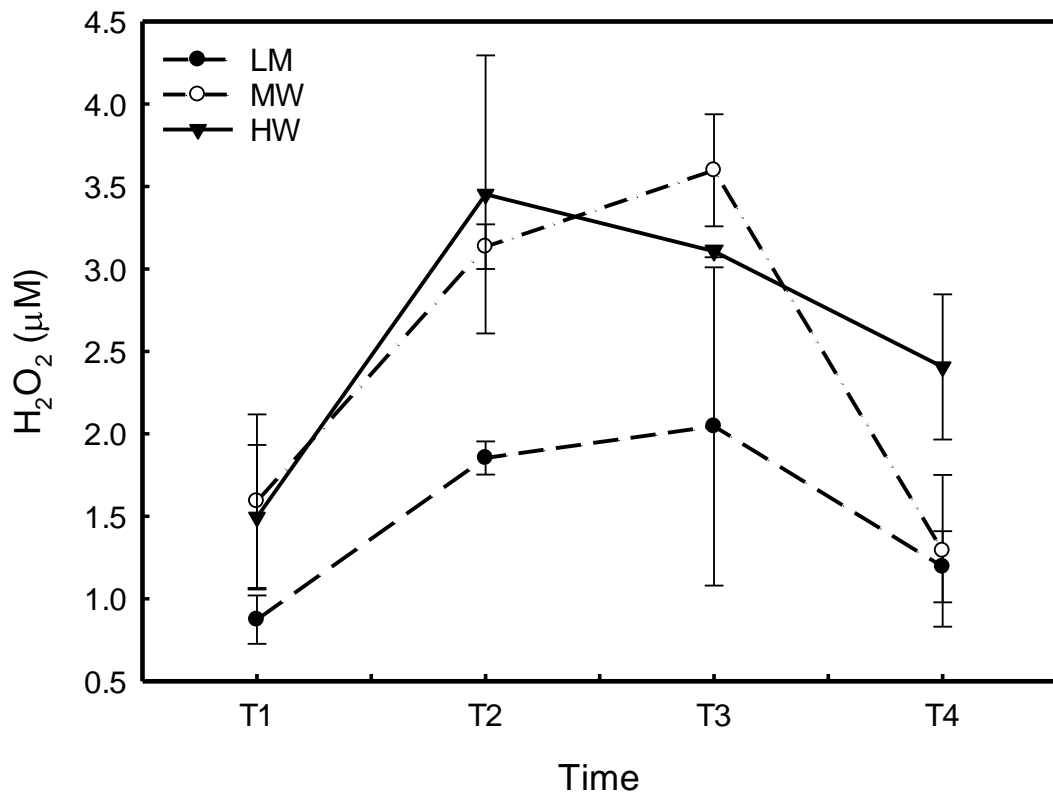


Figure 2.14 Mean levels of H_2O_2 within three rockpool types (LW = Low weediness, MW = Middle weediness and HW = High weediness). See Table 2.1, pools 1-12. Measurements using the CL method were taken at roughly hourly intervals during emersion at four consecutive times. Error bars indicate \pm SEM, $n = 4$.

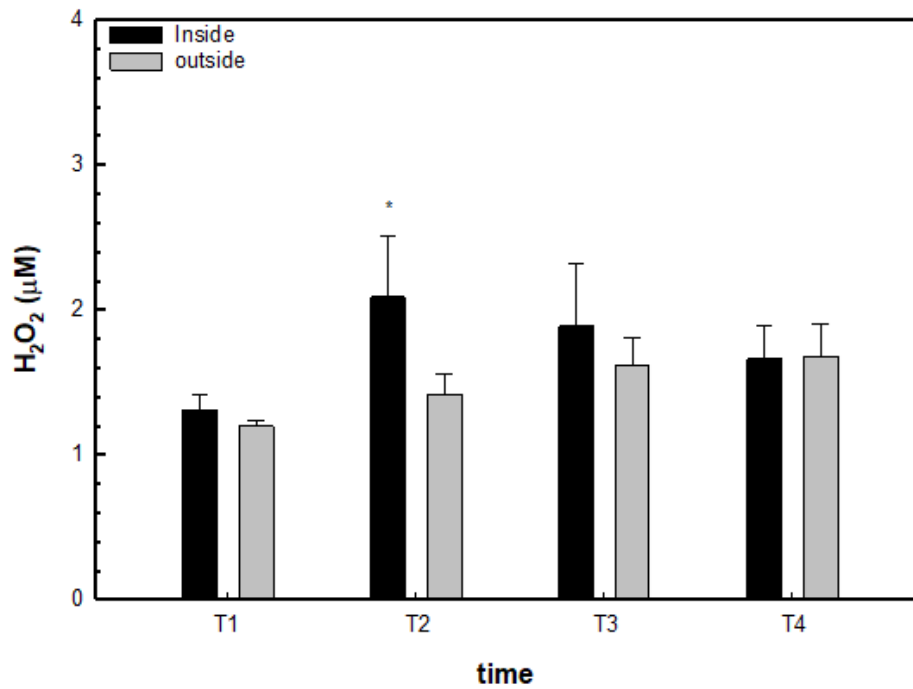


Figure 2.15 Mean levels of H_2O_2 within two adjacent rock pools on Plymouth Hoe (pools 13 and 14 in Table 2.1), sampled from both the middle of the seaweed assemblage and outside the assemblage to look at local concentrations. Triplicate measurements were taken in each pool in and out of the seaweed at roughly hourly intervals during emersion at four consecutive times. Asterisks indicate main significant differences ($P < 0.05$). Error bars indicate \pm SEM, $n = 6$.

2.4 Discussion

2.4.1 Fluorometric and chemiluminescence methods for measuring hydrogen peroxide levels

When H₂O₂ was first found in seawater, van Baalen (1966) predicted that this peroxide could be a significant ecological variable. Since then, many have continued this research and found that H₂O₂ is an important component of natural waters due to its impact on redox chemistry and biological processes. Therefore, to quantify the accurate level of H₂O₂ in seawater using biochemical methods is important.

The fluorescence measurement used in this study is based on the oxidation of homovanillic acid (HVA) into a fluorescent dimer, which is catalysed by horseradish peroxidase (HRP) and depends on the H₂O₂ generated in the seawater. The level of fluorescence detected in this method is close to being directly proportional to the concentration of H₂O₂ (Fig. 2.1) and the λ_{\max} values for excitation and emission were as expected (Staniek and Nohl, 1999). HVA is one of the substrates which offers the best sensitivity and stability in aqueous solutions (Guilbault et al., 1967), but there is a drawback in using it as many sources can produce fluorescence similar to the HVA-HRP reaction mixture contributing to possible misleading results. For example, cytochrome *c* with H₂O₂, Fenton systems and lipoxygenase with H₂O₂ are able to oxidize HVA to its dimer (Foppoli et al., 2000; Gomes et al., 2005). In this study EDTA was added to remove metal such as Fe and Cu from the reaction systems (Foppoli et al., 2000). This HVA-HRP method has been used to estimate H₂O₂ in biological material (Hirsch and Parks, 1982; Baggiolini 1986) but has never been used, as far as I know, in seawater, even though there is a compound, POHPAA (*p*-hydroxyphenylacetic acid) oxidized via a mechanism similar to homovanillic acid that has been used with seawater (Miller and Kaster, 1988).

For all the methods that have been used to evaluate H₂O₂ using the HVA-HRP system, the reaction mixture is incubated for different times up to 2 h and not less than 5 min (Iwai et al., 1983; Paital, 2014; Paździoch-Czochra and Wideńska, 2002; Piotrowski et al., 1996). This might be because of the different concentration of HVA and HRP compared to Paital's (2014) work, because the higher the concentration of HVA and HRP, the faster the rate of oxidation (Hirsch and Parks, 1982; Danielson et al., 2018). Results from the current study found there was a linear relationship between the time taken to reach the end point and the concentration of H₂O₂ (Fig. 2.2). However, even with the

highest concentrations used/encountered here, the time to reach endpoint was short enough (< 1 min) to be convenient in the field, where samples were left to react for 10 min before transfer onto ice packs in the dark in a cool box, after which they were transported back to the lab for the measurement of the fluorescence. Once developed the fluorescence was stable at room temperature for at least 5 h (Fig. 2.3), but ice packs were used as an extra precaution during fieldwork to limit any change in fluorescence after the end point had been reached (Miller and Kester, 1988). It is also important that samples are stored in the dark as under continuous ultraviolet light, HVA oxidation by horseradish peroxidase to produce the fluorescent product (Hirsch and Parks, 1982).

One of the difficulties with measuring H_2O_2 , particularly in water samples from the field, is establishing a reliable blank. This is partly because H_2O_2 may be also be present in the water used to prepare the blank, but also, in the case of the fluorescence method, there may be a component of the fluorescence that is already present and not produced in the HRP-catalysed oxidation of HVA by H_2O_2 (Miller et al., 2005) or other peroxy species such as organic peroxides in coastal waters that can be measured by the HRP method (Burns et al., 2012). These problems can be resolved by using samples to which catalase has been added, in order to determine reagent and H_2O_2 -free blanks in the same seawater for which the analysis is to be done without significant loss of other hydroperoxides (Miller and Kester, 1988). Use of internal standards (spiking) is also important as it gives an indication of the change in the matrix of the original sample. Thus, any fluorescence absorbance which is not eliminated by catalase is not due to H_2O_2 .

Chemiluminescence-based detection is widely used in a wide range of applications, including safety assessment, clinical diagnosis, and environmental monitoring, due to its high sensitivity, wide linear range, and low cost (Khan et al., 2014). Through chemiluminescence (CL), the luminol-peroxidase reaction, which is catalysed by peroxidases, can be utilized to detect peroxides and other reactive oxygen species (Diaz et al., 1996; Nakamura and Nakamura, 1998).

In the results presented here, the effect of pH on calibration curves using H_2O_2 concentrations ranging from 0 to $8.8 \mu\text{M}$ has a significant impact on the level of CL (Fig. 2.6A). First impressions are that the sensitivity of the method increases with increasing pH in the range 8-9 and that there is a threshold below which H_2O_2 is not detected, which decreases with increasing pH. Above this apparent threshold, there is an approximately linear relationship between chemiluminescence and $[\text{H}_2\text{O}_2]$. However, these first impressions are misleading, and if the same data are plotted as $\log_{10}(\text{RLU})$ against $[\text{H}_2\text{O}_2]$

(Fig. 2.6B) then it is apparent that the assay is much more sensitive to changes in $[\text{H}_2\text{O}_2]$ below the apparent threshold than it is above. It is also apparent that the calibrations plotted as $\log_{10}(\text{RLU})$ against $[\text{H}_2\text{O}_2]$ can be fitted with rectangular hyperbolic curves (3 parameter; $y = y_0 + (a \times x) / (b + x)$, the equations for which can be rearranged to give $[\text{H}_2\text{O}_2]$ in terms of $\log_{10}(\text{RLU})$, $x = ((y - y_0) \times b / (a - (y - y_0)))$). While calibration using a series of external standards is applicable in a laboratory setting, using water with defined purity (e.g., distilled water or artificial seawater), in field samples, where the luminescence may be affected by materials present in the water, it is appropriate to use an internal standard, to spike with at least two standards in order to have closeness of agreement between the average value obtained from test results and an accepted reference value.

There was good correlation between two estimates of hydrogen peroxide concentration obtained using the CL method, in one case using two internal standards and in the other external standards, but as would be expected, as the concentration increased there was more discrepancy. This was because the two spikes were further along the hyperbolic curve where the gradient was less steep and therefore the extrapolation was less reliable. The reason for the discrepancy between the measurements using the two methods is not known. In both methods internal standards were used and in principle at least this should have compensated for any potential quenching effects of contaminants in the seawater on either fluorescence or luminescence. As noted above, the FL method suffers from having a high reagent blank reading, whereas the CL method has a reagent blank reading that is orders of magnitude smaller than readings obtained with concentrations of H_2O_2 in the low micromolar range. Error in the measurement of the fluorescence intensity for the reagent blank in the FL method could lead to underestimation of H_2O_2 particularly at low concentrations but would not account for the slope of the linear regression in Figure 2.8 being substantially less than 1.

The CL method clearly has greater sensitivity than the FL method. The luminol-dependent chemiluminescence could potentially be increased by adding an enhancer such as the phenol derivatives, *p*-iodophenol and *p*-phenylphenol (Thorpe et al., 1985), but this was not necessary since the sensitivity is more than enough for the measurement of low micromolar concentrations of H_2O_2 . A disadvantage of the CL method compared to the FL method is that the light input in the CL method rapidly declines and hence the timing of the measurement after mixing the sample with the reagent is critical.

2.4.2 Studies on hydrogen peroxide levels in the field

A rockpool's ecology is determined by a complex interplay of physical, chemical, and biological components (Martins et al., 2007). The findings demonstrated the impact of seaweed cover on physicochemical parameters that have some reciprocal relationships (association of organisms and their environment) in Wembury rockpools. During low tide, oxygen levels gradually increased in all the pools. However, this had a greater impact in pools with seaweed cover. This is explained by an increase in algal abundance, which leads to an increase in photosynthetic activity. Huggett and Griffiths (1986) found that dissolved oxygen production increased with algal abundance and diversity as shore height increased in control pools in South Africa. The asymptotic increase in oxygen showed a decrease in photosynthetic activity at the end of the emerged period, which Morris and Taylor (1983) also observed. This could be due to limiting factors such as a decrease in light intensity towards the end of the day or it could be because the rate of production equals the rate of loss to the atmosphere over time.

In the current study, changes in pH, temperature, and salinity over the low water period were also recorded. Each organism respire, increasing CO₂ levels and decreasing pH. Primary producers, on the other hand, lower CO₂ levels and increase pH; an alkaline pH reflects high rates of photosynthesis. Higher pH was caused by increased algal biomass photosynthesis, which corresponded to higher oxygen production in these pools (Table 2.1). The pH range was narrower in LW pools. This is consistent with previous research findings (Morris and Taylor, 1983; Huggett and Griffiths, 1986). Temperature was affected by environmental and biotic factors in the current study. The most important factors in determining the temperature reached by a fixed-size rockpool are the period of exposure and the rate of heat input. Previous research has shown that air temperature and light intensity increase rockpool temperatures in relation to the area in contact with the air (Ambler and Chapman, 1950; Femino and Mathieson, 1980; Martins et al., 2007). Furthermore, greater algal biomass resulted in a lower temperature increase, as suggested by Ambler and Chapman (1950), who found that canopy cover reduced light irradiance and water mixing. A reduction on water circulation would confine an increase in pool temperature to the surface, so there would be a lower increase in temperature deeper in the pool. Although the increase in salinity showed a significant correlation with temperature during the low water period this did not differ significantly between type of pools, a lower range appeared in pools with a high presence of macroalgae.

The range of H₂O₂ concentrations recorded in the rock pools in Wembury (0.73-4.27 µM) is very similar to concentrations reported in other study sites. In the Wadden sand flats in

Germany, for example, H₂O₂ levels ranged between 1 and 4.5 μM in the summer and stayed below 0.5 μM in the winter (Abele-Oeschger et al., 1997). The concentrations of hydrogen peroxide in rock pools in this study did not show a significant correlation with other parameters, but they may contribute to its production. For example, Abele-Oeschger et al. (1997) found that in oxygenated tidepools H₂O₂ photoproduction outpaces biological and chemical decomposition, resulting in a net accumulation of micromolar H₂O₂ concentrations.

Rockpools had a higher H₂O₂ concentration when compared to the other part of the ocean, which was in nanomolar concentration (Price et al., 1998; Geringga et al., 2004). According to some researchers, H₂O₂ can be produced by photochemical reactions as well as biota, with humic or dissolved organic matter thought to be the primary source (Cooper and Zika, 1983; Palenik and Morel, 1988; Moore et al., 1993; Hanson et al., 2001). Rainwater can carry H₂O₂ into the marine environment (Kieber et al., 2001; Miller and Kester, 1994). Even when only exposed to sunlight, water samples from natural surface and ground waters showed a rapid increase in H₂O₂ concentration (Cooper and Zika, 1983). Those H₂O₂ generations are applied to seawater, but in intertidal pools, the water is stagnant for hours, so on sunny days it receives intense solar radiation, which leads to an increase in water temperatures and may also enhance peroxide accumulation. The results show in this chapter that the highest concentrations of H₂O₂ were found in pools with a high percentage of macroalgae (Fig. 2.14). This could be due to algae photosynthesis or photorespiration. According to Johanson et al. (1989) algal photorespiration under light conditions results in intracellular hydrogen peroxide production, which can directly 'leak' into the water column. This report supported the current study's findings that there are higher H₂O₂ levels in the middle of macroalgae than outside (Fig. 2.15). Furthermore, Moffett and Zika (1987) reported that the presence of biogenic compounds as photosensitizers caused the production of H₂O₂ in seawater. More research, however, is required to reach more conclusive conclusions.

In summary, this study highlighted the use of CL and FL methods in the measurement of H₂O₂ in rockpools and a reciprocal relationship between biotic and abiotic parameters and the physicochemical rockpool environment. Higher algal cover may have resulted in an increase in rockpool H₂O₂ levels because of endogenous leaking of hydrogen peroxide into the seawater medium. In addition, generation of oxygen via photosynthesis may also have resulted in exogenous production of hydrogen peroxide due to higher dissolved oxygen which leading to higher conversion into hydrogen peroxide through photolysis

via dissolved pigments that are referred to as chromophoric dissolved organic matter (CDOM) (O'Sullivan et al. 2005; Johnson et al. 1989). By examining levels of H₂O₂ produced by macroalgae under controlled condition in the laboratory, the work described in Chapter 3 may help to distinguish between these possibilities.

Chapter 3
Production of hydrogen peroxide and physiological responses
to environmental factors by three different macroalgae

3.1 Introduction

Responses to environment perturbation in metabolic processes by plants and algae usually induces formation of reactive oxygen species (ROS). Metabolic processes carried out by chloroplasts, are used to drive electron transport leading to the production of molecular oxygen released as a by-product via oxidation of water at the charge separation site in photosystem II (PSII). As a result, this has allowed oxygen-requiring organisms to survive on the planet but electron transfer from water to produce oxygen is a double-edged sword. Oxygen as such is not particularly reactive but it can potentially be toxic as it can be partially reduced leading to the formation of reactive oxygen species (Halliwell and Gutteridge, 2007).

Macroalgae are distributed in groups parallel along the rocky intertidal zone, where relative abundance along the lower limits is mainly controlled by considerable diurnal changes (Smith and Berry, 1986). They are subjected to various abiotic stressors, including exposure to high solar radiation, changes in temperature and salinity (Davison and Pearson, 1996). Under these conditions, the physiological performance of intertidal macroalgae is influenced significantly by exposure-related stresses and there is a tendency for absorbed light energy to be poorly utilised or exceed levels where the photosynthesis machinery can cope (Murata et al., 2007). This requires the ability of algae to adapt by acclimation to both short- and long-term exposure. Since the light is the primary energy for driving photosynthesis and the light intensity varies from moment to moment, as well as other environmental factors, algae may suffer from photoinhibition which is the condition where excessive photon inhibits the activity of photosystem II (PSII) and disrupts CO₂ fixation (Asada, 2000; Murata et al., 2007). This excess photon energy leads to production of reactive oxygen species (ROS; e.g., H₂O₂) also known as photoproduction of ROS (Asada, 2006; Mano et al., 2016).

Excess photo-excitation energy on the electron acceptor side of PSI can reduce O₂, generating ROS such as superoxide anion radical (O₂^{•-}), hydrogen peroxide (H₂O₂), and hydroxyl radical (•OH) (Mehler, 1951; Asada, 2006; Rutherford et al., 2012). The Mehler reaction generates hydrogen peroxide (H₂O₂) when the light-dependent creation of superoxide radicals (O₂^{•-}) in photosystem I (PSI) is disproportionate to the formation of H₂O₂ spontaneously or via superoxide dismutase (SOD) (Bielski and Allen, 1977; Asada 2006; Krieger-Liszkay et al. 2008). Photorespiration is a process in which O₂ is used as a substrate rather than CO₂ by RubisCO. The process begins in the chloroplasts. As a consequence, glycolate is produced which is dealt with via peroxisomes in combination

with mitochondria. The peroxisomes are responsible for the formation of hydrogen peroxide during the conversion of glycolate to glyoxylate. In PSII, H_2O_2 can also be produced on the electron donor side when exposed to various conditions (Krieger-Liszkay et al. 2008; Pospisil, 2009) that can increase the production. Once formed, like the other forms of active oxygen, H_2O_2 can directly or indirectly cause damage at the site where it is produced (photoinhibition) or H_2O_2 can also diffuse and lead to the formation of the very reactive hydroxyl radical ($\cdot\text{OH}$), which will make substantial damage to organisms by destruction of lipids, proteins and nucleic acids (Asada 2000, Krieger-Liszkay 2005). H_2O_2 also can be produced non-photosynthetically in mitochondria when there is incomplete reduction of oxygen and oxidation reaction that can generate superoxide anion ($\text{O}_2\cdot^-$) and H_2O_2 (Fridovich, 1986).

Since the environmental stresses that depress photosynthetic efficiency can lead to increased ROS (H_2O_2) (Zhu 2001; Mahajan and Tuteja 2005; Vinocur and Altman 2005, Song et al., 2006), measuring chlorophyll *a* concentrations in plants and algae is one of the most widely used ecophysiological techniques for studying the photosynthetic process in these organisms (Murchie and Lawson, 2013), and can be used to gain more information about changes in the photochemistry efficiency of the photosynthetic apparatus (Kalaji et al., 2014, 2017; Guo and Tan, 2015; Ruban, 2016; Stirbet et al., 2018). Chlorophyll fluorescence represents only a small fraction of the absorbed light energy, but it can provide useful information about the function of PSII, and also indirectly about other aspects of photosynthesis such as the efficiency of energy trapping and electron transfer as well as the number of reaction centres per amount of absorbed energy, into a single number (Strasser et al., 2000).

Light energy absorbed by accessory pigments (e.g., chlorophyll *a*; Chl *a*) during photosynthesis in plants is either trapped by the photosystems and converted into a chemically useful form or dissipated as heat or through light re-emission (Chl *a* fluorescence). Ultrafast spectroscopy has revealed the beginning of the electron transfer in PSII (Brudvig, 2008; Govindjee and Seibert, 2010). When enough light is applied to drive photosynthesis, the light quanta are absorbed by antenna complexes, forming excited states of the pigments. The excitation energy trapped in the reaction centre by the primary electron donor P_{680} in the picosecond time scale before primary charge separation occurred. In 3-20 ps, the singlet excited state of P_{680} expel an electron to the primary acceptor pheophytin (Pheo). On the acceptor side, the separated charges from the radical pair $\text{P}_{680}^+ \text{Pheo}^-$ are then stabilized by electron transfer to Q_A (a bound quinone) in 200

ps. The reaction centre is considered 'closed' in this state because Q_A is unable to accept another electron from P680 until it has passed its electron to the next carrier, Q_B . This state causes a decrease in photochemistry efficiency and an increase in Chl *a* fluorescence (Maxwell and Johnson, 2000), which provides information on changes in photochemistry efficiency and dissipation as heat or light (Chl *a*) because these three processes are linked. The electron transport continues in the hundreds of milliseconds time scale from Q_A to Q_B . Following that, an electron is supplied to reduce P_{680}^+ from water via a tyrosine residue (Y_Z) and Mn_4Ca cluster involving oxygen evolution cycle (an S-state) on the donor side to ensure the process's continuation. This process takes ns-ms to complete (Baker and Rosenqvist, 2004; Brudvig, 2008; Govindjee and Seibert, 2010; Rappaport and Diner, 2008; Renger and Holzwarth, 2005; Strasser et al., 2004; Tommos and Babcock, 2000).

As noted in Chapter 1 there is some knowledge of the levels of H_2O_2 in natural waters, but not specifically in rockpools. The work described in Chapter 2 has provided some information on this as well as on how abiotic factors in rock pools may change over a period of emersion. There have been limited studies in the past under controlled conditions in the laboratory in which H_2O_2 production by macroalgae has been investigated, notably the work of Collén and colleagues but this work was limited to a single species of green alga, *Ulva rigida* (Collén et al., 1995; Collén and Pedersén, 1996), and a few furoid species (brown algae), *Fucus spiralis*, *F. evanescens* and *F. distichus* (Collén and Davison, 1999b). The work described in the present chapter aimed to extend the work of Collén et al. to investigate the short time scale (4 h) production of H_2O_2 from macroalgae under controlled conditions but looking at a further range of macroalgal species, including a red alga, and using a greater range of abiotic stressors. The three species investigated were *Chondrus crispus* as representative of the red algae; *Ulva lactuca* belonging to the green algae; and *Fucus serratus*, within the brown algae that are commonly found in the intertidal and in rockpools. Also, the physiological responses of the photosynthetic apparatus resulting from exposure to general environmental stressors found in the intertidal namely light intensity, temperature, pH and salinity, were measured by evaluating different fluorescence parameters as possible indicators for photoinhibition.

3.2 Materials and Methods

3.2.1 Plant material and sample preparation

Three different species of macroalga (*Chondrus crispus*, *Ulva lactuca* and *Fucus serratus*) were collected at low tide from the rocky shore on the Hoe intertidal area of Plymouth (50.3639° N, 4.1492° W), two weeks after full moon to avoid the reproductive cycle. All samples were transported in clear, zip-lock polyethylene bags to the laboratory where they were subsequently cleaned of particulate matter and epibionts under running filtered sea water. Macroalgae were then maintained in an acid-cleaned (10 percent HNO₃ for 24 hours) 10 l polycarbonate tank with filtered natural seawater in a controlled room environment at 15 °C at Plymouth University. When the sample appeared poor or stressed, the seawater was supplemented with Provasoli media for 1-2 days (Saez et al., 2015). Light was provided by cool white fluorescence tubes (Philips) with a light intensity of 25 $\mu\text{mol photon m}^{-2} \text{s}^{-1}$ photosynthetically active radiation (PAR) on a 12:12 h light:dark cycle. The tank was also bubbled with an aerator. The algae were maintained in the laboratory for 4-7 days, to allow recovery from the stress that occurred during the day of collection. Later, samples of macroalgae from this maintenance culture were used as controls. Prior to the exposures, macroalgae were cut into smaller working samples. Vegetative apices of *F. serratus* (without air bladders) used in experiments had fresh weights (FW) between 0.1 and 0.2 g. For *U. lactuca*, the sharpened end of a 20 mm diameter stainless steel cylinder was used to cut discs from the central portions of the thalli (25-30 mg FW) and branch tips with weights 100-200 mg of *C. crispus* were cut using a stainless-steel scalpel. These samples for exposure were acclimated for at least 24 h in new aquaria under the maintenance conditions before use to reduce the effects of wounding responses (Collén and Pedersen, 1996; Collén and Davison, 1999). These cultures were used for both the control and treatment samples. All samples were used within 5 to 14 days of collection prior to the treatments.

3.2.2 Measurement of hydrogen peroxide levels in response to exposure of macroalgae to various environmental conditions

Hydrogen peroxide in seawater medium was measured for each macroalga using either the luminol-dependent chemiluminescence or fluorescence methods described in Chapter 2 (Sections 2.2.3). The fluorescence method, however, was only employed as a reference when the H₂O₂ level in the sample was high. Most of the measurements were made using chemiluminescence (Section 2.2.3) using external standards. Hydrogen peroxide levels were determined under a variety of modified environmental conditions, ranging from the

smallest to the largest values commonly found in the field. The experiments on hydrogen peroxide (H₂O₂) production were performed with 0.40 g of macroalgae discs and branch tips immersed in 40 ml seawater. Physicochemical conditions found in the rock pools were tested into the experiment of production of H₂O₂. Different pH values were set using unbuffered seawater. Adjustment of the determined pH was made using 0.5 M HCl and 1 M NaOH. There were three different pHs (7, 8 and 9); three salinities (15, 32 and 48 psu) in which, distilled water and artificial salt (Instant Ocean®) were used to adjust tested salinity levels; four temperatures (15, 20, 25 and 30 °C); and three light intensities (50, 100 and 200 $\mu\text{mol photon m}^{-2} \text{ s}^{-1}$). Water temperature was not controlled using heaters but raised gradually following the air temperature in the chamber. Light intensity was measured using a light meter (LI-250A; LI-COR Biosciences, Lincoln, NE, USA). All exposures were carried out in a controlled environment chamber (Sanyo, MLR 350T) that was equipped with cool white, fluorescent tubes. These chambers had maximum light intensity of 200 $\mu\text{mol photon m}^{-2} \text{ s}^{-1}$ and maximum air temperature as high as 30 °C.

For the desiccation treatments, thallus samples were exposed to the air for four hours in the same chamber as the normal sample treatment. Temperature and light intensity of the chamber were set to maximum levels, 30 °C and 200 $\mu\text{mol photon m}^{-2} \text{ s}^{-1}$, respectively, while for the control, which consisted of thallus immersed in seawater as above, the pH and salinity were 8 and 32 psu, respectively. The samples were then immediately rehydrated as above, and H₂O₂ levels were measured after 15 min of rehydration. *Fucus serratus* and *Ulva lactuca* were chosen for the desiccation experiment because these macroalgae are frequently completely or partially desiccated at low tide, the former during most tide cycles and the latter occasionally after evaporation of pools on the upper shore.

3.2.3 Chlorophyll fluorescence measurements

Chlorophyll fluorescence measurements of exposed algae were made using a pocket PEA meter (Hansatech Ltd., England). Prior to measurements of maximal quantum yield (F_v/F_m) of PSII photochemistry, macroalgal samples were placed in series of Hansatech Pocket PEA leaf clips with closed shutter plates for dark-adaptation for 30 min to induce an equilibrium state of photosynthetic electron transport, and to ensure all reaction centres were open (Thiele & Krause, 1994; Krause et al., 1984). After the adaptation to the dark, leaf clips were then placed individually on the Hansatech Pocket PEA chlorophyll fluorimeter and the algal samples were exposed to a single high intensity beam of excitation light (up to 3500 $\mu\text{mol photon m}^{-2} \text{ s}^{-1}$ with a peak wavelength of 627 nm) provided by a single light-emitting diode (LED), positioned vertically above the sample

and recorded for 1 s with 12-bit resolution. Fluorescence origin (F_0) and maximum fluorescence yield (F_m), respectively, were measured, and results expressed as the effective quantum yield of PS II and in terms of the ratio of variable to maximum chlorophyll fluorescence ($F_v/F_m = [F_m - F_0]/F_m$).

For chlorophyll *a* fluorescence, the Pocket PEA fluorimeter was set to the following program: the initial fluorescence was at O (50 μ s); J (2 ms) and I (30 ms) were intermediates; and P (500 ms-s) was the peak (see Fig. 3.1). Data procurement was set at every 10 μ s from 10 to 300 μ s; every 0.1 ms from 300 to 3 ms; every 1 ms from 3 to 30 ms; every 10 ms (from 30 to 300 ms); and every 100 ms (from 300 ms to 1 s) and downloaded to a PC through a Bluetooth wireless connection. To gather information from the O-J-I-P transients normalizations and computations were performed using the SigmaPlot (ver. 13). The O-J-I-P transients were analysed according to the equations of the JIP-test (Strasser et al., 2004).

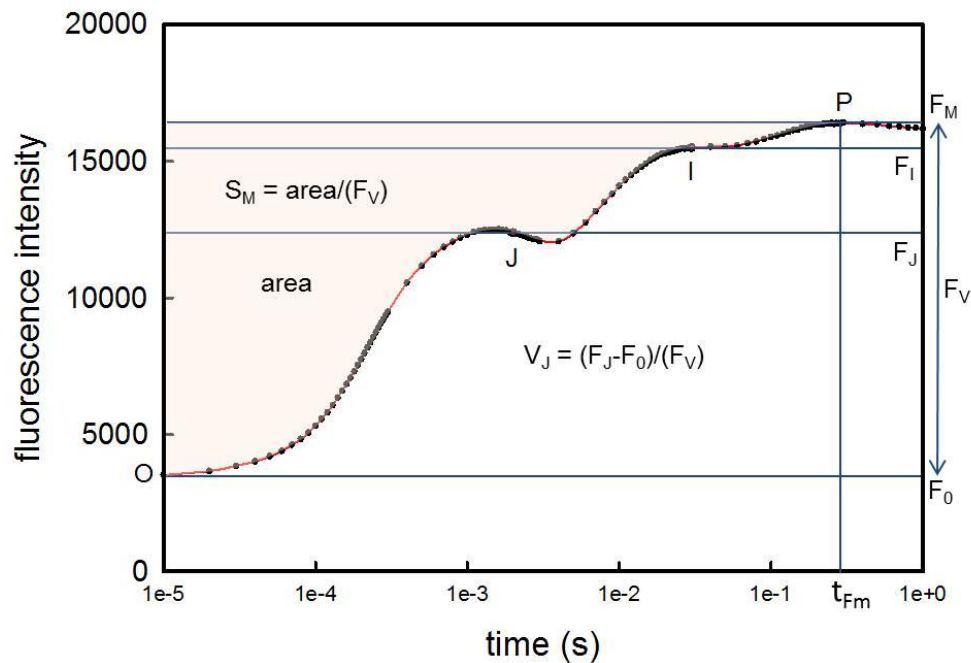


Figure 3.1 Example of changes in the fluorescence of chlorophyll *a* overtime (Moody, A. J., personal communication).

The initial slope at the beginning of the relative variable fluorescence transients (dV/dt_0):

$$\frac{dV}{dt_0} = \frac{F_{300} - F_0}{F_m - F_0}$$

The relative variable fluorescence in the step J (V_J):

$$VJ = \frac{F_J - F_0}{F_m - F_0}$$

The maximum quantum yield of primary photochemistry (ωP_0):

$$\omega P_0 = 1 - \frac{F_0}{F_m}$$

The quantum yield of electron transport (ωE_0):

$$\omega E_0 = \left[1 - \left(\frac{F_0}{F_m}\right)\right] - (1 - VJ)$$

Proportion of energy trapped via photochemistry leading to electron transfer – ETC* relative to PSII function (ψ_0):

$$\psi_0 = 1 - VJ$$

The total number of active reaction centre per absorption (RC/ABS):

$$\frac{RC}{ABS} = \frac{1 - (F_0/F_m)}{M_0/VJ}$$

The amount of active PSII reaction centres per excited cross (RC/CS):

$$\frac{RC}{CS} = F_m \omega P_0 \frac{VJ}{M_0}$$

Proportional to absorbed energy per reaction centre (ABS/RC):

$$\frac{ABS}{RC} = M_0 \times \frac{1}{VJ} \times \frac{1}{\omega P_0}$$

Maximal trapping rate of PSII, the maximal rate by which an excitation is trapped by the RC (TR_0/RC):

$$\frac{TR_0}{RC} = M_0 \times \frac{1}{VJ}$$

Proportional to electron transport per active RC, reaction centre (ET_o/RC):

$$\frac{ET_o}{RC} = M_o \times \frac{1}{VJ} \times \Psi_o$$

Proportional to dissipated energy per reaction centre (DI_o/RC):

$$\frac{DI_o}{RC} = \frac{ABS}{RC} - \frac{TR_o}{RC}$$

where F_o is the original fluorescence, F_J the fluorescence intensity at the phase J, F_m the maximal fluorescence, and M_o = TR_o/RC - ET_o/RC

3.2.4 Statistical analyses

All statistical analyses were carried out using SPSS (IBM SPSS Statistics for Windows, Version 26.0., Armonk, NY: IBM Corp). General linear model (GLM) analysis of variance (ANOVA) was used to compare responses of the three species to the abiotic factors. A post hoc Tukey Multiple Comparison procedure, with P ≤ 0.05, was used to identify significant differences between individual means. If significant interaction was observed, Tukey's test was performed in order to identify the treatments that contributed to this interaction. Shapiro-Wilk and Levene's tests were used on datasets to assess the normality and homogeneity of variance, respectively. When assumptions of normality or homogeneous variance were not met, data were transformed using the square root function.

3.3 Results

3.3.1 Levels of extracellular H₂O₂ produced by macroalgae

The concentration of H₂O₂ in the seawater seen in Fig. 3.2 had slightly different time courses for each species. As shown in the graph, when the concentration of hydrogen peroxide in seawater was increased over time by three different macroalgae, the concentration reached a steady state level within four hours.

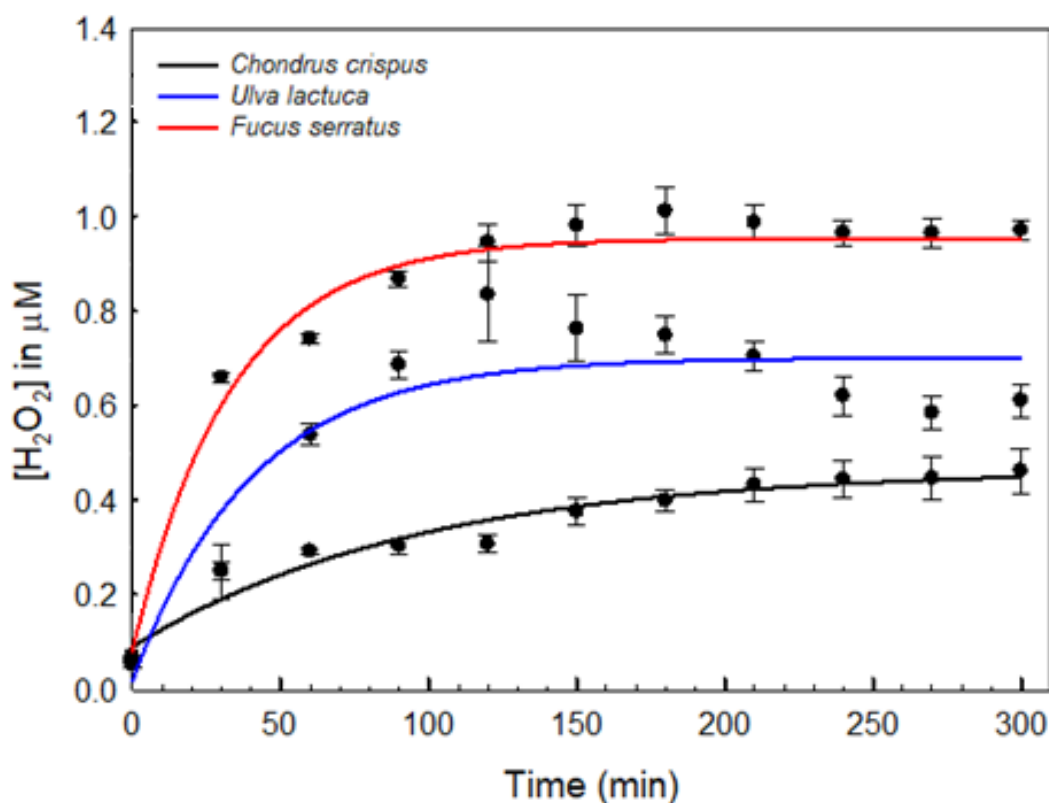


Figure 3.2 Time courses of H₂O₂ excretion from *F. serratus*, *U. lactuca* and *C. crispus* under a photon irradiance of 50 μmol photon m⁻² s⁻¹ at 20 °C. Fresh macroalgal samples (0.4 g) were incubated in 40 ml filtered seawater. H₂O₂ concentrations were measured using the CL method (Section 2.2.3) with external standards. Rectangular hyperbolas (3 parameters) were used to fit the H₂O₂ data. Means ± standard error are shown ($n = 3$).

There was a rapid increase in level of H₂O₂ for *F. serratus* in the first 30 min with steady state levels being reached in about 2 h. *U. lactuca* similarly led to an increase in H₂O₂ over 2 h but then the concentration decreased thereafter to reaching a stable level by 4 h. In contrast, *C. crispus* has two phases of increase which is from the first hour, stable and raised to steady level of 0.4 μM. Overall, after 4 h treatment the level of H₂O₂ did reach a steady state level.

3.3.2 Effects of abiotic stressors on H₂O₂ steady state levels produced by macroalgae

3.3.2.1 pH

After incubation for 4 h, hydrogen peroxide levels for all species of macroalgae were significantly different in response to pH, $F_{(2,18)} = 67.816$, $P < 0.001$ (Fig. 3.3). The results show that the steady state concentration increased with increasing pH. However, there was no significant different level of H₂O₂ between *F. serratus* and *U. lactuca* at pH 7 which was on level $2.8 \pm 0.08 \mu\text{M}$ (mean \pm S.E.M.). With one-way ANOVA, it was found that there are no significant differences in levels for the seawater control and the levels of hydrogen peroxide in the presence of the macroalgae were much higher than in the control seawater. A significant interaction was observed between pH and ‘macroalgal species’, $F_{(4,18)} = 13.568$, $P < 0.001$; this reflects the difference in behaviour between the seawater alone and seawater plus macroalgae. For *U. lactuca* and *F. serratus*, at pH 8 and pH 9 levels of hydrogen peroxide are significantly different to pH 7, ($F_{(2,6)} = 8.425$, $P = 0.01$) and ($F_{(2,6)} = 81.632$, $P < 0.001$), while only at pH 9 were levels significantly different for *C. crispus* ($F_{(2,6)} = 16.802$, $P = 0.003$).

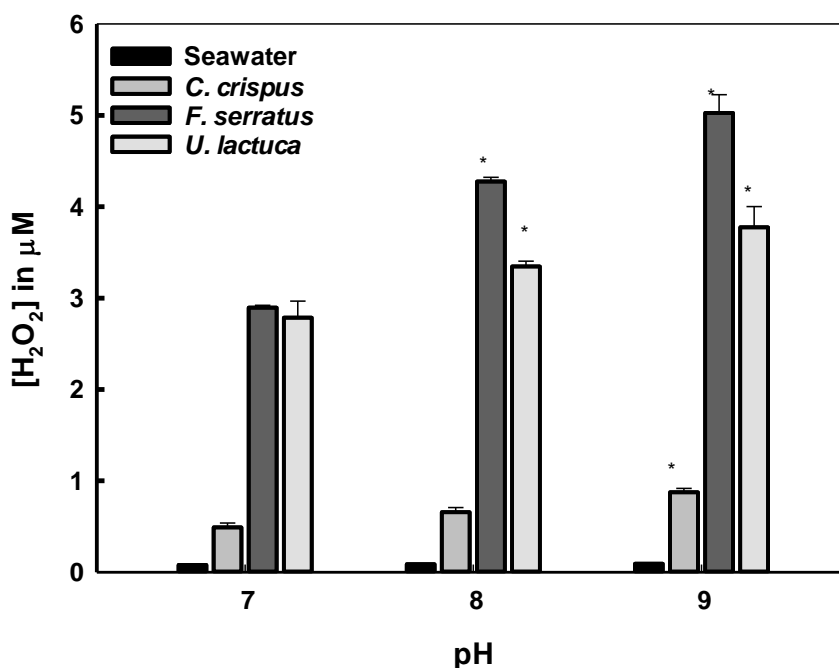


Figure 3.3 The effects of pH on the level H₂O₂ in seawater after *F. serratus*, *U. lactuca* and *C. crispus* samples were exposed in seawater to a photon irradiance of $200 \mu\text{mol photon m}^{-2} \text{s}^{-1}$ at 20 °C for 4 h. Data shown are means \pm S.E.M. ($n = 3$). Fresh macroalgal samples (0.4 g) were incubated in 40 ml filtered seawater. The pH was measured before exposure as nominal values and the control was filtered seawater without macroalgae. H₂O₂ concentrations were measured using the CL method (Section 2.2.3) with external standards. Asterisks indicate significant differences between treatments ($P < 0.05$) found after Tukey's *post hoc* test.

3.3.2.2 Light intensity

After a four-hour incubation period, hydrogen peroxide levels for all macroalgae species were significantly different in response to intensity level ($F_{(2,18)} = 8.251$, $P = 0.003$; Fig. 3.4). With *Chondrus crispus* there were no significant differences in hydrogen peroxide levels with increasing levels of light intensity ($F_{(2,6)} = 0.018$, $P = 0.983$) similar to seawater. However, with *Fucus serratus* and *Ulva lactuca* there was a significant effect on H_2O_2 steady state levels which increased with increasing light intensity level ($F_{(2,6)} = 11.228$, $P = 0.009$, and $F_{(2,6)} = 7.902$, $P = 0.021$, respectively). Light intensity, like pH, was found to have a significant interaction with 'macroalgae species', $F_{(4,18)} = 3.917$, $P = 0.019$ (Fig. 3.4). However, again this is down to the difference in behaviour between seawater alone and seawater plus macroalgae.

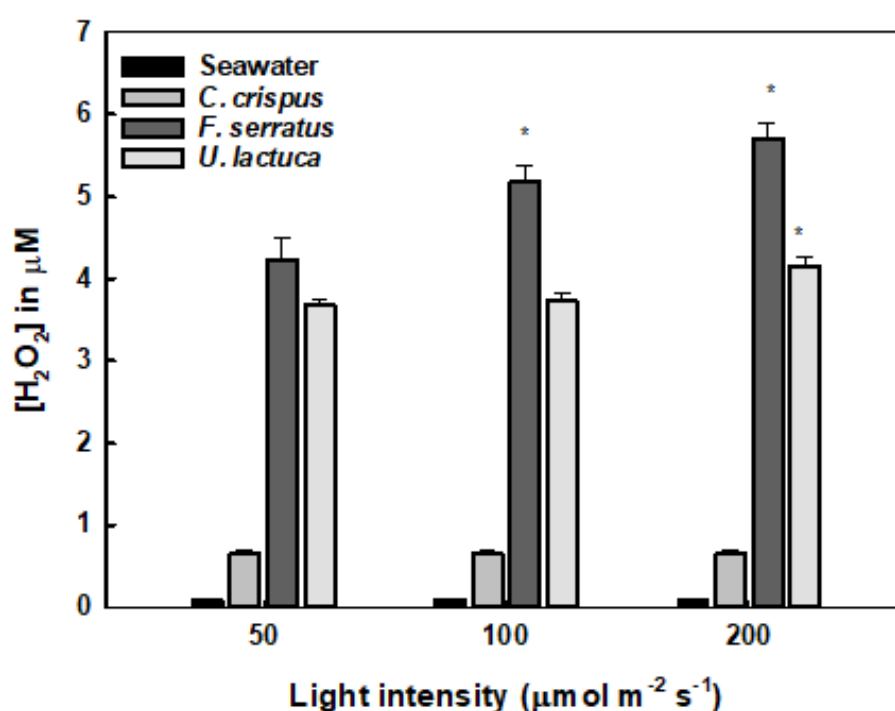


Figure 3.4 Effects of light intensity on levels of H_2O_2 for three different macroalgae with seawater as a control. Macroalgae (0.4 g) in 40 ml filtered seawater were exposed at 20 °C to different light intensities for 4 h. H_2O_2 concentrations were measured using the CL method (Section 2.2.3) with external standards. Means \pm standard error are shown ($n = 3$). Asterisks indicate significant differences between treatments ($P < 0.05$) found after Tukey's *post hoc* test.

3.3.2.3 Temperature

There were no statistical differences in the level of hydrogen peroxide (Fig. 3.5) between any treatments following 4 h of exposure to different temperatures below 30 °C. Hydrogen peroxide levels in *U. lactuca* and *F. serratus* were similar across the three lower temperatures compared to 30 °C, where there was a significant increase ($F_{(3,8)} = 9.212$, $P = 0.006$ and $F_{(3,16)} = 13.146$, $P = 0.002$, respectively). However, *Chondrus crispus* had a difference response to temperature compared to the other two macroalgae. As a result, a significant interaction between temperature and macroalgae species was observed ($F_{(3,16)} = 5.054$, $P = 0.012$).

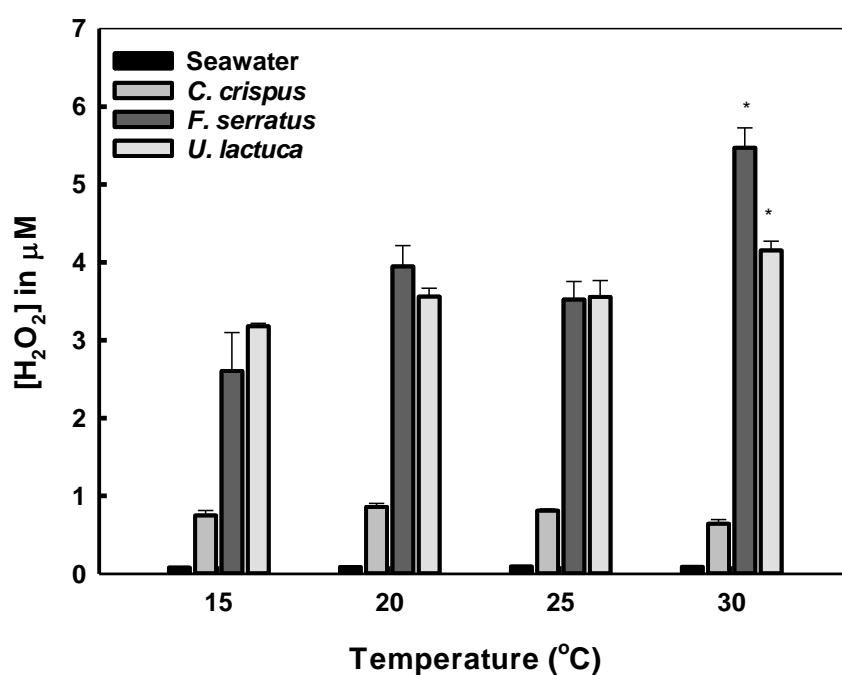


Figure 3.5 Effects of temperature on levels of H_2O_2 for three different macroalgae with seawater as control. Macroalgae (0.4 g) in 40 ml filtered seawater were exposed to different temperatures for 4 h. H_2O_2 concentrations were measured using the CL method (Section 2.2.3) with external standards. Means \pm standard error is shown ($n = 3$). Asterisks indicate significant differences between treatments for each species ($P < 0.05$) found after Tukey's *post hoc* test.

3.3.2.4 Salinity

Salinity had no effect on steady state hydrogen peroxide levels for any of these species. Even though, compared to the other two species, *F. serratus* seemed to produce a higher H_2O_2 concentration under hypersaline conditions, this difference was not statistically significant ($F_{(2,6)} = 1.095$, $P = 0.35$).

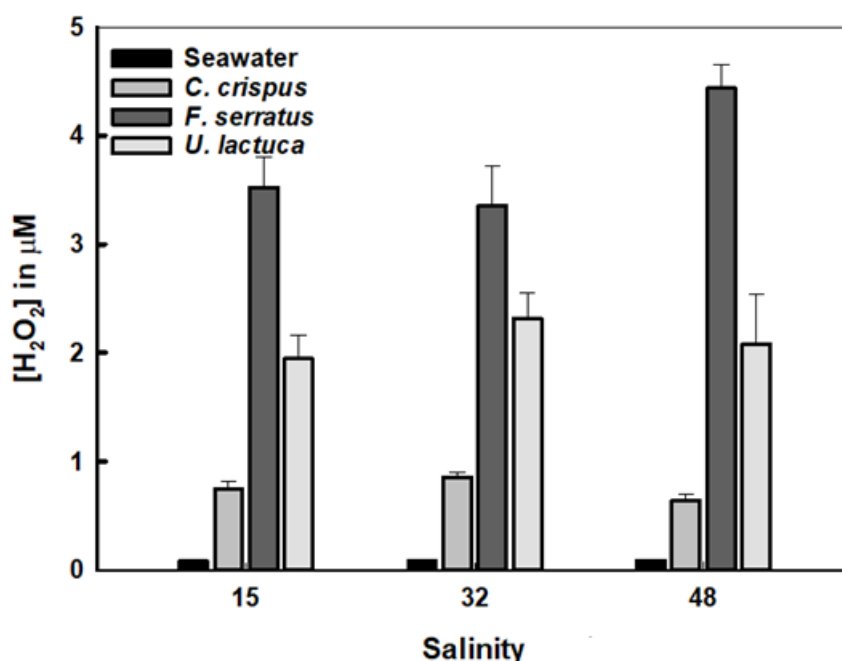


Figure 3.6 Effects of salinity (psu) on levels of H_2O_2 for three different macroalgae with seawater as control. Macroalgae (0.4 g) in 40 ml filtered seawater were exposed various salinities over 4 h. H_2O_2 concentrations were measured using the CL method (Section 2.2.3) with external standards. Means \pm standard error is shown ($n = 3$).

3.3.2.5. Experiments in which macroalgae were either desiccated or combined together

It is interesting to note that when hydrogen peroxide levels were measured in the seawater medium after macroalgae had been desiccated under $200 \mu mol \text{ photon } m^{-2} s^{-1}$ and a temperature of $30^\circ C$ for 4 h, levels increased significantly almost 2-fold compared to the control, the same treatment but without desiccation (see Section 3.2.2) for *Fucus serratus* and *Ulva lactuca* (Fig. 3.7). In contrast, when either of those two macroalgae species were combined with *C. crispus*, the level of H_2O_2 was apparently reduced (Fig. 3.8). However, this experiment is challenging to comprehend due to the absence of controls with *Ulva lactuca* and *Chondrus crispus* alone. Nevertheless, relative to that produced by *Fucus serratus* (100%), the quantities of H_2O_2 produced by these algae are 81.2% for *U. lactuca* (range: 69.2-90.1%) and 19.5% for *C. crispus* (range: 15.0-25.0%) as shown in Figs. 3.3-

3.6. The levels produced from simple additive behaviour when combining the algae can be expected, 59.7% for F+C (range 57.5-62.9%), 49.0% for U+C (range 46.7-55.9%), and 90.4% for F+U (range 84.6-95.1%), and compared with the actual values achieved (32.6% for F+C; 36.1% for U+C; and 86.5% for F+U) (Fig. 3.8). It is clear that the actual values for combinations involving *C. crispus* are lower than expected, but the value for the combination of *F. serratus* and *U. lactuca* is as expected.

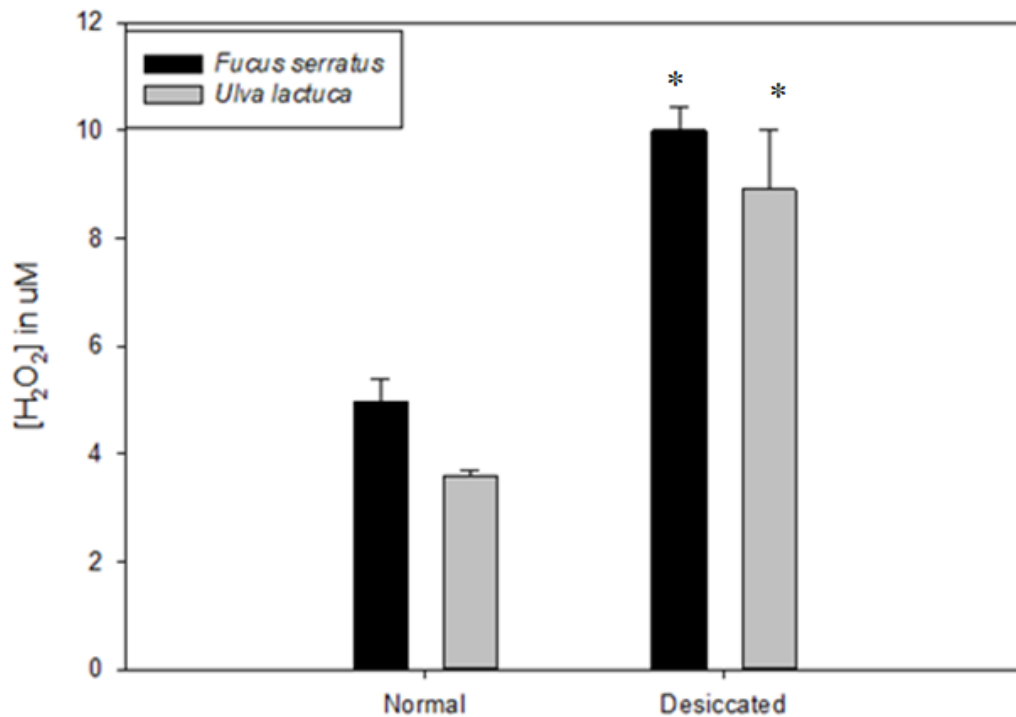


Figure 3.7 Levels of H₂O₂ in seawater surrounding two species of macroalgae that had either been desiccated beforehand for 4 h under a light intensity of 200 $\mu\text{mol photon m}^{-2} \text{s}^{-1}$ and temperature 30 °C or non-desiccated (see Section 3.2.2). H₂O₂ concentrations were measured using the CL method (Section 2.2.3) with external standards. Means \pm standard error are shown ($n = 3$). Asterisks indicate significant differences between treatments for each species ($P < 0.05$) found after Tukey's *post hoc* test.

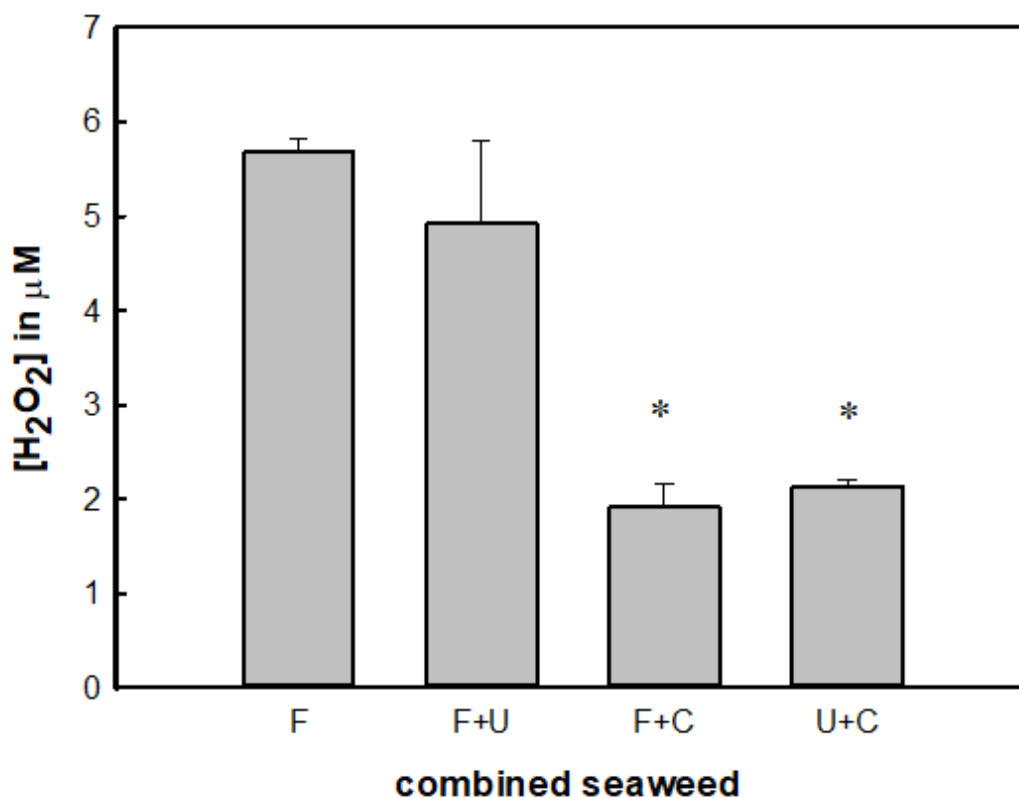


Figure 3.8 Levels of H₂O₂ in seawater surrounding combinations of macroalgae. 400 mg (200 mg of each species) of seaweed was put together in 40 ml filtered seawater at 30 °C and 200 μmol photon m⁻² s⁻¹ for 4 h. F; *Fucus* alone (400 mg) F+U: *Fucus* and *Ulva*, F+C; *Fucus* and *Chondrus*, U+C; *Ulva* and *Chondrus*. H₂O₂ concentrations were measured using the CL method (Section 2.2.3) with external standards. Means ± standard error are shown (*n* = 3). Asterisks indicate significant differences between treatments for each species (*P* < 0.05) found after Tukey's *post hoc* test.

3.3.3 Effects of abiotic stress on chlorophyll *a* fluorescence

The maximum efficiency of PSII photochemistry, as measured by the ratio of variable to maximum fluorescence (F_v/F_m) and the Performance Index (PI), decreased as irradiance, salinity, and temperature increased. Maximum quantum yield (F_v/F_m) was found to be significantly lower (30% with *F. serratus*; 40% with *C. crispus*; and 50% with *U. lactuca*) at 200 μmol photon m⁻² s⁻¹. Temperature and salinity both reduced F_v/F_m by 15% with *F. serratus* at 30 °C and *U. lactuca* at 48 psu, respectively compared to control (Fig. 3.9).

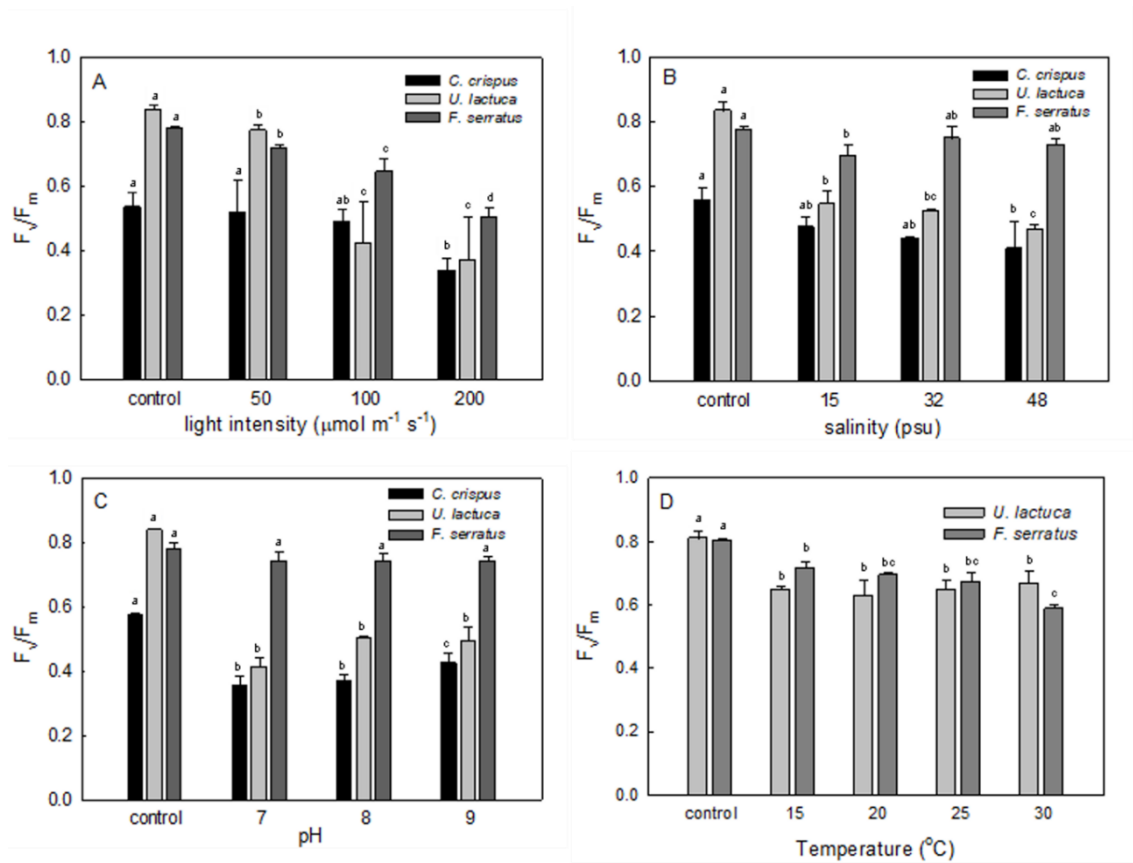


Figure 3.9 The maximum quantum yield (F_v/F_m) with three species of macroalga (*Chondrus crispus*, *Ulva lactuca* and *Fucus serratus*) exposed to four abiotic stressors, light intensity (A), salinity (B), pH (C) and temperature (D). Results are presented as mean of three independent measurements \pm S.E.M. Statistical analysis was performed using ANOVA. Bars with the same letter as not significantly different, while those with different letters are ($P < 0.05$). In each case the control was macroalgal thallus prior to treatment. Asterisks indicate significant differences between treatments for each species ($P < 0.05$) found after Tukey's post hoc test.

The performance index on chlorophyll basis (PI) was lower for the majority of the experimental conditions when compared to the control. The results show that when light intensity was increased, PI for all three macroalgae decreased significantly ($P < 0.05$), but only *F. serratus* showed a significant decrease in PI when subjected to elevated temperature. In addition, *U. lactuca* showed a decrease in PI under hypersaline conditions (Fig. 3.10-3.12). While all of the abiotic stressors had a substantial effect on steady state H_2O_2 levels produced by the macroalgae studied (Figs. 3.3-3.6), it was only in the case of light intensity that there were corresponding decreases in photosynthetic efficiency as measured by F_v/F_m and PI. For example, H_2O_2 levels increased with increasing pH in all three algae (Fig. 3.3), but there were no significant changes in F_v/F_m and PI under the same conditions (Figs. 3.9-3.12). F_v/F_m is a fundamental measurement that represents the maximum quantum yield of PSII, whereas PI integrates various elements of photosynthesis, including those that occur downstream of PSII. The characteristics of PSII photochemistry were investigated by OJIP analysis to further understand possible reasons for the decreases in PI caused by increased light intensity. OJIP analysis followed the polyphasic rise of fluorescence transients under different treatments to suggest what caused a decrease in the F_v/F_m ratio in photoinhibited cells. Figure 3.13 shows changes in absorption flux, trapping flux, electron transport flux, and dissipation flux per PSII reaction centre, i.e., ABS/RC , TR_o/RC , ET_o/RC , and DI_o/RC values obtained from polyphasic fluorescence transient observations (Section 3.2.3). Light absorption (ABS/RC ; Fig. 3.13A) increased with increasing light intensity, but this rise was not significant in *C. crispus*. Although light absorption increased, the efficiency of light energy trapping (TR_o/RC ; Fig. 3.13B) was unchanged in two species and increased somewhat in the third, *U. lactuca*. The amount of light energy dissipated, partly as fluorescence, DI_o/RC (Fig. 3.13D), increased in two species but was not significant in the third, *C. crispus*. The electron transport flow (ET_o/RC ; Fig. 3.13C), which indicates processes downstream of PSII in photosynthesis, was of particular interest. There were non-significant declines in two of the species, but a considerable decrease in *F. serratus*.

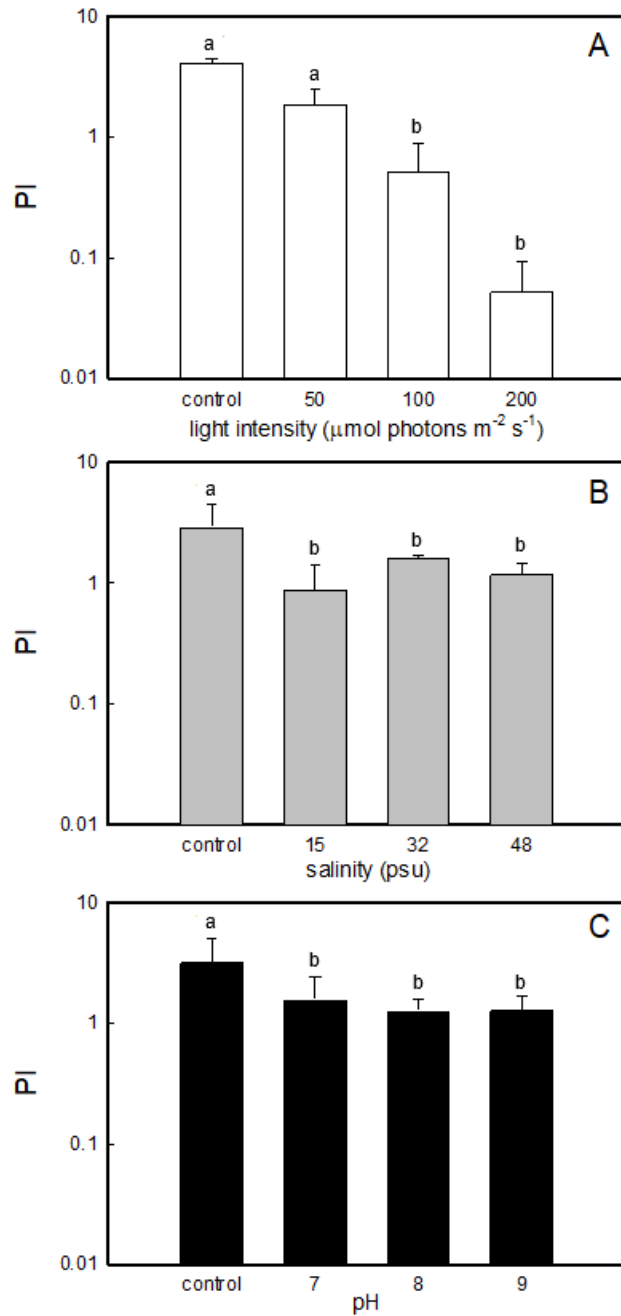


Figure 3.10 Performance index (PI) of *Chondrus crispus* exposed to three abiotic stressors, pH, light intensity and salinity. Results are presented as means of three independent measurements \pm S.E.M. Statistical analysis was performed using ANOVA. Bars with the same letter as not significantly different, while those with different letters are ($P < 0.05$). In each case the control was macroalgal thallus prior to treatment.

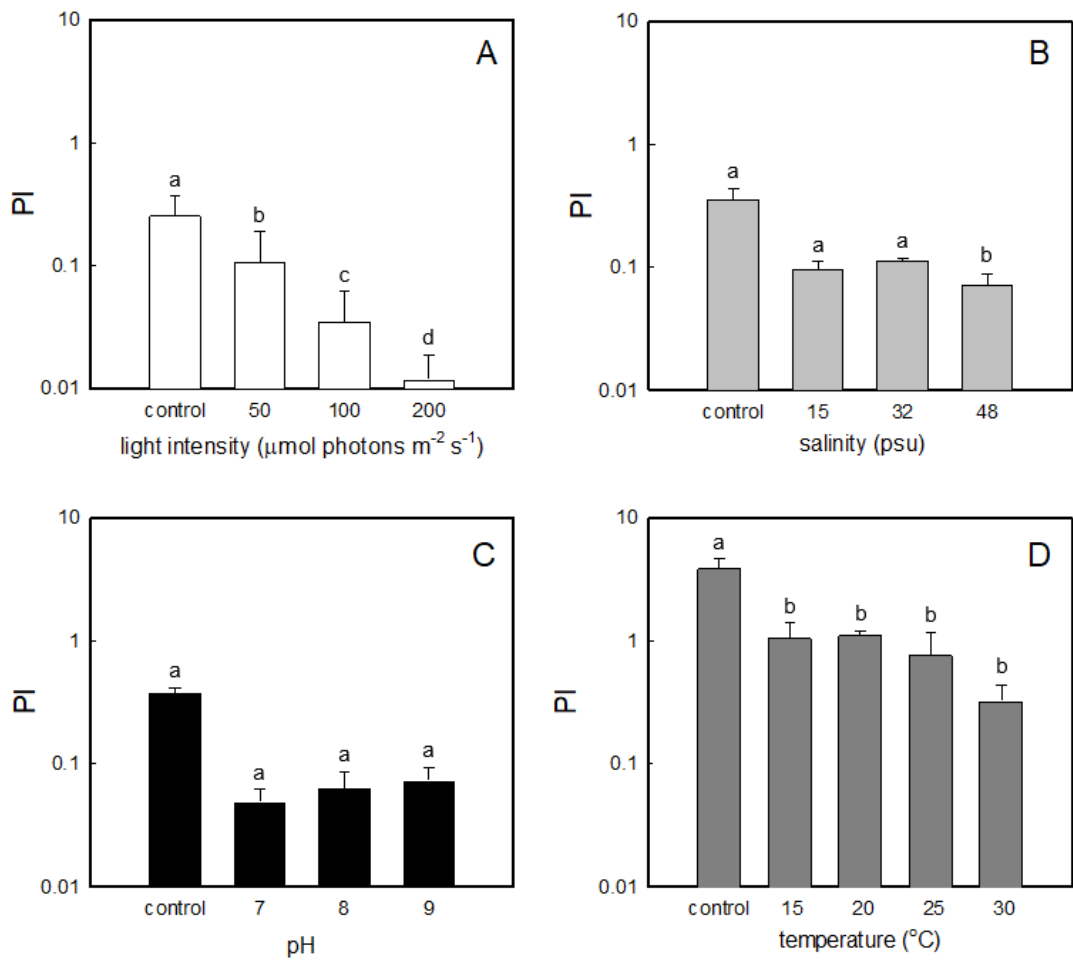


Figure 3.11 Performance index (PI) of *Fucus serratus* exposed to four abiotic stressors, pH, light intensity, temperature and salinity. Results are presented as means of three independent measurements \pm S.E.M. Statistical analysis was performed using ANOVA. Bars with the same letter as not significantly different, while those with different letters are ($P < 0.05$). In each case the control was macroalgal thallus prior to treatment.

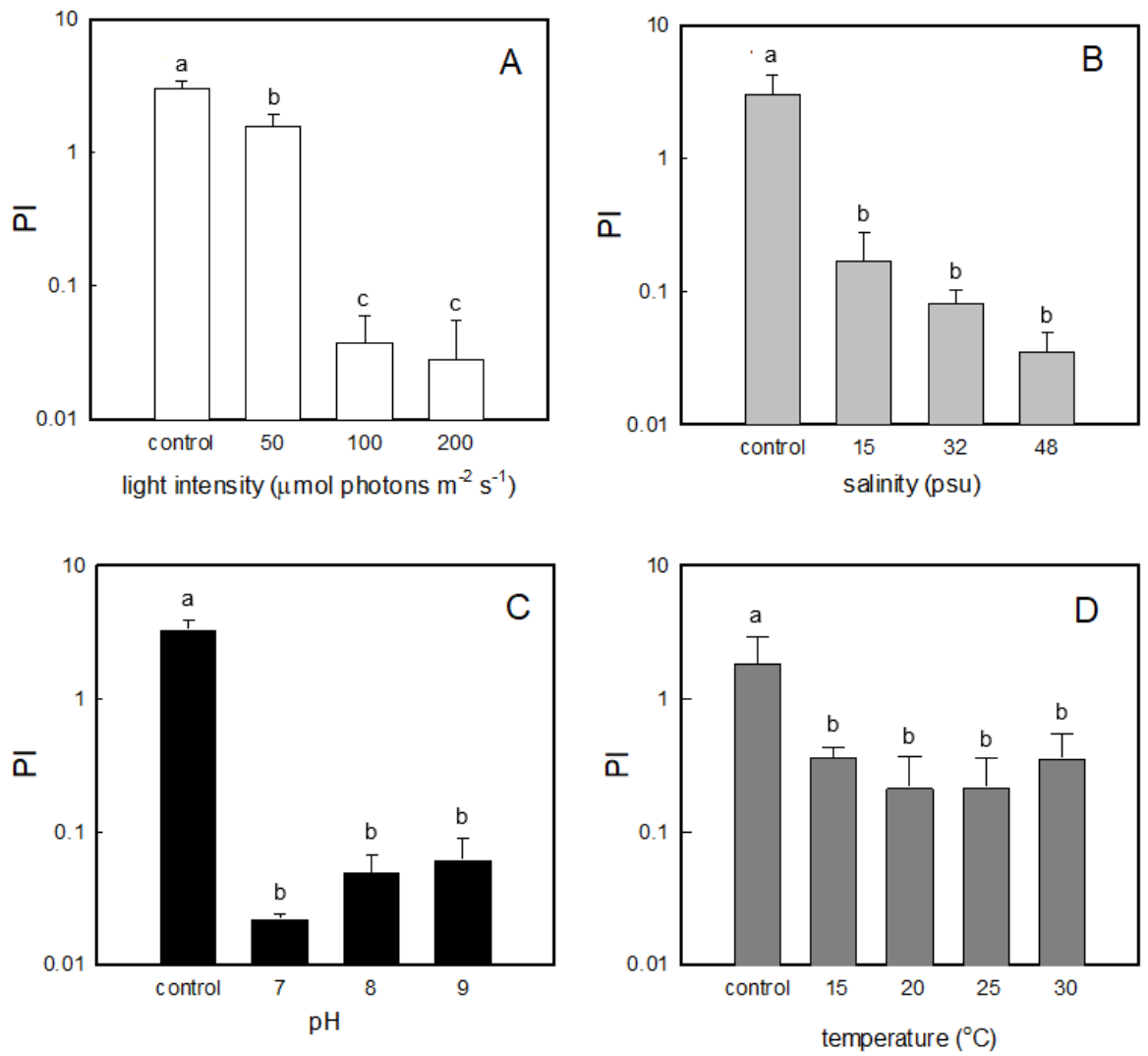


Figure 3.12 Performance index (PI) of *Ulva lactuca* exposed to four abiotic stressors, pH, light intensity, temperature and salinity. Results are presented as means of three independent measurements \pm S.E.M. Statistical analysis was performed using ANOVA. Bars with the same letter as not significantly different, while those with different letters are ($P < 0.05$). In each case the control was macroalgal thallus prior to treatment.

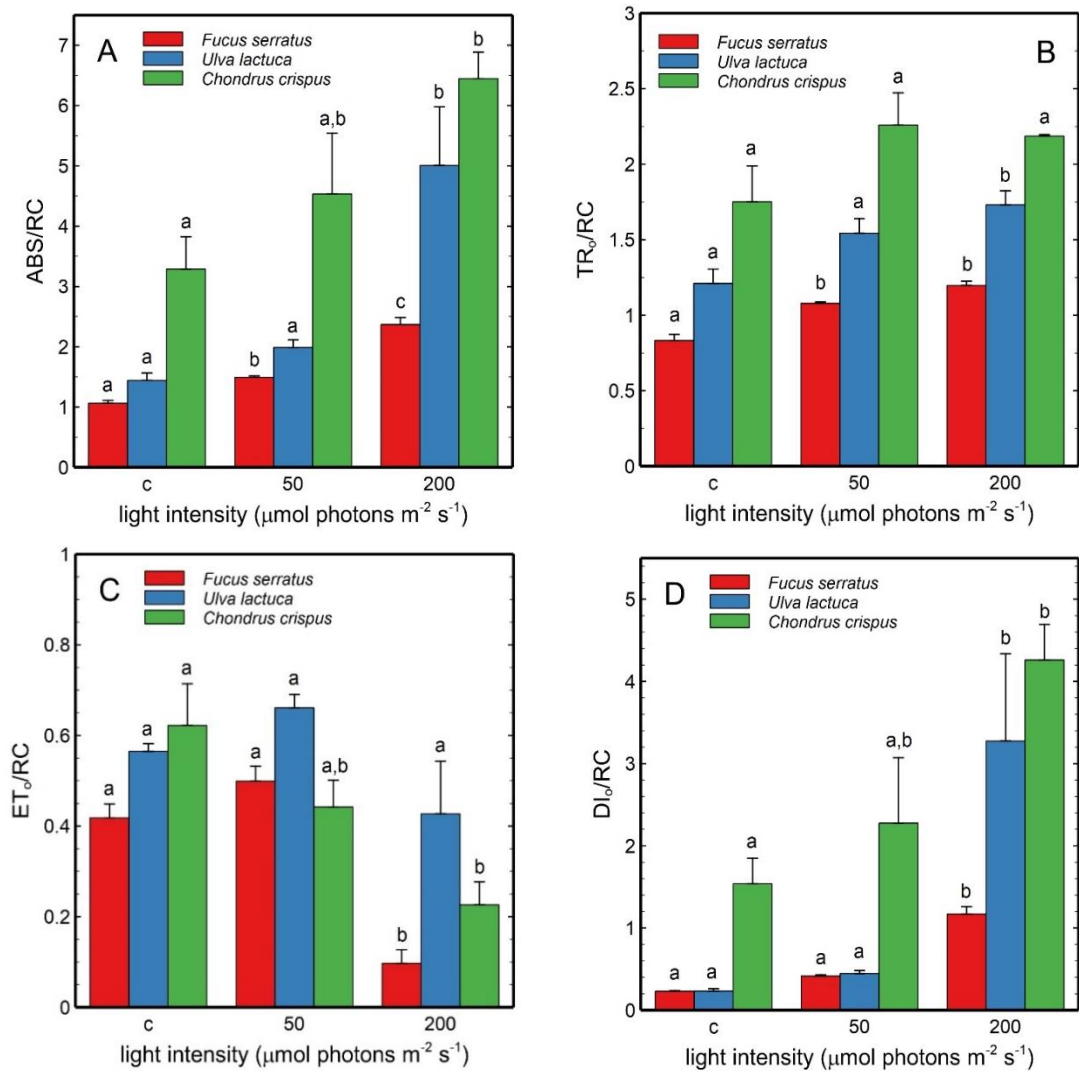


Figure 3.13 Four flux ratios derived from OJIP analysis for three species of macroalga (*Chondrus crispus*, *Ulva lactuca* and *Fucus serratus*) exposed to different light intensities. Results are presented as mean of three independent measurements \pm S.E.M. Statistical analysis was performed using ANOVA. Bars with the same letter as not significantly different, while those with different letters are ($P < 0.05$). In each case the control was macroalgal thallus prior to treatment.

3.4 Discussion

Significant increases were observed in levels of H₂O₂ in response to diverse environment factors, between only seawater compared to the seawater with macroalgae throughout the experiment. This shows that the H₂O₂ has been formed in the experiment. Researchers have found that the production of H₂O₂ functions as a sink for energy (Collén et al., 1996). They discovered that an increase in the level of H₂O₂ excreted by macroalgae exposed to irradiance still continued even though photosynthesis was already saturated. However, the observed pattern may explain why the dynamic level of H₂O₂ in the seawater exhibited both an increase and a reduction. Throughout the experiments in this study, levels of H₂O₂ increased and then slightly decreased to reach a steady state level after 4 h exposure to the abiotic treatments, e.g., light (Fig. 3.2). A possible explanation for this might be the role of H₂O₂ scavenging enzymes. When H₂O₂ is produced, it may be eliminated via enzymatic detoxifying systems such as catalase (CAT), ascorbate peroxidase (APX) and glutathione peroxidase (GPX), as well the antioxidant ascorbic acid and other small molecule antioxidants (Hertwig et al. 1992; Dummermuth, 2003; Zhu et al., 2017), to levels that do not exceed the macroalgae's threshold values of tolerance.

The results presented in this study give information about the levels of H₂O₂ produced by intertidal macroalgae under artificial abiotic stress using luminol-dependent chemiluminescence and OJIP analysis for investigating the characteristics of PSII photochemistry, in short-term stress experiments. In the four abiotic treatments, the plants with higher level of H₂O₂ under exposure, were *Fucus serratus* as representative of the brown algae, *Ulva lactuca* belonging to the green algae and *Chondrus crispus* within the red algae, respectively.

This provides evidence that environmental factors can induce production of H₂O₂, yet macroalgae responded differently depending on species (Dummermut et al., 2003). The result show that *C. crispus* was not sensitive to the treatments. This species did not appear to produce more H₂O₂ when the light, temperature and salinity were increased. This phenomenon could be caused by two factors: first, H₂O₂ is destroyed by enzymes and the antioxidant before it is released into seawater, or there is an increase in the production of H₂O₂-scavenging enzymes that are released extracellularly into seawater. Previous research in coral (*Stylophora pistillata*) has confirmed that the antioxidants released by the corals are anti-H₂O₂ enzymes, most likely catalase (Armoza-Zvuloni and Shaked, 2014). The antioxidant released by the coral was found to range from 10⁻⁴ to 10⁻³ catalase-like units per cm² coral. Another study also revealed that when *C. crispus* was exposed

to a high concentration H_2O_2 (100 μM) the extracellular concentration of H_2O_2 was decreased 95% in 30 min (Collén and Davidson, 1999). That experiment is consistent with the results of this study and indicates that this species of red algae is able to lessen the level of H_2O_2 on its surrounding seawater (Fig. 3.8).

Increased light intensity, temperature, and pH, on the other hand, induced increased H_2O_2 levels in *F. serratus* and *U. lactuca*. When photosynthesis is inhibited by suboptimal conditions, it is claimed that an increased amount of reactive oxygen is produced (Asada, 1999). The excretion of H_2O_2 from the green alga, *U. rigida*, was light-dependent and increased exponentially as photon irradiance increased (Collén and Pedersen, 1996). Their findings revealed that a 30 mg disc of *Ulva rigida* produced a H_2O_2 concentration of 4 μM in 3.25ml of seawater after 30 min and that this excretion increased exponentially with photon irradiance. Furthermore, in their study looking at the H_2O_2 production of three *Fucus* species exposed to desiccation and high intensity light, Collén and Davison (1999) observed that all three species produced H_2O_2 at similar levels to each other.

According to Abrahamson (2003), temperature stress resulted in a significant increase in H_2O_2 levels, because high temperatures may disrupt the equilibrium between respiration and photosynthesis, and they are affected differently by temperature increase. Above certain threshold values, which vary between species, respiration accelerates at a rate faster than photosynthesis, causing a metabolic imbalance. Increased the temperature raised the production of H_2O_2 in green algae and also brown algae (Abrahamson, 2003). In the present investigation, the content of H_2O_2 tend to increase with increasing temperature for both species (*U. lactuca* and *F. serratus*), demonstrating that oxidative stress generated by heat stress was considerable at 30 °C.

While other treatments cause the concentration of H_2O_2 to increase in only one or two species, at pH 9 the level of H_2O_2 was increased in all three species. This finding was similar to Collén et al. (1995). *U. rigida* was exposed to light intensity of 700 $\mu\text{mol m}^{-2} \text{s}^{-1}$ for one hour with different pHs. The result showed that the H_2O_2 level was three time higher at pH 9 in comparison to pH 8. This might cause by decreased availability of CO_2 as a consequence the rate of photosynthesis is lowered. The reactions connected with the direct photoreduction of oxygen (Mehler reaction) to the superoxide radical, which occur when the concentration of CO_2 is limiting for photosynthesis and caused by reduced electron transport components associated with PSI, are referred to as oxidative reactions (Badger, 1985); and an increased amount of superoxide radicals is also formed when the ratio of NADPH/NADP⁺ to O_2 is high (Scandalios 1993; Badger et al., 2000). However,

looking at the result of this study on chlorophyll fluorescence data pH has no effect on F_v/F_m or PI (Fig. 3.11 and 3.12), suggesting that any differences in levels of hydrogen peroxide under the different conditions are not down to dysfunction in photosynthesis. Hence the current study is more in agreement with Collén et al. (1996) who found that the increased H_2O_2 is related to the increasing pH of the medium rather than a greater capacity to produce H_2O_2 . This is based on the fact that the pH of the medium rises as the day progresses, causing an increase in H_2O_2 .

Photosystem II (PSII) is thought to be very vulnerable to photoinhibition, which can be caused by light in the presence or absence of other stressors. The responses of the photosynthetic apparatus to different stresses induced by various abiotic stress changes can be detected and photoinhibition and general stress effects estimated for photosynthetic organisms by means of the fast Chl *a* fluorescence transient. There is an issue with most of the data sets since both F_v/F_m and PI are lower for most of the experimental conditions compared to the control (Figs. 3.9-3.12). Nevertheless, F_v/F_m shows a consistent decrease as light intensity increases for all three species indicative of a lowered quantum yield in PSII. In general, this is an indicator of photoinhibition (Hanelt et al., 1993; Cabello-Pasini et al., 2000). The effect of increasing irradiance on photosynthetic both F_v/F_m and PI indicates that increased light intensity over this range leads to dysfunction of photosynthesis. Photoinhibitory processes dissipate such excess of absorbed energy through fluorescence and heat, and functions as a protective mechanism for the photosynthetic apparatus (Hanelt et al., 1993; Hader et al., 1997).

In accordance with what is described in the Results, even though majority of abiotic stressors generated increases in steady-state levels of H_2O_2 , only an increase in light intensity caused corresponding reductions in F_v/F_m and PI. In contrast to the relatively basic F_v/F_m measurement, which determines the maximum quantum yield of PSII, the PI value considers a broader array of photosynthesis-related parameters. In order to have a deeper comprehension of this, an OJIP analysis was conducted, and various flow ratios were obtained (Fig. 3.13). These ratios are prone to vary due to the fact that they represent energy fluxes in relation to the number of PSII reaction centres. On the other hand, considering only a short period of time, it is presumed that this is not the case. As expected, the ABS/RC ratio increases as the light intensity rises; however, there was no corresponding increase in the TR_o/RC ratio, which quantifies the quantity of light energy captured. With the increase in light intensity, TR_o/RC for two of the macroalgae was unchanged, while for the third, *U. lactuca*, it increased only slightly. Additionally, significant increases in the amount of energy that has been lost (DI_o/RC) have been

observed in two macroalgae (the increase in the third, *C. crispus*, was not significant), which is consistent with the decreased efficiency of PSII at increasing light intensities, as indicated by the declines in F_v/F_m (Misra et al., 2001). ET_o/RC , the final flux ratio, is connected to the electron transport that occurs after light absorption and the photochemistry that occurs in PSII (Yusuf et al., 2010). In addition to changes in the maximum quantum yield of PSII, alterations in ET_o/RC may contribute to the decreases in PI observed for all three species in response to an increase in incident light intensity. However, this only appears to be the case for *F. serratus*, where a significant decrease in ET_o/RC was observed at high light intensities.

Under stress, the decreases in F_v/F_m indicated that the reaction centres in PSII were damaged/photochemically less active. However, PI assesses overall photosynthetic performance including PSI and other electron acceptors, and its values may represent the photosynthetic transport chain's energy flow efficiency beyond PSII, where low efficiency could lead to over reduction and an increase in $O_2^{\bullet-}$ (and hence H_2O_2) via the Mehler reaction. Hence, it seems that in *F. serratus* dysfunction in photosynthetic electron transfer can account for the increase in H_2O_2 with increased light intensity.

Chapter 4
Effects of hydrogen peroxide on the snakelocks anemone
(Anemonia viridis)

4.1 Introduction

The results presented in Chapters 2 and 3 has helped establish the range of H₂O₂ concentrations that organisms living in intertidal rockpools might encounter, using both measurements in the field and under controlled conditions in the laboratory. This, in line with the work of other researchers (Abele-Oeschger et al., 1997; Collén et al., 1995; Collén and Pedersén, 1996), suggests that H₂O₂ concentrations in this environment are in the low micromolar range but may be higher locally. The concern now is whether H₂O₂ concentrations of this level can be harmful to other organisms in rockpools. Abele-Oeschger et al. (1994) discovered that 5 µM H₂O₂ reduced oxygen consumption by the polychaete worm *Nereis diversicolor*, while Abele-Oeschger and Buchner (1995) discovered that the same concentration reduced filtration rate by 40% in the bivalve *Cerastoderma edule*, but both of these species reside in tidal mud rather than rockpools. Other work from the same group may be more relevant; Abele-Oeschger et al. (1996) demonstrated a similar effect of 20 µM H₂O₂ on oxygen consumption by *Crangon crangon*, an epibenthic shrimp found in rockpools with sandy bottoms.

The snakelocks anemone, *Anemonia viridis*, is often found in the intertidal zone of rocky shores in temperate countries (Muller-Parker & Davy, 2001), and is considered a model organism for research on Cnidarians (e.g., Dani et al., 2017; Moya et al., 2012; Richier et al., 2005; Richier et al., 2006). The choice of the symbiotic snakelocks anemone as the study organism here was driven by the extensive literature on corals, closely related symbiotic organisms, which are known to be susceptible to oxidative stress (Dias et al., 2019; Downs et al., 2002). There are two different variants or colour morphs of *A. viridis*, namely *var. rustica* and *rufescens*, the brown and green morphs, respectively (Porro et al., 2019). The difference in colour is because there is no detectable fluorescence in the brown morph while there is expression of green and red-orange fluorescent proteins in the green one; despite being phenotypically different they are classed as the same species (Mallien et al., 2017). *A. viridis* has a mutualistic association with endosymbiotic algae (referred to as zooxanthellae), the zooxanthellae providing organic nutrients via photosynthesis to support metabolism, growth and reproduction while the animal host provides CO₂ and essential nutrients such as nitrogen (Furla et al., 1998). The most common symbiotic algae found in sea anemones are dinoflagellates of the genus *Symbiodinium* (Casado-Amezúa et al., 2014). They are normally located within endodermal cells and concentrate in the tentacles and oral disc (Furla et al., 1998).

As photosynthetic organisms, zooxanthellae are sensitive to changes in light, because this can result in ROS-mediated damage that can be harmful to the host (Smith et al., 2005). Living in habitats such as rockpools that are shallow, relatively warm, and strongly illuminated species such as *A. viridis* can experience large changes in environmental conditions over short time periods. Under such conditions, elevated concentrations of photochemically produced ROS such as H₂O₂ are likely, and as has been seen in Chapter 2 and 3, the same is true for ROS production by macroalgae. On top of this the host anemone may experience high internal levels of ROS from the photosynthetic activity of their zooxanthellae (Downs et al. 2002; Richier et al. 2006; Saragosti et al., 2010).

The increase in the production of H₂O₂ in many algae, including zooxanthellae, corresponds with increased excitation pressure upon photosystem II (PSII) (Dykens and Shick, 1984; Tchernov et al. 2004) or a reduction in the quantum yield of photochemistry associated with increases in the rate of protein turnover in the oxygen-generating reaction centres of PSII, or of elevated temperatures (Downs et al., 2002). It has been suggested that such an elevation in ROS production, especially of H₂O₂, by zooxanthellae is associated with events that lead to bleaching, i.e., loss of the zooxanthellae as a protective measure. Hydrogen peroxide is an important primary signalling molecule between zooxanthellae and the symbiotic host, but at elevated concentrations, it triggers the expulsion mechanism (Shick et al., 1996; Smith et al., 2005; Suggett and Smith, 2019).

Organisms have developed complex cellular defensive responses to the generation and elevation of H₂O₂ levels. These include both enzymatic (e.g., superoxide dismutase [SOD] and catalase [CAT]) and non-enzymatic antioxidants, low molecular mass substances (e.g., reduced glutathione, GSH) that can reduce superoxide radicals (O₂^{•-}) and hydrogen peroxide (H₂O₂) to nontoxic forms such as oxygen and water, thereby reducing the likelihood of damage to key cellular processes (Richier et al., 2006). SOD catalyses the dismutation of superoxide into oxygen and H₂O₂, and CAT is responsible for inactivating H₂O₂ into water and oxygen. H₂O₂ may also be removed via peroxidase enzymes, e.g., selenium-dependent glutathione, which uses GSH to reduce H₂O₂ to water, with GSH being regenerated from oxidised glutathione by NADPH, catalysed by glutathione reductase (Halliwell and Gutteridge, 2007).

Despite extensive studies on the effects of stressors such as high temperature that induce ROS production in Cnidarians including corals and anemones (Lesser et al. 1990; Dykens et al., 1992; Downs et al., 2002; Richier et al., 2006), the application of exogenous H₂O₂ to assess the oxidative stress response in these organisms is still limited. This study

examined the potential impact of H₂O₂ on the ecology of rockpools using the snakelocks anemone, *Anemonia viridis*, which, of all the rockpool fauna on which H₂O₂ could have a negative impact, may be particularly susceptible because of the presence of the symbiotic photosynthetic zooxanthellae. Changes in the antioxidant enzymes SOD and CAT, concentrations of total glutathione and products of lipid peroxidation (MDA), and the density of zooxanthellae were measured in *A. viridis* exposed to an environmentally relevant range of H₂O₂ concentrations.

4.2 Materials and Methods

4.2.1 Sample collection and maintenance

Individuals of the snakelocks anemone, *Anemonia viridis*, ($n = 15$ of each morph) were collected by hand from the upper shore at west of Wembury Point in the South Hams, Devon, UK (50.3167° N, 4.1086° W; Grid ref. SX5048). Once in the laboratory, anemones were maintained in closed-circuit filtered seawater ($0.1 \mu\text{m}$) in a 50-l container within a temperature-controlled culture room. Seawater was constantly aerated by submerged air stones with 50% renewed weekly, and a 100% water change every 4 weeks. Temperature was maintained at $15 \pm 0.18^{\circ}\text{C}$; irradiance was set at $150 \mu\text{mol photon m}^{-2} \text{s}^{-1}$ (provided by cool white fluorescence tubes; Philips) on a 12 h:12 h L:D cycle to photoacclimate the *Symbiodinium* (Harland and Davies, 1994); and salinity was 32.8 ± 0.35 psu with a pH of 8.2 ± 0.04 . During the acclimation period, anemones were fed frozen *Artemia salina* (Gamma blister, Tropical Marine Centre, Bristol, UK) ad libitum on a weekly basis. After a month of laboratory acclimation, anemones were exposed to different hydrogen peroxide concentrations. All experiments were carried out under the same culture conditions outlined above.

4.2.2 Exposure of *A. viridis* to H_2O_2

Individuals ($n = 12$ for both morphs) that had a pedal disc measuring less than or equal to 2 cm in diameter were selected and placed in individual 1 l acid-washed glass beakers filled with 800 ml of filtered seawater for 1 h habituation. Immediately before the experiments, a nominal 10 mM H_2O_2 stock solution was prepared and the concentration confirmed by measuring the UV absorbance at 240 nm ($\epsilon_{240} = 43.6 \text{ M}^{-1} \text{ cm}^{-1}$; Hildebrandt and Roots, 1975); this high stock concentration was prepared to minimize variability in volume between the treatments. Three replicates of each morph were exposed to one of four H_2O_2 concentrations: 0 (control), 1, 10 and 100 μM H_2O_2 . Exposure lasted for 4 h during which time the hydrogen peroxide was topped up every 2 h to maintain the original concentration (Fig. 4.1).

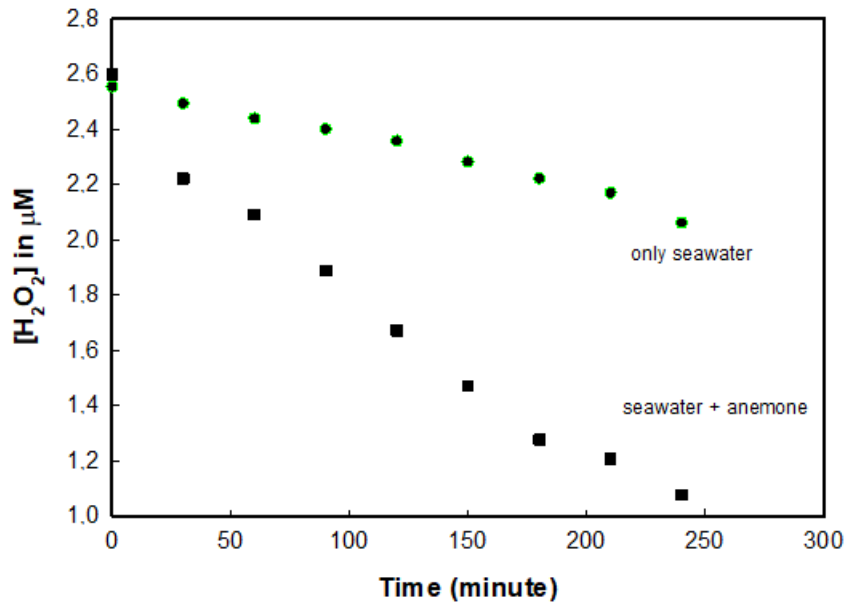


Figure 4.1 The H₂O₂ concentration profile in seawater over 4 h exposure to control (no anemone present) and with an anemone in 2.6 μM H₂O₂.

4.2.3 Quantification of zooxanthellae density

At the end of the 4 h exposure period, three tentacles per individual were cut off using scissors and homogenised to extract the zooxanthellae. The tissue was homogenised using a glass Potter homogeniser with 0.5 ml cold extraction buffer, 50 mM potassium phosphate, pH 7.8, containing 0.4 M sorbitol. The homogenate was thereafter centrifuged at 9,000 *g*_{av} for 5 min at 4 °C (Hawk 15/05, Sanyo). After the pellet of zooxanthellae was broken up using a pipette tip, the homogenate was re-centrifuged at 21,000 *g*_{av} for 2 min. The supernatant was pipetted after removing any floating mucus and stored at -20 °C to await analyses of protein and enzyme activity. The pellet (containing zooxanthellae) was re-suspended in 0.3 ml extraction buffer and filtered through 100 μm nylon mesh (Nitex) to remove larger pieces of remaining animal tissue. The number of cells in the suspension was counted using a Fuchs-Rosenthal haemocytometer. A haemocytometer has a central area, which is slightly lower (0.1 mm) than the rest of the surface, and which forms two counting chambers. Each counting chamber has a series of finely ruled areas forming grids. The grids and 0.1 mm depression of the counting chambers define known volumes. Hence the number of cells in a known volume can be counted.

4.2.4 Thiobarbituric acid reactive substances assay

The thiobarbituric acid reactive substances (TBARS) assay, based on Yagi et al. (1998) was used to detect lipid peroxides or their products, such as malondialdehyde (MDA). Levels of MDA in *A. viridis* tissues were determined by measuring the colorimetric change that occurs when MDA reacts with thiobarbituric acid (TBA). Tissue extract (40 μl) was pipetted into 1.5 Eppendorf tubes, and 150 μl of 0.1 M potassium phosphate buffer was added to bring the volume to 190 μl . Fifty microlitres of 10% (w/v) trichloroacetic acid (TCA) were added to the extracts in order to precipitate the protein. These were then mixed with 75 μl of 1.3% (w/v) TBA dissolved in 0.35% NaOH and placed in an aluminium heating block at 80 °C for 30 min. The mix was then centrifuged in a Harrier 18/80R centrifuge (MSE Ltd, London, UK) for 5 min at 4 °C. Three hundred microlitres of each supernatant were transferred to fresh Eppendorf tubes. After cooling for 10 min, 260 μl of each extract were transferred into the wells of a 96-well plate and placed in a microplate reader (Spectramax 190, Molecular Devices) to measure A_{532} . Calibration was made using 1,1,3,3-tetramethoxypropane standards (TEP) in the range of 0-25 μM treated in the same way as the samples. The linear calibration graph (Fig. 4.2) allowed for the absorbance of the samples to be converted into MDA concentrations that were then expressed as nmol g^{-1} protein.

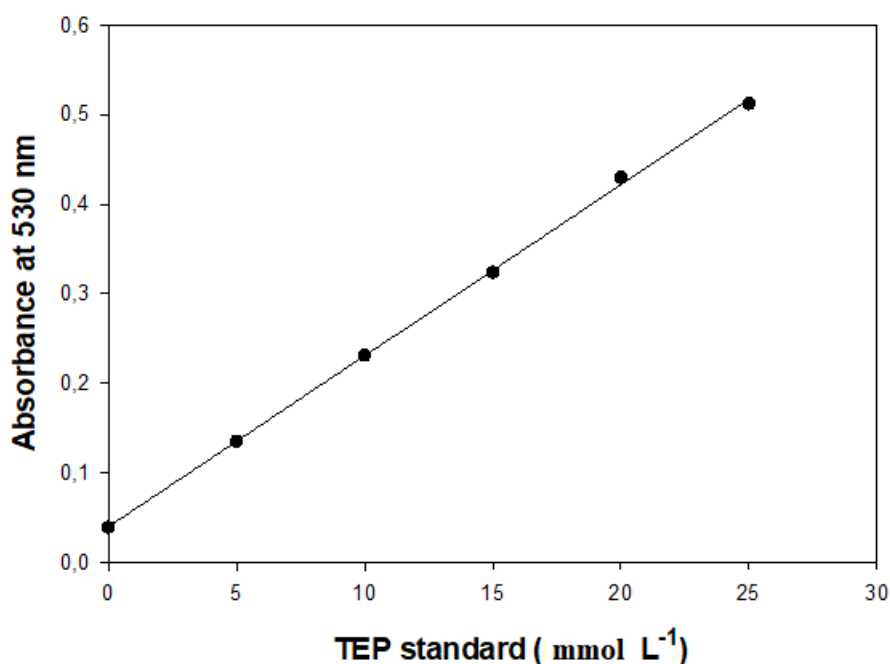


Figure 4.2 Calibration graph of MDA standards using TEP at the absorbance 530 nm.

4.2.5 Measurement of total glutathione content

Total glutathione (glutathione and glutathione disulphide) content in the tentacles was determined using a glutathione assay based on Owens and Belcher (1965) with some modifications in the protocol as described by Al-Subiai et al. (2009) from Adams et al., 1983. This is a kinetic assay in which catalytic amounts of glutathione cause a continuous reduction of 5,5'-dithiobis-(2-nitrobenzoic) acid (DTNB) to TNB. The oxidised glutathione formed is recycled by glutathione reductase and NADPH. When a reducing agent, such as glutathione, is added to DTNB it causes an increase in colour (yellow; the total glutathione content is quantified by the rate of colour change that is directly proportional to the concentration of total glutathione). The tissue extracts were first mixed in a 1:1 ratio with a buffered DTNB solution (pH 7.5, containing 100 mM potassium phosphate and 5 mM potassium EDTA) (Adams et al., 1983). Forty microlitres of the DTNB-treated samples were pipetted into the wells of a 96 well plate (Sterilin Limited, UK) to which 210 μ l of assay buffer containing glutathione reductase (G3664; 0.6 U) was subsequently added. The reaction was then started with the addition of 60 μ l of 1 mM NADPH (D23423) to the wells. The plate was, thereafter, placed in a microplate reader (Optimax, Molecular Devices, USA) which monitored the change at 412 nm for 15 min. Six samples were analysed simultaneously along with a blank containing assay buffer and a 20 μ M glutathione standard. Fig. 4.3 shows that the changes in absorbance were linear over the 15 min of measurement. The rate of change of the reaction was then used, in addition to that of the blank and the standard. Total glutathione content was calculated from the absorbance/time graphs and expressed as nmol mg^{-1} protein.

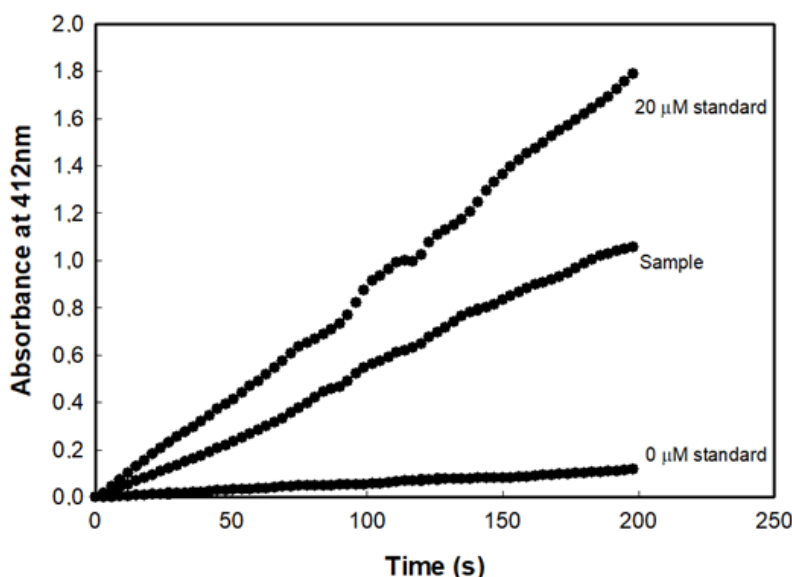


Figure 4.3 Example time courses for the glutathione assay, with a blank, a 20 μ M standard and a sample.

4.2.6 Measurement of superoxide dismutase activity

The assay method was adapted from McCord and Fridovich (1969). Xanthine oxidase acting enzymatically upon xanthine generates superoxide radicals ($O_2^{\bullet-}$), and the reduction of cytochrome *c* is used as an indicator of $O_2^{\bullet-}$ production. The reduction of cytochrome *c*, which can be followed at 550 nm, is inhibited by superoxide dismutase (e.g. see high-SOD control in the example time courses shown in Fig. 4.4). For the measurement of SOD activity, a reaction buffer was prepared with 50 mM potassium phosphate buffer (pH 7.8), the reaction mixture contained 25 mg ml⁻¹ cytochrome *c*, 0.5 mM xanthine and 100-fold dilution of xanthine oxidase (Sigma X4500) with the buffer. Ten microlitres of the sample or commercial SOD (Sigma S8409) were added into 250 μ l of the reaction mixture in the plate, and absorbance increase was monitored for 5 min in a microplate reader (SpectraMax 190, Molecular Devices). To estimate the initial rate of increase of A_{550} the time course data were fitted with an exponential rise to maximum (3 parameters) or a linear regression. All rates were corrected by subtracting the SOD-insensitive rate (high SOD). A reasonable estimate of this rate was obtained by using 10 μ l of the 1:9 diluted commercial SOD. The number of units of SOD activity per ml of the sample was calculated by dividing the control rate by rate of each sample and subtracting 1 (Moody A. J., personal communication). The result was then multiplied by 100 for 10 μ l sample to obtain the activity concentration in U ml⁻¹. The results were then expressed in U mg⁻¹ protein.

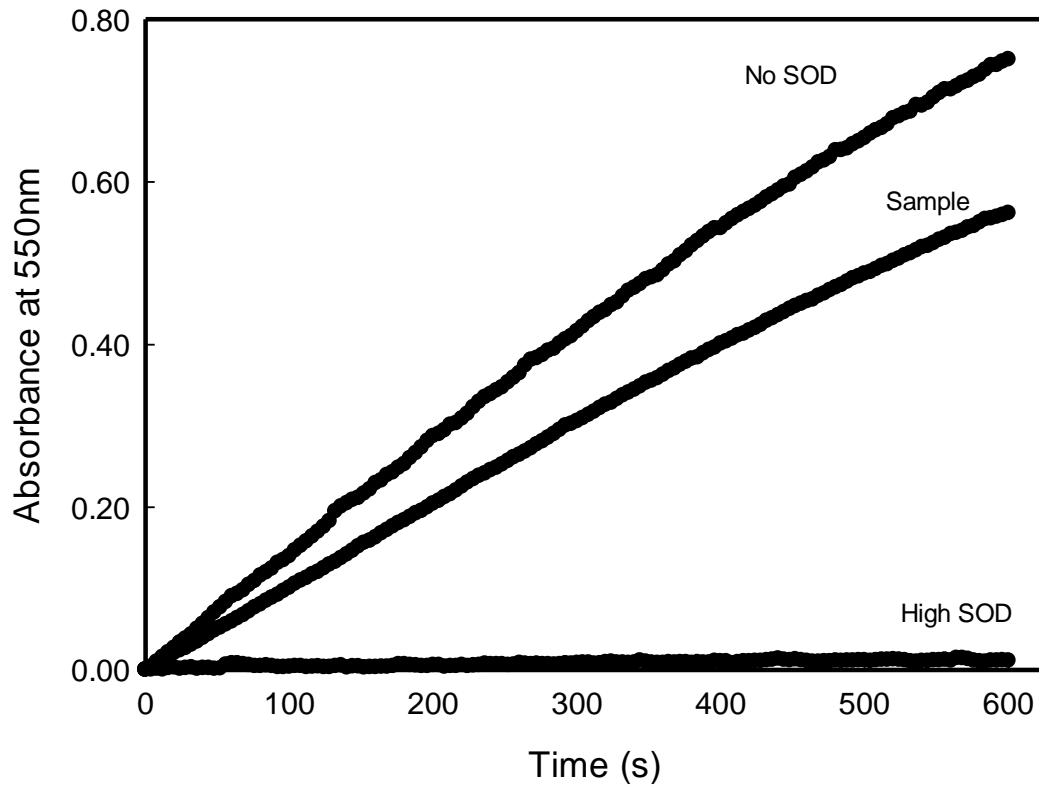


Figure 4.4 Example time courses for the SOD assay showing the High SOD-insensitive rate, the control rate in which SOD was absent, and the rate when a sample was added.

4.2.7 Measurement of catalase activity

Catalase activity in tissue extracts was monitored through the decomposition of hydrogen peroxide (H_2O_2) using a spectrophotometric method modified from that of Beers & Sizer (1952). Samples (10 μl) were added to a 96-well flat-bottom UV-transparent microplate reader (Spectramax 190, Molecular Devices) and the reaction with H_2O_2 started by adding 290 μl of 10 mM H_2O_2 solution (0.11 ml of 30% (w/w) H_2O_2 diluted with 100 ml of 100 mM potassium phosphate buffer solution, pH 7.0) at 25 °C. The rate of decomposition of H_2O_2 was measured at 240 nm. The change in absorbance was monitored for 100 s. One catalase unit was defined as the decomposition of 1 μmol of H_2O_2 min^{-1} and was calculated by using the molar extinction coefficient of H_2O_2 at 240 nm of $43.6 \text{ M}^{-1} \text{ cm}^{-1}$ (Merle et al. 2007). The catalase activity of the samples was expressed in $\mu\text{mol min}^{-1} \text{ g}^{-1}$ protein.

4.2.8 Measurement of total protein

Protein content in the sample material was measured spectrophotometrically using a BCA Protein Assay Kit (Pierce, Bonn, Germany). The BCA method reagent was prepared

according to the manufacturer's instructions using the microplate procedure. A bovine serum albumin (BSA; Sigma, Munich, Germany) stock concentration was made in bulk quantity prior to the measurements. BSA standard curves were made accordingly, and aliquots were stored to ensure an identical BSA content for each set of measurements. Undiluted samples (25 μ l) were added to the reagent solution (200 μ l BCA working reagent) and incubated at 37 °C for 30 min. Sample absorbance was measured at 562 nm at room temperature. The protein content of anemone extract was measured from the linear part of standard curve (Fig. 4.5) of bovine serum albumin and calculated in milligrams per ml.

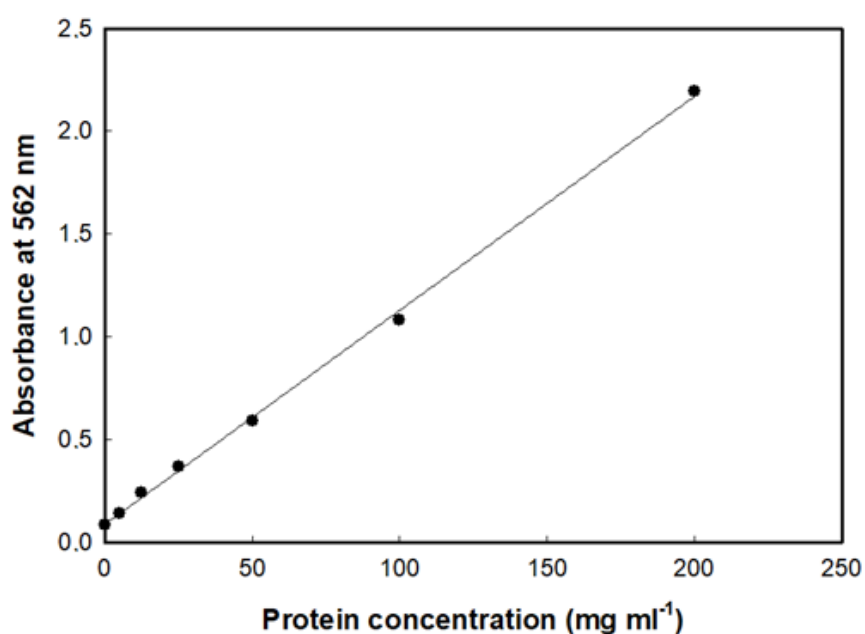


Figure 4.5 Calibration graph of protein using BCA assay at 562 nm.

4.2.9 Statistical analysis

Data were analysed using SPSS 25.0 statistical package (IBM Inc Armonk, NY, and the USA). Before all parametric tests, the data were tested for homogeneity of variance and normality (Sokal and Rohlf, 1995). Zooxanthellae density, total glutathione content, lipid peroxidation levels, SOD and catalase activity, were compared using two-way ANOVA with Tukey HSD posthoc tests to determine significance between the H₂O₂ treatment in two colour morphs. In cases where additional analyses were needed, one-way ANOVA was performed to check differences. In all analyses, differences were considered to be significant at a probability of 5% ($P < 0.05$).

4.3 Results

The effect of hydrogen peroxide (H_2O_2) oxidative stress was investigated in individuals of the two morphs of *Anemonia viridis*. Four levels of nominal H_2O_2 concentration, including a control, were set up and maintained for four hours.

4.3.1 Changes in zooxanthellae density

Figure 4.6 shows the effects of H_2O_2 on zooxanthellae density in the tentacle tissue. No significant interaction between H_2O_2 treatments and morphs were observed during the four hours of exposure ($P > 0.05$). For both morphs, the zooxanthellae density after all H_2O_2 treatments was not significantly changed, with less than a 10% increase or decrease from the control. Thus, no bleaching was observed with the elevated H_2O_2 exposure within the four-hour experiments.

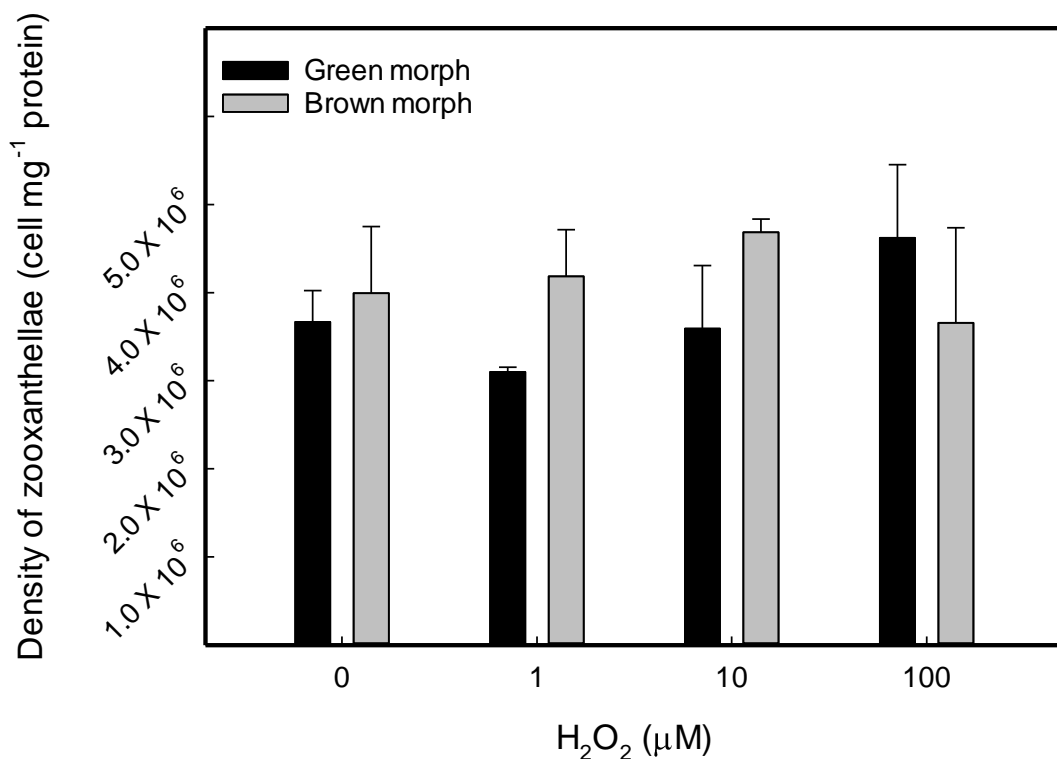


Figure 4.6 Zooxanthellae densities of *A. viridis* (tentacle tissue) under three different concentrations of H_2O_2 . Each data point is the mean \pm S.E.M. ($n = 3$).

4.3.2 Lipid peroxidation

Analysis of lipid peroxidation levels was performed by evaluating the MDA content and

any product of lipid peroxidation in the tissue. Effects of H₂O₂ concentration on lipid peroxidation within morphs were analysed by two-way ANOVA (morph × treatment). With both morphs, apparent effects of H₂O₂ were found (P = 0.018). Anemones exposed to 100 μM H₂O₂ showed the highest MDA value (20% increase) that was significantly different from the control (P = 0.021). Moreover, no significant differences in lipid peroxidation were observed between 1, 10 and 100 μM H₂O₂ concentrations. A similar pattern was found for the brown morph (Fig. 4.7) in TBARs analysis to that of the green morph, but the values were lower (3% increase) than the green morph and statistical significance was not found (P = 0.11).

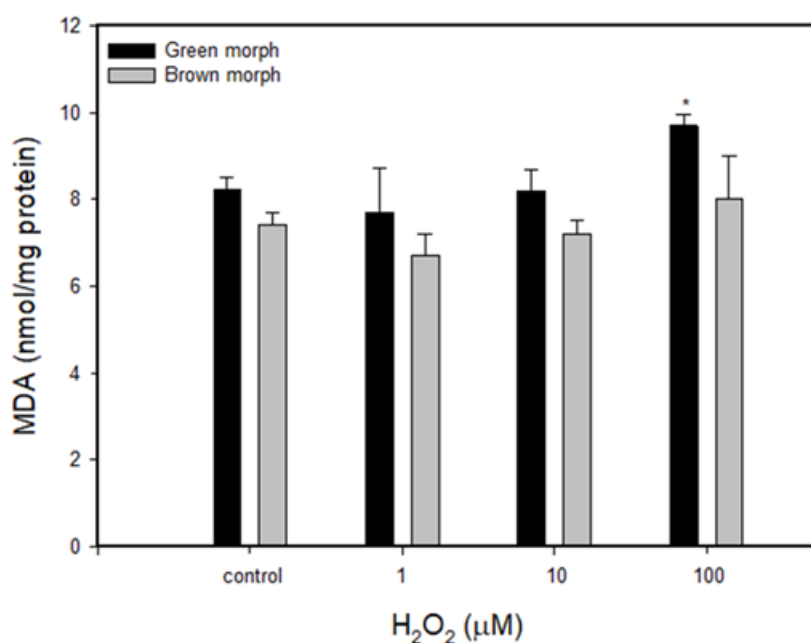


Figure 4.7 Effects of hydrogen peroxide on malondialdehyde content in tentacle extracts from green and brown morphs of *A. viridis* exposed to four different H₂O₂ treatments (0, 1, 10 and 100 μM). The asterisk indicates the treatment which is significantly different from the control (P = 0.021). Bars indicate means ± S.E.M. (n = 3).

4.3.3 Changes in non-enzymatic and enzymatic antioxidant content and activities

The analysis of total glutathione content data (Fig. 4.8) shows a non-significant decrease with increasing H_2O_2 ($P > 0.05$). The green morph shows a decrease of 25% at 100 μM of H_2O_2 compared to the control, while in the brown morph glutathione decreases less than 2% compared to the control at the same H_2O_2 concentration.

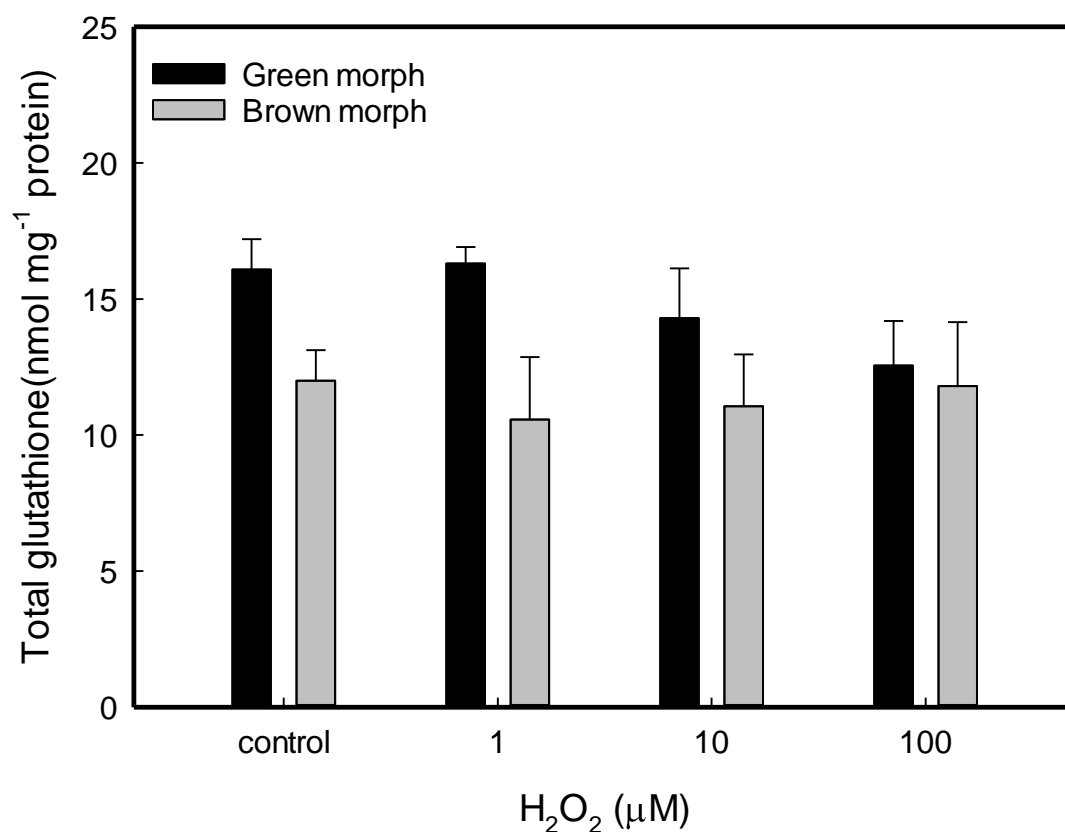


Figure 4.8 Total glutathione levels of *A. viridis* (tentacle tissue) of green and brown morphs under three different treatments with H_2O_2 over the course of 4 h. No significant difference was found in total glutathione levels among treatments ($P = 0.20$ and $P = 0.68$, respectively, $n = 3$). Error bars indicate standard error.

However, there was a significant difference of total glutathione between morphs at the control and 1 μM H_2O_2 treatment ($P = 0.02$).

With H_2O_2 exposure, there were no significant differences in SOD activity in either green or brown morphs ($P > 0.05$), during the 4 h exposure period (Fig. 4.9). The SOD activities of both types of anemones were variable between 1 μM and 10 μM , even though SOD activity of green morph after treatment with 100 μM H_2O_2 was the highest 28% compared to brown morphs that increase only 2% (Fig. 4.9).

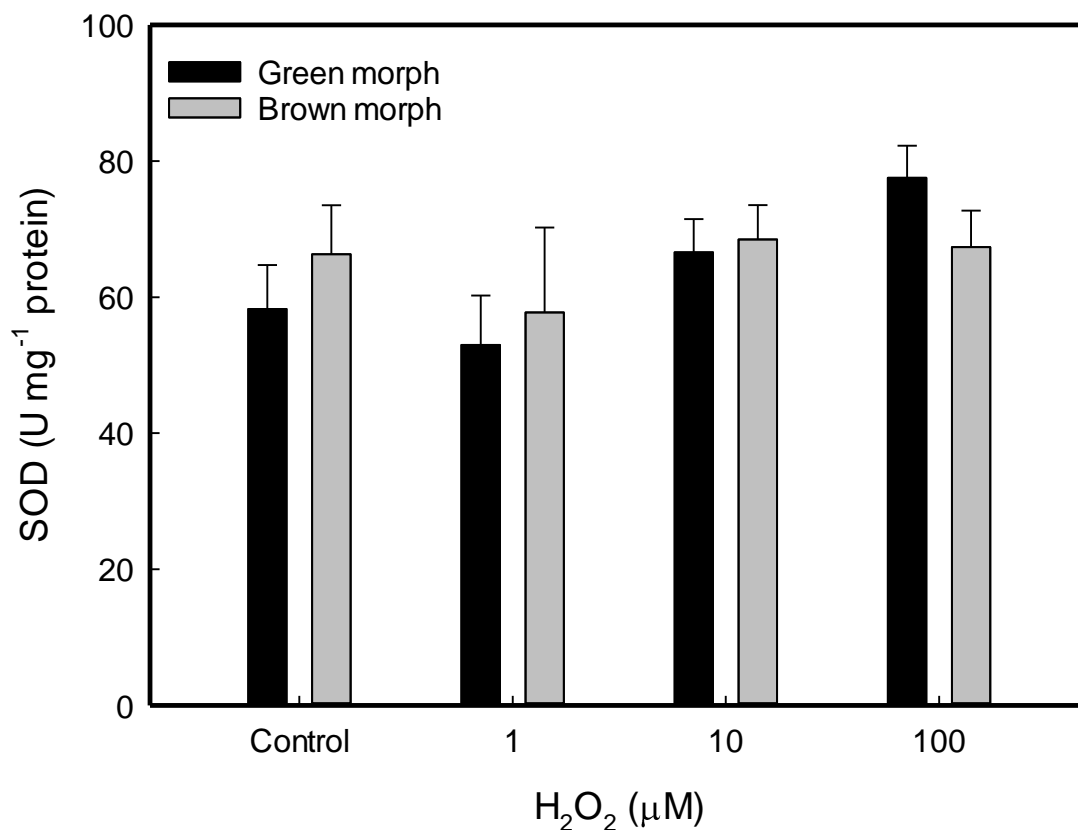


Figure 4.9 Effects of hydrogen peroxide on superoxide dismutase (SOD) activity in tentacle extracts from green and brown morphs of *A. viridis* exposed to four different H₂O₂ treatments (0, 1, 10 and 100 μM). Data (n = 3) are expressed in nmol g⁻¹ protein. No significant difference was found in the enzyme activity among treatments (P = 0.61 and P = 0.89, respectively). Error bars indicate standard error.

However, significant differences for H₂O₂ concentration treatment (P = 0.0001) and between the morphs (P = 0.044) were observed for catalase (CAT) activity. Figure 4.10 shows the effects of H₂O₂ on the activity of CAT in the tentacle tissue increased as the concentration in the treatment increased. The CAT activity significantly increased in both morphs at 10 and 100 μM (P = 0.032 and P = 0.0001, respectively). At 10 μM exposure there was a 29% increase in CAT activity in both morphs and was found to be significant according to t-test (P = 0.0013 for green morph and P = 0.034 for brown morph).

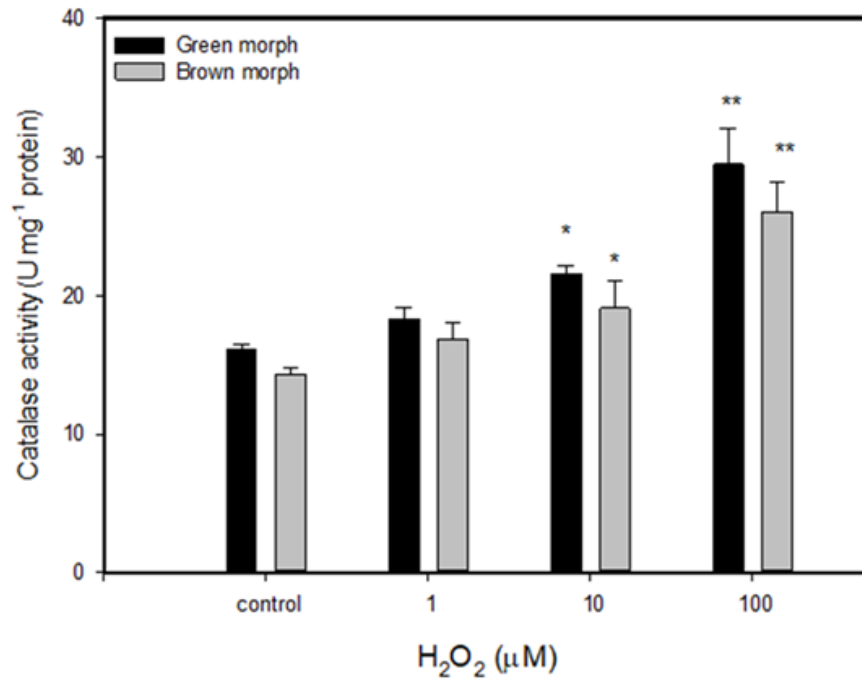


Figure 4.10 Effects of hydrogen peroxide on catalase (CAT) activity in tentacle extracts from green and brown morph of *A. viridis* exposed to four different H₂O₂ treatments (0, 1, 10 and 100 μM). Data (n = 3) are expressed in nmol g⁻¹ protein. The asterisk indicates the treatment which is significantly different from the control (*; P < 0.05; **; P < 0.001). Error bars indicate standard error.

4.4 Discussion

Exogenous H₂O₂ was applied to assess the oxidative stress responses of the sea anemone *Anemonia viridis*. Results presented in Chapter 2 and from other studies (Abele-Oeschger et al., 1997; Collén et al., 1996) show that in the rock pools concentration of H₂O₂ can reach 5 µM, probably because of photochemical production by algae. In addition, other studies found that the levels of H₂O₂ in rainwater can be substantially higher than this; for example; measurable concentrations of up to 82 µM have been reported in oceanic rainwater (Yuan et al., 2000) and up to 247 µM in continental rainwater (Sakugawa et al., 1990; Vione et al., 2003). As a result, precipitation events can substantially increase H₂O₂ levels in surface waters (Cooper et al., 1987; Yuan et al., 2000) and in particular intertidal rock pools. Therefore, this is an appropriate way to investigate the biological response of a coastal marine invertebrate, *Anemonia viridis*, likely to encounter elevated H₂O₂ levels in its habitat that could trigger oxidative stress (Abele-Oeschger et al., 1997). Furthermore, H₂O₂ is the most abundant and long-lived ROS in marine environments and can diffuse freely across membranes.

Anthozoans (such as *A. viridis*) can live in oligotrophic environments due to their symbiotic relationship with unicellular dinoflagellates known as zooxanthellae. However, zooxanthellae are susceptible to light and temperature-mediated damage, which causes oxidative stress in the cnidarian host. As a result, zooxanthellae can be ejected and/or lose their pigments, causing the host's overall colour to be bleached. In this study it was found that there were no differences in the density of zooxanthellae in the anemones, even with exposure to a nominal concentration of 100 µM H₂O₂ (Fig. 4.6). Thus, no bleaching of either colour morph was observed. A similar result was also found by Higuchi et al. (2008) when another symbiotic Cnidarian, the tropical reef coral, *Galaxea fascicularis*, was exposed to H₂O₂ for five days. The coral was exposed to a ten-fold increase in H₂O₂ compared to the control, but showed no bleaching, although the maximum concentration used (3 µM) was much lower than here. According to Gates et al. (1992) five separate biological mechanisms are known to be involved in symbiont removal from Cnidarian host tissues: necrosis, apoptosis, detachment of the host cell, exocytosis *in situ*, and annihilation of the symbiont. These symbiont loss events are believed as an ultimate defence of Cnidarians against oxidative stress (Downs et al., 2002). No bleaching was observed at the highest level of H₂O₂ tested in *Anemonia viridis*, even though H₂O₂ is thought to be in some way associated with bleaching (Lesser, 1997). This might be because the oxidative stress was not due to the *in-situ* generation of H₂O₂ via the

symbiotic algae. This suggests that bleaching is more likely to occur when H₂O₂ is produced by zooxanthellae under stress conditions, as is the case with corals and anemones exposed to hyperthermic stress (Dunn et al., 2004; Franklin et al., 2004; Strychar et al., 2004; Higuchi et al., 2009). Temperature stress causes photoinhibition and damage of the symbiont chloroplast apparatus, which act in concert to initiate the bleaching cascade. For example, damage to the D1 protein caused the rate of photodamage to exceed the capacity to repair the damage, resulting in the loss of PSII functional reaction centres (Warner et al., 1999), which in turn affected carbon fixation (Smith et al., 2005) and the Mehler reaction (Asada, 200; Weis, 2008). The host may have a mechanism that actively destroys symbionts, ultimately digesting or expelling them due to their different concentrations (Higuchi et al., 2012).

The other possibility is that the oxidative stress-tested by the 100 µM H₂O₂ in seawater was within the range that *A. viridis* is able to tolerate normally or perhaps acclimatise to, the adaptive bleaching hypothesis (ABH) (Shick, 1991; Buddemeier et al., 2004, Fautin & Buddemeier 2004). According to this hypothesis symbiotic Cnidarians, including anemones may use the strategy of switching from a less favourable symbiont partner to a more favourable one when they encounter a wide range of environmental stressors in their habitat beforehand (Chen et al., 2005; Brading et al., 2007; Silverstein et al. 2015). In coral, quantitative PCR and chlorophyll fluorometry was used to examine the structure and function of *Symbiodinium* colonies within coral hosts, as well as repeated bleaching and recovery studies on the coral *Montastraea cavernosa*. Three months later, a second heat stress (also 32 °C for 10 days) was applied, and previously bleached corals that were now dominated by D1a *Symbiodinium* suffered less photodamage and symbiont loss than control corals that had not previously bleached and were thus still dominated by *Symbiodinium* C3 when the second heat stress was applied (Silverstein et al. 2015). It appears from these findings that D1a symbionts, which were previously unidentified, only grew more widespread after bleaching was performed. The snakelocks anemones collected in this study may have suffered from heat exposure at low tide throughout the summer and may have utilized the same strategy to thrive in their particular ecosystem (Jarrold et.al., 2012; Silverstein et al. 2015) because they came from rock pools rather than deeper water where the temperature might be more stable.

The second indication of oxidative stress chosen to determine the effects of H₂O₂ on *A. viridis* was lipid peroxidation (LPO). LPO (measured as the LPO product, MDA, in this study) is believed to be caused by high ROS levels and subsequent cellular damage.

Measuring lipid peroxidation provides information as a biomarker for ROS-induced cellular membrane damage (Flores-Ramírez & Liñán-Cabello 2007). The TBARS assay used in this study showed a tendency for MDA levels to increase as the concentration of H₂O₂ increased and did show more effects in the green morphs but not in their brown counterparts. These results agree with most of the literature on the subject. In most cases, lipid peroxidation increases with oxidative stress, indicating cellular damage (Downs et al., 2002; Richier et al., 2005; Teixeira et al., 2013). For example, in gastropods *Mytilus galloprovincialis*, MDA levels escalated 115% as a result of H₂O₂ exposure for four days (Cavaletto et al., 2002). The same trends have also been observed in another invertebrate as observed by Storch et al. (2000), who found that MDA levels in the lugworm *Arenicola marina* significantly increased following the application of peroxide. Another study by Jordão (2011) found that the anemone *Actinia equina* do not exhibit a significant increase of lipid peroxidation when exposed to mercury (Hg) for 96 h. It was suggested that this might be related to increased antioxidant activity that has been acting as the protector of the cells (Jordão, 2011).

The changes of lipid peroxidation in this study are similar to a study by Caparkaya et al. (2010). They found that MDA levels in the green morph of *A. viridis* increased significantly; on the other hand, no significant change was observed in MDA levels in the brown morph when the anemones were exposed to UV light (Caparkaya et al., 2010). The colour morphs of *A. viridis* differ because of the much higher levels of expression of green fluorescent protein (GFP) and related chromoproteins (CP) in the green morph compared to the brown (Leutenegger et al., 2007). It might be expected that levels of lipid peroxidation would be lower in the green morph as GFP and CP have been suggested to have a photoprotective function (Krasowska et al., 2006) and/or antioxidant function, showing SOD activity (Bou-Abdallah et al., 2006).

To further explore the potential responses of *A. viridis* to H₂O₂ exposure, the antioxidant defences of the anemones were investigated. The anemone, like other aerobic organisms, possesses comprehensive enzymatic and non-enzymatic antioxidant defences to cope with overproduction of ROS. Increases in antioxidant enzyme activities are indicative of increased concentrations of ROS (Lesser et al., 1990). The insignificant lipid peroxidation detected during the H₂O₂ exposure could be indicative of the presence of an effective antioxidant defence system. All data concerning the enzymatic and the non-enzymatic antioxidant defence systems indicate an approach of their boundaries of physiological tolerance during exposure to a higher concentration of H₂O₂. In this study, the activity of

catalase (CAT) was found to gradually rise with each level of H₂O₂ treatment, with significant increases at higher H₂O₂ concentrations. Superoxide dismutase (SOD) also showed an increase, but this was not statistically significant, while total glutathione tended to decrease but again not significantly.

The increased CAT activity, in response to H₂O₂ exposure that did not cause bleaching, which was significantly different from the controls (10 and 100 µM), for both colour morphs, suggested that the enzymatic antioxidant catalase may play a key role in the acclimation of *A. viridis* to peroxide stress. Catalase works by catalysing the decomposition of toxic H₂O₂ into water and molecular oxygen (Fridovich 1998), because an excess of H₂O₂ must be avoided in order to prevent changes in cell physiology. This is primarily due to the presence of free Cu and Fe cations in the cytosol, which react with H₂O₂ in the Fenton reaction to produce hydroxyl radicals, which can cause oxidative damage to cells. Rosa and colleagues (2005) found that the lack of high CAT response resulted in oxidative stress, as evidenced by higher levels of LPO and DNA damage in H₂O₂ exposed polychaeta *Laeonereis acuta*. Another study, however, found that even though catalase activity was increased significantly after exposure to hydrogen peroxide, lipid peroxidation still occurred as a result of oxidative stress (Cavaletto et al., 2002). This study's findings are consistent with those of previous related studies by Higuchi et al (2009). They discovered that the activity of CAT in coral tissue and isolated zooxanthellae increased significantly in response to H₂O₂ exposure. Since H₂O₂, in that study, was exposed externally, the host animal must have been directly exposed to H₂O₂. CAT activities increased within a few minutes to several hours, according to Levy et al. (2006). The tissue distribution of catalase activity was measured in *A. viridis* by Merle and colleagues (2007), and they found that, generally, the ectodermal fraction had the highest catalase activity, accounting for 67% of the total catalase activity. This is in comparison to less than 10% catalase activity in zooxanthellae and less than 25% catalase activity in the endodermal fraction. Other studies on supplementary symbiotic marine organisms have found that catalase activity is higher in animal tissue than in zooxanthellae (Tyler, and Trench, 1988; Lesser and Shick, 1989). It is possible that the anemone tissue containing the CAT enzyme is very responsive. Hydrogen peroxide enters cells by diffusion; then catalase in host tissue plays an important role in the detoxification.

In this study, total glutathione was also assessed as an antioxidant. The cell contains both reduced (GSH) and oxidized (GSSG) forms of glutathione. To combat reactive oxygen species (ROS), eukaryotic cells require glutathione. Typically, this occurs because GSH

works as a cofactor in the elimination of H_2O_2 via glutathione peroxidase activity (Dickinson & Forman 2002, Sunagawa et al., 2008). Changes in GSH levels (decreases or increases) have been highlighted as a potential stress biomarker in marine invertebrates (Regoli and Principato, 1995; Ringwood et al., 1998). However, tissue extracts from *A. viridis* anemones subjected to the greatest concentration of H_2O_2 (100 μM) exhibited no significant decrease in total glutathione content. This result was comparable to that of Cavaletto et al. (2002), who detected no significant glutathione content in blue mussels (*Mytilus galloprovincialis*) and found that treatment with H_2O_2 for four days resulted in a non-significant decrease of -22% in glutathione content, concurrent with an increase in MDA levels. They suggested that glutathione is not involved in the defence of mussels against H_2O_2 . Mitchelmore et al. (2003) reported in a separate study on heavy metal (Cd) exposure that the symbiotic anemone *Anthopleura elegantissima* exhibited a high degree of Cd accumulation but no significant drop in GSH compared to its aposymbiotic counterpart. They also found that symbiotic anemones had higher GSH levels than aposymbiotic ones. However, although Cd may cause oxidative stress the role of glutathione in the detoxification of Cd may be different to its potential role in detoxification of H_2O_2 since phytochelatin, metal-chelating polymers of GSH, are known to be present in Cnidarians (Goldstone, 2008).

During the four-hour exposure to H_2O_2 , there were no significant variations in SOD activity in anemone tissue. The anemone's SOD activity rose, but the rise was not statistically significant, despite exposure up to 100 μM . Since SOD catalyses the transformation of superoxide ($\text{O}_2^{\cdot-}$) into oxygen and H_2O_2 , this was anticipated. Increases in antioxidant enzyme activity indicate an increase in reactive oxygen species (ROS) concentrations (Lesser et al. 1990). Given that variations in SOD activity reflect changes in $\text{O}_2^{\cdot-}$ concentrations, the results indicate that H_2O_2 exposure during the incubation period did not generate $\text{O}_2^{\cdot-}$ production in the anemone tissue.

In conclusion, the findings provided support the hypothesis that the symbiotic snakelocks anemone's reaction to H_2O_2 involves an increase in antioxidant capacity. This implies that short-term (4 h) H_2O_2 exposure stress might cause rapid oxidative stress, culminating in a rise in MDA in the green morph at 100 μM . CAT played a crucial part in anemone H_2O_2 stress conditions, with higher CAT activities caused by elevated H_2O_2 concentrations in the tissue. This suggests that H_2O_2 from the surrounding saltwater diffused to the anemone's ectoderm and entered the cytoplasm (Higuchi et al., 2009). This data also indicates that symbiont ejection is not triggered by external H_2O_2 exposure, but rather to

the synthesis of endogenous H₂O₂ by symbiont algae in response to environmental stress (Lesser, 1997).

Chapter 5

General Discussion

Macroalgae have been recognized as a possible source of reactive oxygen species (ROS) (e.g., H₂O₂) in some rockpools and other enclosed settings, and the accumulation of these ROS may be detrimental to other organisms. The research detailed in this thesis examined the impact of abiotic stressors on the H₂O₂ levels generated by marine macroalgae (seaweeds), as well as the effect of H₂O₂ on a co-occurring organism in rockpools. The potential relationships between these two variables were investigated through field observations and controlled laboratory studies. In the first chapter methods were developed for measuring H₂O₂ in the field and these were applied to samples collected from rockpools with various levels of seaweed cover. Physicochemical parameters were also measured in the rockpools.

The initial challenge of the study was to develop a viable and trustworthy method for quantifying H₂O₂ levels in seawater pools. A fluorescence method (FL) was initially used because this is by far the most common type of method used and it could be adapted so that the fluorescent product was generated in the field but measured on return to the laboratory. However, it was not sensitive enough to concentrations of H₂O₂ below 1 µM. Because of this and because it is unaffected by the absorbance and/or fluorescence of high concentrations of DOM, a much more sensitive chemiluminescence method (CL) was developed, which could be carried out entirely in the field. In both cases reactions with H₂O₂ in seawater are catalysed by horseradish peroxidase (HRP), and both approaches have been used previously to detect peroxide in oligotrophic waters (Miller et al., 2005). However, the CL method developed here used a novel approach of measuring chemiluminescence using a portable luminometer. This type of luminometer is normally used to determine the amount of ATP in the environment using the firefly bioluminescence system. These measurements are routinely employed to detect microbial contamination of surfaces, for example, in the context of hospital or food safety (Davidson et al., 1999), resulting in the development of very portable, low-cost equipment capable of logging a series of readings. To our knowledge, this is the first time that such an instrument has been used to measure luminol-dependent chemiluminescence, which produces light with a significantly different wavelength than firefly bioluminescence. Because of the relatively low cost of the portable luminometer this CL method could have applications in contexts other than rockpools where levels of H₂O₂ need to be measured in the field.

The levels of H₂O₂ in the rockpools revealed in Chapter 2 are higher (mostly in the micromolar range) than the levels of H₂O₂ in other parts of the ocean. Other researchers

have observed H₂O₂ profiles from the ocean surface to the various ocean basins, which are in the pico to nanomolar range (Table 1.2). Most of the pools studied here were routinely intertidal on all tides with a couple refreshed with seawater only during spring tides. Hence in most cases the water would remain stagnant for several hours, exposed to solar radiation that can promote H₂O₂ generation via photochemical reduction of oxygen (Cooper and Zika, 1983). In the open ocean the emphasis has been on photochemical reduction of oxygen as the source of H₂O₂ generation via UV interaction with DOM (Abele-Oeschger et al., 1997; Thornton, 2014) but it is also recognised that H₂O₂ can be produced biogenically in saltwater via phytoplankton, e.g., as a by-product of photosynthesis (Johanson et al., 1989; Zika et al., 1985a). The results of this investigation indicate that the highest concentrations of H₂O₂ were detected in pools with a high macroalgae content (Fig. 2.14) suggesting the importance of biogenic H₂O₂ produced by the algae through photosynthesis, photorespiration or other metabolic processes. The range of concentrations found in ‘weedy’ rockpools corresponds well with those found (micromolar) with individual species of macroalgae under controlled laboratory conditions as described in the work in Chapter 3 and is consistent with levels found previously with other species of macroalga under controlled conditions by Collén and co-workers (Collén et al., 1995; Collén & Pedersén, 1996; Collén and Davison, 1999b). Together the results from Chapters 2 and 3, suggest that H₂O₂ in rockpools with high levels of macroalgae is mainly biogenic rather than photochemical in origin. However, levels of H₂O₂ produced by all macroalgae are not the same; the results from Chapter 3 show that a brown alga, *Fucus serratus*, and a green alga, *Ulva lactuca*, produced 4-5 times higher levels of H₂O₂ than a red alga, *Chondrus crispus*. Whether this is a general property of red algae could be the subject of further investigation; Collén et al. only looked at examples of brown and green algae, so the result obtained here is the only example of a comparison between these groups and a red alga. Chloroplasts in these different groups of macroalga differ in many ways, e.g., origin, morphology (Solymosi, 2012) and types of accessory pigments {red algae have higher concentrations of carotenoids, phycocyanin and phycoerythrin (Osório et al. 2020; Al Solami 2020)}, and have different photosynthetic properties, e.g., the lower basal value of F_v/F_m seen in red algae compared to brown and green algae as well as vascular plants (Fig. 3.9; Kearns & Turner, 2016; Baumann et al., 2009).

As well as producing lower steady state levels of H₂O₂ on its own some evidence was presented in Chapter 3 that the red alga, *C. crispus*, in combination with either *F. serratus* or *U. lactuca*, could decrease the levels of H₂O₂ in the surrounding seawater compared to

that expected from simple addition of the concentrations of H₂O₂ produced by the algae alone. In future the quality of this evidence could be improved and extended to other combinations of macroalgae, but it suggests that the levels of H₂O₂ seen in rockpools in the field in Chapter 2 are a product of the different levels of production and removal in particular pools. The lower level of H₂O₂ produced by *C. crispus*, may be due to lower rates of production, but it could also be that red algae have greater antioxidant capacity than green or brown algae, and there is some evidence that this is the case; Al Solami (2020) found higher activities of the antioxidant enzymes SOD and catalase in red algae versus green. However, this cannot explain the lower level of H₂O₂ seen when *C. crispus* was combined with either of the other two algae, leading to the possibility that *C. crispus* may release ‘catalase’ activity into the surrounding water. It is already known that seawater has the capacity to decompose H₂O₂ (Petasne and Zika, 1997). This could be investigated in future research, as could further combinations of green, brown and red algae, and related to field studies (Chapter 2) comparing H₂O₂ levels in rockpools with different macroalgal assemblages.

In the work described in Chapter 4, the effect of H₂O₂ on an organism that lives in rockpools, the snakelocks anemone, *Anemonia viridis*, was investigated, considering the levels of H₂O₂ that were found in both in the field (Chapter 2) and in the laboratory (Chapter 3). Based on the findings of this work, it appears that exposure to H₂O₂ for a short period of time (four hours) did not have major immediate consequences, and only led to a slight increase in lipid peroxidation at the highest concentration of H₂O₂ and no decrease in levels of total glutathione. This is despite this organism potentially being particularly sensitive to H₂O₂ because of the presence of the symbiotic photosynthetic dinoflagellate (zooxanthellae), *Symbiodinium*, in its tissues, leading to its being used as a model for understanding temperature-induced bleaching in other Cnidarians, e.g., corals (Richier et al., 2005; Richier et al., 2006). However, even at 100 µM there appeared to be no change in zooxanthellae density in *A. viridis* over 4 h. The only major effect of H₂O₂ that was observed was a marked increase in catalase activity, suggesting that catalase is essential for the survival of these anemones when they are subjected to H₂O₂ stress. Given this outcome of the work described in Chapter 4, combined with the information obtained in Chapters 2 and 3, it seems that oxidative stress caused by H₂O₂ not be an issue, even though levels of H₂O₂ may be higher in rockpools than in open ocean. However, it may be premature to reach this conclusion.

Firstly, the study in Chapter 4 was limited to 4 h exposure to H₂O₂, whereas in rockpools

on the upper shore there are likely to be anemones that are exposed to elevated H_2O_2 levels for longer than this in rockpools where the seawater is not refreshed over a series of neap tides. In addition, results from Chapter 3 suggest that desiccation of macroalgae followed by rehydration, a common occurrence in the intertidal, can lead the production of much higher levels of H_2O_2 . This is consistent with studies by Flores-Molina et al. (2013) into the effects of desiccation stress in a range of intertidal macroalgae who found higher cellular levels of H_2O_2 both during and following desiccation than those seen before desiccation. However, the data in Chapter 3 was limited to a single time point after hydration, so this approach needs to be extended to understand how H_2O_2 production changes following rehydration, and how this might impact on levels in rockpools. Finally, there is also some evidence in Chapter 2 that levels of H_2O_2 in rockpools may be locally higher. This work also needs to be extended; the pools investigated were dominated by *U. lactuca* so it would be interesting to repeat this in pools with more mixed assemblages of macroalgae. Taken together, more knowledge of the potential range of H_2O_2 concentrations that may occur in rockpools could feed into the design of experiments like that described in Chapter 4.

More generally, to establish whether levels of H_2O_2 in rockpools are detrimental would require extension of the work in Chapter 4 to other organisms. Possible candidates include the shrimp, *Palaemon elegans*, which although having a relatively impermeable exoskeleton, may still be vulnerable to H_2O_2 via their gills. A detrimental effect of $20 \mu\text{M}$ H_2O_2 on oxygen consumption has already been demonstrated in the epibenthic shrimp, *Crangon crangon*, but *Palaemon elegans* is more likely to be found in rockpool. It should also be pointed out that H_2O_2 is only one example of the ROS that may be present in rockpools, being chosen because of its relative stability. One way of measuring levels of ROS other than H_2O_2 is to use the changes in fluorescence on the oxidation of dichlorohydrofluorescein diacetate to dichlorofluorescein by ROS (Collén and Davison, 2002). It may be possible to do this in the field using the same approach as that used here in the FL method for measuring H_2O_2 in the field, i.e., to carry out the fluorogenic reaction in the field and then do the fluorescence measurement in the laboratory. However, it is not entirely clear what is being measured using this method (Halliwell and Gutteridge, 2007).

Given the difficulty of measuring ROS other than H_2O_2 another possibility might be to bring together aspects of the work in Chapters 3 and 4, and use mesocosm experiments where rockpool organisms are exposed under controlled conditions to the mixture of ROS

produced by co-incubating organisms with individual species or combinations of species of macroalgae. As well as eliminating the need to measure ROS levels, another advantage of this approach is that the algae can maintain steady state levels of ROS during the experiment. A problem with the exposure of *A. viridis* to H₂O₂ described in Chapter 4 is that the level of H₂O₂ was only nominal because it declined throughout the experiment (Fig. 4.1).

A further direction that needs to be explored in relation to the potential detrimental effects of H₂O₂ generated by macroalgae in rockpools on rockpool organisms is the consequences of combining stressors. When two stressors are applied simultaneously, there may be antagonistic or synergistic interactions between the stressors, the latter being of particular interest here. In the experiment described in Chapter 4, the anemones were maintained under normal seawater conditions in terms of the pH (8.2) and salinity (33 psu) during the exposure to H₂O₂, and the temperature and light intensity were mid-range for *A. viridis*. However, it would be interesting, for example, to combine the exposure to H₂O₂ with elevated pH and/or temperature and/or light intensity; in the rockpools monitored in Chapter 2 the pH increased over time in emersed pools and exceeded 9 after 4 h, as did temperature. Like other Cnidarians, it is already known that increased temperature may cause bleaching, loss of the photosynthetic zooxanthellae, in symbiotic anemones (Sawyer and Muscatine, 2001); the combination of elevated temperature and H₂O₂, may lower the threshold for bleaching in *A. viridis*, having more profound consequences.

Potentiated toxicity, which is related to the concept of 'stress on stress,' is one of two types of a more general phenomena known as synergistic toxicity, which happens when two substances in sublethal concentrations that do not harm individually cause significant harm when combined (Todgham and Stillman, 2013). Many potentially harmful contaminants enter the marine environment, but copper is of special relevance since it may end up in rockpools as a component of antifouling paint particles (Turner, 2010). Antifouling paint contains copper, which helps to inhibit the growth of epiphytes and other organisms on ship hulls. Copper is well known for its toxicity (Gaetke and Chow, 2003); by its redox activity, it can produce oxidative stress via Fenton-like reactions (Haber-Weiss reaction) with O₂^{•-} and H₂O₂, potentially leading to the formation of hydroxyl radicals (•OH; Halliwell and Gutteridge, 2007). As a result, the presence of copper may exacerbate the effects of H₂O₂, and it would be interesting to investigate the effect of exposing rockpool organisms like *A. viridis* to copper and H₂O₂ at

environmentally relevant amounts.

Finally, in the study described in Chapter 4 the capacity of *A. viridis* to acclimatise to at least a short-term exposure to H_2O_2 was established, since there was a significant (within 4 h) increase in catalase activity. Other rockpool organisms may be able to acclimatise in a similar way, while others may be able to use behavioural changes to cope with elevated H_2O_2 levels in rockpools, e.g., which can reduce their activity and close their shells using their opercula. Capacity to acclimatise to H_2O_2 may be an adaptation that organisms from 'weedy' rockpools have that organisms that do not live in such rockpools do not. It would be interesting to establish whether the capacity to deal with exogenous H_2O_2 differs between these groups of organisms.

References

- Abele, D., Burlando, B., Viarengo, A. & Pörtner, H.-O. (1998) Exposure to elevated temperatures and hydrogen peroxide elicits oxidative stress and antioxidant response in the Antarctic intertidal limpet *Nacella concinna*. *Comp. Biochem. Phys. B*, 120, 425-435.
- Abele-Oeschger, D., Oeschger, R., & Theede, H. (1994) Biochemical adaptations of *Nereis diversicolor* (Polychaeta) to temporarily increased hydrogen peroxide levels in intertidal sandflats. *Mar. Ecol. Prog. Ser.*, 106, 101–110.
- Abele-Oeschger, D. & Buchner, T. (1995) Effect of environmental hydrogen peroxide accumulation on filtration rates of the intertidal bivalve clam *Cerastoderma edule*. *Verh Dtsch Zool Ges.*, 88, 93
- Abele-Oeschger, D., Sartoris, E. J. & Pörtner, H. O. (1996) Effect of elevated hydrogen peroxide levels on aerobic metabolic rate, lactate formation, ATP homeostasis and intracellular pH in the sand shrimp *Crangon crangon*. *Comp. Biochem. Physiol. C*, 117, 123-129.
- Abele-Oeschger, D., Tüg, H. & Röttgers, R. (1997) Dynamics of UV-driven hydrogen peroxide formation on an intertidal sandflat. *Limnol. Oceanogr.*, 42, 1406-1415.
- Allen, J.F., 2003. Cyclic, pseudocyclic and noncyclic photophosphorylation: new links in the chain. *Trends Plant Sci.* 8, 15–19.
- Alric, J., Pierre, Y., Picot, D., Lavergne, J. & Rappaport, F. (2005) Spectral and redox characterization of the heme c_1 of the cytochrome b_6/f complex. *Proc. Natl. Acad. Sci. USA* 102, 15860–15865.
- Alscher, R. G., Erturk, N. & Heath, L. S. (2002) Role of superoxide dismutases (SODs) in controlling oxidative stress in plants. *J. Exp. Bot.*, 53, 1331-1341.
- Al Solami, M. A. (2020). Comparative response of red and green algae to the quality of coastal water of Red Sea, Haql, Saudi Arabia. *J. Environ. Prot.*, 11, 793-806.
- Arakaki, T., Ikota, H., Okada, K., Kuroki, Y., Nakajima, H. & Tanahara, A. (2007) Behavior of hydrogen peroxide between atmosphere and coastal seawater around Okinawa Island. *Chikyukagaku Geochem.*, 41, 35-41.
- Armoza-Zvuloni, R. & Shaked, Y. (2014) Release of hydrogen peroxide and antioxidant

by the coral *Stylophora pistillata* to its external *milieu*. Biogeosciences Discuss., 11, 33-59.

Arnér, E. S. & Holmgren, A. (2000) Physiological functions of thioredoxin and thioredoxin reductase. Eur. J. Biochem., 267, 6102-6109.

Asada, K. (1999) The water-water cycle in chloroplasts: scavenging of active oxygens and dissipation of excess photons. Annu. Rev. Plant Biol., 50, 601-639.

Bader, H., Sturzenegger, V. & Hoigne, J. (1988) Photometric method for the determination of low concentrations of hydrogen peroxide by the peroxidase catalyzed oxidation of N, N-diethyl-p-phenylenediamine (DPD). Water Res., 22, 1109-1115.

Ballesteros, E., Ballesteros, E., & Romero, J. (1988). Zonation patterns in tideless environments (Northwestern Mediterranean): looking for discontinuities in species distributions. Inv Pasq., 52(4), 595-616.

Baniulis, D., Hasan, S.S., Stofleth, J.T., Cramer, W.A. (2013) Mechanism of enhanced superoxide production in the cytochrome *b₆f* complex of oxygenic photosynthesis. Biochemistry (Mosc.) 52, 8975–8983.

Barber, J. & Tran, P. D. (2013). From natural to artificial photosynthesis. J. Roy. Soc. Interface, 10, 20120984.

Barbier, E. B., Hacker, S. D., Kennedy, C., Koch, E. W., Stier, A. C. & Silliman, B. R. (2011) The value of estuarine and coastal ecosystem services. Ecol. Monogr., 81, 169-193.

Barja, G. (2002) Minireview: the quantitative measurement of H₂O₂ generation in isolated mitochondria. J. Bioenerg.Biomembr., 34, 227-233.

Bartosz, G. (2009) Reactive oxygen species: destroyers or messengers? Biochem. Pharmacol., 77, 1303-1315.

Baumann, H. A., Morrison, L. & Stengel, D. B. (2009) Metal accumulation and toxicity measured by PAM—chlorophyll fluorescence in seven species of marine macroalgae. Ecotox. Environ Safety, 72, 1063-1075.

Bendall, D. & Manasse, R. (1995) Cyclic photophosphorylation and electron transport. BBA Bioenergetics, 1229, 23-38.

- Bertness, M.O., Gaines, S. & Hay, M.E. 2001. Marine community ecology. Sinauer Associates Incorporated.
- Bertness, M. D. & Callaway, R. (1994) Positive interactions in communities. *Trends Ecol. Evol.*, 9, 191-193.
- Bhattacharjee, S. (2012) The language of reactive oxygen species signaling in plants. *J. Bot.*, 2012, 22 pages
- Bieza, S. A., Boubeta, F., Feis, A., Smulevich, G., Estrin, D. A., Boechi, L., & Bari, S. E. (2015). Reactivity of inorganic sulfide species toward a heme protein model. *Inorg. Chem.*, 54, 527-533.
- Bischof, K. & Rautenberger, R. (2012) Seaweed responses to environmental stress: reactive oxygen and antioxidative strategies. In *Seaweed biology* (pp. 109-132). Springer, Berlin, Heidelberg.
- Bou-Abdallah, F., Chasteen, N. D. & Lesser, M. P. (2006) Quenching of superoxide radicals by green fluorescent protein, *Biochim. Biophys. Acta*, 1760, 1690-1695.
- Bulleri, F., Benedetti-Cecchi, L., Acunto, S., Cinelli, F. & Hawkins, S. J. (2002) The influence of canopy algae on vertical patterns of distribution of low-shore assemblages on rocky coasts in the northwest Mediterranean. *J. Exp. Mar. Biol. Ecol.*, 267(1), 89-106.
- Bulleri, F., Bertocci, I. & Micheli, F. (2002) Interplay of encrusting coralline algae and sea urchins in maintaining alternative habitats. *Mar. Ecol. Prog. Ser.*, 243, 101-109.
- Burns, J. M., Cooper, W. J., Ferry, J. L., King, D. W., Dimento, B. P., McNeill, K., Miller, C. J., Miller, W. L., Peake, B. M. & Rusak, S. A. (2012) Methods for reactive oxygen species (ROS) detection in aqueous environments. *Aquat. Sci.*, 74, 683-734.
- Burritt, D. J., Larkindale, J., & Hurd, C. L. (2002). Antioxidant metabolism in the intertidal red seaweed *Stictosiphonia arbuscula* following desiccation. *Planta*, 215(5), 829-838.
- Burrows, M. T., Harvey, R., Robb, L., Poloczanska, E. S., Mieszkowska, N., Moore, P. & Benedetti-Cecchi, L. (2009) Spatial scales of variance in abundance of intertidal species: effects of region, dispersal mode, and trophic level. *Ecology*, 90, 1242-1254.
- Caparkaya, D., Cengiz, S., Dincel, B., Demir, S. & Cavas, L. (2010). The effects of UV

exposure on the antioxidant enzyme systems of anemones. *Mediterr. Mar. Sci.*, 11, 259-275.

Casado-Amezúa, P., Machordom, A., Bernardo, J., González-Wangüemert, M. (2014) New insights into the genetic diversity of Mediterranean zooxanthellae. *Symbiosis*, 63, 41-46.

Cavaletto, M., Ghezzi, A., Burlando, B., Evangelisti, V., Ceratto, N. & Viarengo, A. (2002). Effect of hydrogen peroxide on antioxidant enzymes and metallothionein level in the digestive gland of *Mytilus galloprovincialis*. *Comp. Biochem. Phys. C*, 131, 447-455.

Chappuis, E., Terradas, M., Cefali, M. E., Mariani, S. & Ballesteros, E. (2014) Vertical zonation is the main distribution pattern of littoral assemblages on rocky shores at a regional scale. *Estuar. Coast. Shelf Sci.*, 147, 113-122.

Collén, J. & Davison, I. R. (1999a) Reactive oxygen metabolism in intertidal *Fucus* spp. (Phaeophyceae). *J. Phycol.*, 35, 62-69.

Collén, J. & Davison, I. R. (1999b) Production and damage of reactive oxygen in intertidal *Fucus* spp. (Phaeophyceae). *J. Phycol.*, 35, 54-61.

Collén, J. & Pedersén, M. (1996) Production, scavenging and toxicity of hydrogen peroxide in the green seaweed *Ulva rigida*. *Eur. J. Phycol.*, 31, 265-271.

Collén, J., Rio, M. J., García-Reina, G. & Pedersén, M. (1995) Photosynthetic production of hydrogen peroxide by *Ulva rigida* C. Ag. (Chlorophyta). *Planta*, 196, 225-230.

Company, R., Serafim, A., Cosson, R.P., Fiala-Medioni, A., Camus, L., Colaco, A., Serrao Santos, R., Bebianno, M.J. (2008) Antioxidant biochemical responses to long-term copper exposure in *Bathymodiolus azoricus* from Menez-Gwen hydrothermal vent. *Sci. Total Environ.*, 389, 407-417.

Connell, J. H. (1961) The influence of interspecific competition and other factors on the distribution of the barnacle *Chthamalus stellatus*. *Ecology*, 710-723.

Connell, J. H. (1972) Community interactions on marine rocky intertidal shores. *Annual Review of Ecology and Systematics*, 169-192.

Contreras, L., Moenne, A., & Correa, J. (2005) Antioxidant responses in *Scytosiphon lomentaria* (Phaeophyceae) inhabiting copper-enriched coastal environments. *J. Phycol.*,

41, 1184-1195.

Cooper, W. J. & Zepp, R. G. (1990) Hydrogen peroxide decay in waters with suspended soils: evidence for biologically mediated processes. *Can. J. Fish. Aquat. Sci.*, 47, 888-893.

Cooper, W. J. & Zika, R. G. (1983) Photochemical formation of hydrogen peroxide in surface and ground waters exposed to sunlight. *Science (Washington)*, 220, 711-712.

Cooper, W. J., Saltzman, E. S. & Zika, R. G. (1987) The contribution of rainwater to variability in surface ocean hydrogen peroxide. *J. Geophys. Res.-Oceans*, 92, 2970-2980.

Costanza, R., De Groot, R., Sutton, P., Van der Ploeg, S., Anderson, S. J., Kubiszewski, I. & Turner, R. K. (2014) Changes in the global value of ecosystem services. *Global Environ. Change*, 26, 152-158.

Crofts, A.R. & Wraight, C.A. (1983) The electrochemical domain of photosynthesis. *BBA Bioenerg.* 726, 149-185.

Cruz, J. A., Avenson, T. J., Kanazawa, A., Takizawa, K., Edwards, G. E., Kramer, D. M. (2005) Plasticity in light reactions of photosynthesis for energy production and photoprotection. *J. Exp. Bot.*, 56, 395-406.

Cruz-Motta, J. J., Miloslavich, P., Palomo, G., Iken, K., Konar, B., Pohle, G. & Sardi, A. (2010) Patterns of spatial variation of assemblages associated with intertidal rocky shores: a global perspective. *PloS One*, 5(12), e14354.

Dani, V., Priouzeau, F., Mertz, M., Mondin, M., Pagnotta, S., Lacas-Gervais, S., Davy, S. K. & Sabourault, C. (2017) Expression patterns of sterol transporters NPC1 and NPC2 in the cnidarian–dinoflagellate symbiosis. *Cell Microbiol.* 19, e12753.

Daniel, M. & Boyden, C. (1975) Diurnal variations in physico-chemical conditions within intertidal rockpools, *Fld Stud.* 4: 161-176.

Dat, J., Vandenaabeele, S., Vranová, E., Van Montagu, M., Inzé, D. & Van Breusegem, F. (2000) Dual action of the active oxygen species during plant stress responses. *Cell. Mol. Life Sci.*, 57, 779-795.

De Groot, R., Brander, L., Van Der Ploeg, S., Costanza, R., Bernard, F., Braat, L. & Hussain, S. (2012) Global estimates of the value of ecosystems and their services in

monetary units. *Ecosyst. Serv.*, 1(1), 50-61.

Dias, M., Madeira, C., Jogee, N., Ferreira, A., Gouveia, R., Cabral, H., Diniz, M & Vinagre, C. (2019). Oxidative stress on scleractinian coral fragments following exposure to high temperature and low salinity. *Ecol. Indic.*, 107, 105586.

Díaz, A. N., Sanchez, F. G. & García, J. G. (1996) Hydrogen peroxide assay by using enhanced chemiluminescence of the luminol-H₂O₂-horseradish peroxidase system: Comparative studies. *Anal. Chim. Acta*, 327, 161-165.

Dickinson, D. A. & Forman, H. J. (2002) Cellular glutathione and thiols metabolism. *Bioch. Pharmacol.*, 64, 1019-1026.

Downs, C., Fauth, J. E., Halas, J. C., Dustan, P., Bemiss, J. & Woodley, C. M. (2002) Oxidative stress and seasonal coral bleaching. *Free Rad. Biol. Med.*, 33, 533-543.

Dugan, J. E., Hubbard, D. M. & Quigley, B. J. (2013) Beyond beach width: Steps toward identifying and integrating ecological envelopes with geomorphic features and datums for sandy beach ecosystems. *Geomorphology*, 199, 95-105.

Dyken, J. A. & Shick, J. M. (1984) Photobiology of the symbiotic sea anemone, *Anthopleura elegantissima*: defenses against photodynamic effects, and seasonal photoacclimatization. *Biol. Bull.*, 167, 683-697.

Dynowski, M., Schaaf, G., Loque, D., Moran, O. & Ludewig, U. (2008) Plant plasma membrane water channels conduct the signalling molecule H₂O₂. *Biochem. J.*, 414, 53-61.

Eisenberg, G. (1943) Colorimetric determination of hydrogen peroxide. *Ind. Eng. Chem.*, 15, 327-328.

Ellis, D. V. (2003) Rocky shore intertidal zonation as a means of monitoring and assessing shoreline biodiversity recovery. *Mar. Pollut. Bull.*, 46(3), 305-307.

Emamverdian, A., Ding, Y., Mokhberdorran, F. & Xie, Y. (2015) Heavy metal stress and some mechanisms of plant defense response. *Sci. World J.*, 2015, 756120.

Erlandsson, J., McQuaid, C. D. & Sköld, M. (2011) Patchiness and co-existence of indigenous and invasive mussels at small spatial scales: the interaction of facilitation and competition. *PloS One*, 6(11), e26958.

- Foppoli, C., Coccia, R., Blarzino, C. & Rosei, M. A. (2000) Formation of homovanillic acid dimer by enzymatic or Fenton system-catalyzed oxidation. *International J. Biochem. Cell B*, 32, 657-663.
- Fork, D. C. & Herbert, S. K. (1993) Electron transport and photophosphorylation by photosystem I in vivo in plants and cyanobacteria. *Photosynth. Res.*, 36(3), 149-168.
- Foyer, C. H. & Noctor, G. (2003) Redox sensing and signalling associated with reactive oxygen in chloroplasts, peroxisomes and mitochondria. *Physiol. Plantarum*, 119, 355-364.
- Foyer, C. H. & Shigeoka, S. (2011) Understanding oxidative stress and antioxidant functions to enhance photosynthesis. *Plant physiol.*, 155, 93-100.
- Foyer, C.H. & Harbinson, J. (1999) Relationship between antioxidant metabolism and carotenoids in the regulation of photosynthesis, in: Frank, H.A., Young, A.J., Britton, G., Cogdell, R.J., *The photochemistry of carotenoids*. Kluwer Academic Publishers, Dordrecht, The Netherlands, pp. 305-325.
- Furla, P., Bénazet-Tambutté, S., Jaubert, J. & Allemand, D. (1998) Functional polarity of the tentacle of the sea anemone *Anemonia viridis*: role in inorganic carbon acquisition. *Am. J. Phys.* 274, R303-310.
- Fraschetti, S., Terlizzi, A. & Benedetti-Cecchi, L. (2005) Patterns of distribution of marine assemblages from rocky shores: evidence of relevant scales of variation. *Mar. Ecol. Prog. Ser.*, 296, 13-29.
- Fromme, P. & Mathis, P. (2004) Unraveling the photosystem I reaction center: a history, or the sum of many efforts. *Photosynth. Res.* 80, 109-124.
- Gaetke, L. M. & Chow, C. K. (2003) Copper toxicity, oxidative stress, and antioxidant nutrients. *Toxicology*, 189, 147-163.
- Gaines, S. D. & Denny, M. W. (2007) *Encyclopedia of tidepools and rocky shores* (No. 1). Univ. of California Press.
- Ganning, B. (1971) Studies on chemical, physical and biological conditions in Swedish rockpool ecosystems. *Ophelia*, 9, 51-105.
- Gao, S., Shen, S., Wang, G., Niu, J., Lin, A. & Pan, G. (2011) PSI-driven cyclic electron

flow allows intertidal macro-algae *Ulva* sp. (Chlorophyta) to survive in desiccated conditions. *Plant Cell Physiol.*, 52(5), 885-893.

Gechev, T. S., van Breusegem, F., Stone, J. M., Denev, I. & Laloi, C. (2006) Reactive oxygen species as signals that modulate plant stress responses and programmed cell death. *Bioessays*, 28, 1091-1101.

Gerringa, L. J., Rijkenberg, M. J., Timmermans, R., & Buma, A. G. (2004). The influence of solar ultraviolet radiation on the photochemical production of H₂O₂ in the equatorial Atlantic Ocean. *Journal of Sea Research*, 51(1), 3-10.

Gill, S. S. & Tuteja, N. (2010) Reactive oxygen species and antioxidant machinery in abiotic stress tolerance in crop plants. *Plant Physiol. Biochem.*, 48, 909-930.

Goldstone, J. V., (2008) Environmental sensing and response genes in Cnidaria: the chemical defensome in the sea anemone *Nematostella vectensis*. *Cell Biol. Toxicol.*, 24, 483-502.

Gomes, A., Fernandes, E. & Lima, J. L. (2005) Fluorescence probes used for detection of reactive oxygen species. *J. Biochem. Biophys. Meth.*, 65, 45-80.

Green, J. M. (1971) Local distribution of *Oligocottus maculosus* Girard and other tidepool cottids of the west coast of Vancouver Island, British Columbia. *Can. J. Zool.*, 49, 1111-1128.

Guilbault, G. G., Brignac Jr, P. J. & Zimmer, M. (1968) Homovanillic acid as a fluorometric substrate for oxidative enzymes. Analytical applications of the peroxidase, glucose oxidase, and xanthine oxidase systems. *Anal. Chem.*, 40, 190-196.

Halliwell, B. & Gutteridge, J. M. (2007) Free radicals in biology and medicine. 4th edition, Oxford University Press, Oxford.

Halliwell, B. (2006) Reactive species and antioxidants. Redox biology is a fundamental theme of aerobic life. *Plant Physiol.*, 141, 312-322.

Halliwell, B., Clement, M. V., Ramalingam, J. & Long, L. H. (2000) Hydrogen peroxide. Ubiquitous in cell culture and *in vivo*? *IUBMB Life*, 50(4-5), 251-257.

Hanson, A. K., Tindale, N. W. & Abdel-Moati, M. A. R. (2001) An equatorial Pacific rain event: influence on the distribution of iron and hydrogen peroxide in surface waters.

Mar. Chem., 75(1-2), 69-88.

Harland, A. D. and Davies, P. S. (1994) Time-course of photoadaptation in the symbiotic sea anemone *Anemonia viridis*. Mar. Biol., 119, 45-51.

Hawkins, S. J. & Hartnoll, R. G. (1985) Factors determining the upper limits of intertidal canopy-forming algae. Mar. Ecol. Prog. Ser., 20(3), 265-271.

Hawkins, S. J. & Jones, H. D. (1992) Rocky Shores (Marine Conservation Society, Marine Field Course Guide 1).

Heber U, Walker D (1992) Concerning a dual function of coupled cyclic electron transport in leaves. Plant Physiology 100:1621-1626.

Heber, U. & Walker, D. (1992) Concerning a dual function of coupled cyclic electron transport in leaves. Plant Physiol., 100, 1621-1626.

Heber, U., Bilger, W., Türk, R. & Lange, O. L. (2010) Photoprotection of reaction centres in photosynthetic organisms: mechanisms of thermal energy dissipation in desiccated thalli of the lichen *Lobaria pulmonaria*. New Phytol., 185(2), 459-470.

Henzler, T. & Steudle, E. (2000) Transport and metabolic degradation of hydrogen peroxide in *Chara corallina*: model calculations and measurements with the pressure probe suggest transport of H₂O₂ across water channels. J. Exp. Bot., 51, 2053-2066.

Higuchi, T., Fujimura, H., Arakaki, T. & Oomori, T. (2009) The synergistic effects of hydrogen peroxide and elevated seawater temperature on the metabolic activity of the coral *Galaxea fascicularis*. Mar. Biol., 156, 589-596.

Iwai, H., Ishihara, F. & Akihama, S. (1983) A fluorometric rate assay of peroxidase using the homovanillic acid-*o*-dianisidine-hydrogen peroxide system. Chem. Pharmaceut. Bull., 31, 3579-3582.

Jarrold, M. D., Calosi, P., Verberk, W. C., Rastrick, S. P., Atfield, A., & Spicer, J. I. (2013). Physiological plasticity preserves the metabolic relationship of the intertidal non-calcifying anthozoan-Symbiodinium symbiosis under ocean acidification. Journal of experimental marine biology and ecology, 449, 200-206.

Johnson G. N. (2005) Cyclic electron transport in C₃ plants: fact or artefact? J. Exp. Bot., 56, 407-416.

Johnson, G. N. (2011). Physiology of PSI cyclic electron transport in higher plants. *BBA Bioenerg.*, 1807(3), 384-389.

Johnson, K. S., Willason, S. W., Wiesenburg, D. A., Lohrenz, S. E. & Arnone, R. A. (1989) Hydrogen peroxide in the western Mediterranean Sea: A tracer for vertical advection. *Deep-Sea Res. Part I*, 36, 241-254.

Joliot, P., & Johnson, G. N. (2011) Regulation of cyclic and linear electron flow in higher plants. *PNAS USA*, 108, 13317-13322.

Karkas, M. D., Verho, O., Johnston, E. V. & Åkermark, B. (2014) Artificial photosynthesis: molecular systems for catalytic water oxidation. *Chem. Rev.*, 114(24), 11863-12001.

Kearns, J. & Turner, A. (2016) An evaluation of the toxicity and bioaccumulation of bismuth in the coastal environment using three species of macroalga. *Environ. Poll.*, 208, 435-441.

Khosravi, A., Vossoughi, M., Shahrokhian, S. & Alemzadeh, I. (2013) Magnetic labelled HRP-polymer nanoparticles: A recyclable nanobiocatalyst. *Journal of the Serbian Chemical Society*, 78, 921-931.

Kieber, D. J., Peake, B. M. & Scully, N. M. (2003) Reactive oxygen species in aquatic ecosystems. In *UV effects in aquatic organisms and ecosystems*. *Roy. Soc. Chem.*, 251-288.

Kieber, R.J., Cooper, W.J., Willey, J.D. & Avery, G.B. (2001) Hydrogen peroxide at the Bermuda Atlantic Time Series Station. Part 1: Temporal variability of atmospheric hydrogen peroxide and its influence on seawater concentrations. *J. Atmos. Chem.*, 39(1), 1-13.

Kiirikki, M. (1996) Mechanisms affecting macroalgal zonation in the northern Baltic Sea. *Eur. J. Phycol.*, 31(3), 225-232.

Kiirikki, M. (1996) Experimental evidence that *Fucus vesiculosus* (Phaeophyta) controls filamentous algae by means of the whiplash effect. *Eur. J. Phycol.*, 31, 61-66.

Klugh, A. B. (1924) Factors controlling the biota of tide-pools. *Ecology*, 5, 192-196.

Kok, G. L., Holler, T. P., Lopez, M. B., Nachtrieb, H. A. & Yuan, M. (1978) Chemiluminescent method for determination of hydrogen peroxide in the ambient

atmosphere. *Environ. Sci. Technol.*, 12, 1072-1076.

Krasowska, J., Pierzchała, K., Bzowska, A., Forró, L., Sienkiewicz, A., & Wielgus-Kutrowska, B. (2021). Chromophore of an enhanced green fluorescent protein can play a photoprotective role due to photobleaching. *Int. J. Mol. Sci.*, 22, 8565.

Kurisu, G., Zhang, H., Smith, J.L. & Cramer, W.A. (2003) Structure of the cytochrome *b₆f* complex of oxygenic photosynthesis: tuning the cavity. *Science*, 302, 1009-1014.

Laloi, C., Przybyła, D. & Apel, K. (2006) A genetic approach towards elucidating the biological activity of different reactive oxygen species in *Arabidopsis thaliana*. *J. Exp. Bot.*, 57, 1719-1724.

Leutenegger, A., Kredel, S., Gundel, S., D'Angelo, C., Salih, A. & Wiedenmann, J. (2007) Analysis of fluorescent and non-fluorescent sea anemones from the Mediterranean Sea during a bleaching event. *J. Exp. Mar. Biol. Ecol.*, 353, 221-234.

Levy, O., Achituv, Y., Yacobi, Y., Dubinsky, Z. & Stambler, N. (2006). Dieltuning' of coral metabolism: physiological responses to light cues. *J. Exp. Biol.*, 209, 273-283.

Lewis, J. R. (1964). *The ecology of rocky shores*. English Universities Press.

Lewis, S., May, S., Donkin, M. & Depledge, M. (1998) The influence of copper and heat shock on the physiology and cellular stress response of *Enteromorpha intestinalis*. *Mar. Environ. Res.*, 46, 421-424.

Little, C. & Kitching, J. A. (1996) *The biology of rocky shores*. Oxford University Press.

Lu, I.-F., Sung, M.-S. & Lee, T.-M. (2006) Salinity stress and hydrogen peroxide regulation of antioxidant defense system in *Ulva fasciata*. *Mar. Biol.*, 150, 1-15.

Lushchak, V. I. (2011) Environmentally induced oxidative stress in aquatic animals. *Aquat. Toxicol.*, 101, 13-30.

Macieira, R. M. & Joyeux, J.-C. (2011) Distribution patterns of tidepool fishes on a tropical flat reef. *Fish. B.-NOAA*, 109, (3).

Mallien, C., Porro, B., Zamoum, T., Olivier, C., Wiedenmann, J., Furla, P. & Forcioli, D. (2017) Conspicuous morphological differentiation without speciation in *Anemonia viridis* (Cnidaria, Actiniaria). *Syst. Biodivers.* 1-16.

- Mamboya, F., Lyimo, T. J., Landberg, T. & Björk, M. (2009) Influence of combined changes in salinity and copper modulation on growth and copper uptake in the tropical green macroalga *Ulva reticulata*. *Estuar. Coast. Shelf Sci.*, 84, 326-330.
- Mangialajo, L., Chiantore, M., Susini, M. L., Meinesz, A., Cattaneo-Vietti, R. & Thibaut, T. (2012) Zonation patterns and interspecific relationships of fucoids in microtidal environments. *J. Exp. Mar. Biol. Ecol.*, 412, 72-80.
- Martínez, B., Arenas, F., Rubal, M., Burgués, S., Esteban, R., García-Plazaola, I. & Trilla, A. (2012) Physical factors driving intertidal macroalgae distribution: physiological stress of a dominant fucoid at its southern limit. *Oecologia*, 170(2), 341-353.
- Matsumoto, M. (2004) Advanced chemistry of dioxetane-based chemiluminescent substrates originating from bioluminescence. *J. Photochem. Photobiol. C*, 5, 27-53.
- McGregor, D. (1965) Physical ecology of some New Zealand supralittoral pools. *Hydrobiologia*, 25, 277-284.
- Menconi, M., Benedetti-Cecchi, L. & Cinelli, F. (1999) Spatial and temporal variability in the distribution of algae and invertebrates on rocky shores in the northwest Mediterranean. *J. Exp. Mar. Biol. Ecol.*, 233(1), 1-23.
- Menge, B. A. & Sutherland, J. P. (1987) Community regulation: variation in disturbance, competition, and predation in relation to environmental stress and recruitment. *Am. Nat.*, 130(5), 730-757.
- Metaxas, A. & Scheibling, R. E. (1993) Community structure and organization of tidepools. *Mar. Ecol. Prog. Ser.*, 98, 187-198.
- Miller, G. W., Morgan, C. A., Kieber, D. J., King, D. W., Snow, J. A., Heikes, B. G., Mopper, K. & Kiddle, J. J. (2005) Hydrogen peroxide method intercomparison study in seawater. *Mar. Chem.*, 97, 4-13.
- Miller, W. L. & Kester, D. R. (1988) Hydrogen peroxide measurement in seawater by (*p*-hydroxyphenyl) acetic acid dimerization. *Anal. Chem.*, 60, 2711-2715.
- Mitchell, P. (1975) The protonmotive Q cycle: a general formulation. *FEBS Lett.* 59, 137-139.
- Mitchelmore, C. L., Ringwood, A. H., & Weis, V. M. (2003). Differential accumulation

of cadmium and changes in glutathione levels as a function of symbiotic state in the sea anemone *Anthopleura elegantissima* as a function of symbiotic state. J. Exp. Mar. Biol. Ecol. 284, 71-85.

Mittler, R. (2002) Oxidative stress, antioxidants and stress tolerance. Trends Plant Sci., 7, 405-410.

Moffett, J. W. & Zafiriou, O. C. (1993) The photochemical decomposition of hydrogen peroxide in surface waters of the Eastern Caribbean and Orinoco River. J. Geophys. Res.-Oceans, 98, 2307-2313.

Moffett, J.W. & Zika, R.G. (1987) Reaction-kinetics of hydrogen-peroxide with copper and iron in seawater. Environ. Sci. Technol., 21(8), 804-810.

Møller, I. M., Jensen, P. E. & Hansson, A. (2007) Oxidative modifications to cellular components in plants. Annu. Rev. Plant Biol., 58, 459-481.

Moore, C. A., Farmer, C. T. & Zika, R. G. (1993) Influence of the Orinoco River on hydrogen peroxide distribution and production in the eastern Caribbean. J. Geophys. Res.-Oceans, 98, 2289-2298.

Morris, S. & Taylor, A. C. (1983) Diurnal and seasonal variation in physico-chemical conditions within intertidal rock pools. Estuar. Coast. Shelf Sci., 17, 339-355.

Morrow, K. M. & Carpenter, R. C. (2008) Macroalgal morphology mediates particle capture by the corallimorpharian *Corynactis californica*. Mar. Biol., 155(3), 273-280.

Moya, A., Ganot, P., Furla, P. & Sabourault, C. (2012) The transcriptomic response to thermal stress is immediate, transient and potentiated by ultraviolet radiation in the sea anemone *Anemonia viridis*. Mol. Ecol., 21, 1158-1174.

Muller-Parker, G. & Davy, S. K. (2001) Temperate and tropical algal-sea anemone symbioses. Invert. Biol., 120, 104-123.

Munekage, Y., Hashimoto, M., Miyake, C., Tomizawa, K.-I., Endo, T., Tasaka, M., Shikanai, T. (2004) Cyclic electron flow around photosystem I is essential for photosynthesis. Nature, 429, 579-589.

Nakamura, M., & Nakamura, S. (1998). One-and two-electron oxidations of luminol by peroxidase systems. Free Radical Biology and Medicine, 24(4), 537-544.

- Nakamura, T. (2010) Importance of water-flow on the physiological responses of reef-building corals. *Galaxea, Journal of Coral Reef Studies*, 12, 1-14.
- Neill, S. O., Gould, K. S., Kilmartin, P. A., Mitchell, K. A. & Markham, K. R. (2002) Antioxidant capacities of green and cyanic leaves in the sun species, *Quintinia serrata*. *Funct. Plant Biol.*, 29, 1437-1443.
- Niu, L. & Liao, W. (2016) Hydrogen peroxide signaling in plant development and abiotic responses: crosstalk with nitric oxide and calcium. *Front. in Plant Sci.*, 7, 230.
- Osório, C., Machado, S., Peixoto, J., Bessada, S., Pimentel, F. B., C. Alves, R. & Oliveira, M. B. P. (2020) Pigments content (chlorophylls, fucoxanthin and phycobiliproteins) of different commercial dried algae. *Separations*, 7, 33.
- O'Sullivan, D. W., Neale, P. J., Coffin, R. B., Boyd, T. J., & Osburn, C. L. (2005). Photochemical production of hydrogen peroxide and methylhydroperoxide in coastal waters. *Marine Chemistry*, 97(1-2), 14-33.
- Paital, B. (2014) A modified fluorimetric method for determination of hydrogen peroxide using homovanillic acid oxidation principle. *Biomedical Research International*, ID 342958, 8 p.
- Palenik, B. & Morel, F. (1988) Dark production of H₂O₂ in the Sargasso Sea. *Limnol. Oceanogr.*, 33, 1606-1611.
- Palenik, B., Zafiriou, O. & Morel, F. (1987) Hydrogen peroxide production by a marine phytoplankter 1. *Limnol. Oceanogr.*, 32, 1365-1369.
- Paździoch-Czochra, M. & Wideńska, A. (2002) Spectrofluorimetric determination of hydrogen peroxide scavenging activity. *Ana. Chim. Acta*, 452, 177-184.
- Peltier, G., Tolleter, D., Billon, E. & Cournac, L. (2010) Auxiliary electron transport pathways in chloroplasts of microalgae. *Photosynth. Res.*, 106(1-2), 19-31.
- Petasne, R. G. & Zika, R. G. (1987). Fate of superoxide in coastal sea water. *Nature*, 325, 516-518.
- Piotrowski, W. J., Pietras, T., Kurmanowska, Z., Nowak, D., Marczak, J., Marks-Kończalik, J. & Mazerant, P. (1996) Effect of paraquat intoxication and ambroxol treatment on hydrogen peroxide production and lipid peroxidation in selected organs of

rat. J. Appl. Toxicol., 16, 501-507.

Poremba, K., Tillmann, U. & Hesse, K. J. (1999) Tidal impact on planktonic primary and bacterial production in the German Wadden Sea. *Helgoland Mar. Res.*, 53(1), 19-27.

Porro, B., Mallien, C. Hume, B. C. C., Pey, A., Aubin, E., Christen, R., Voolstra, C.R., Furla, P. & Forcioli, D. (2020) The many faced symbiotic snakelocks anemone (*Anemonia viridis*, Anthozoa): host and symbiont genetic differentiation among colour morphs. *Heredity*, 124, 351-366.

Price, D., Mantoura, R. F. C., & Worsfold, P. J. (1998). Shipboard determination of hydrogen peroxide in the western Mediterranean Sea using flow injection with chemiluminescence detection. *Analytica chimica acta*, 377(2-3), 145-155.

Pyefinch, K. (1943) The intertidal ecology of Bardsey Island, North Wales, with special reference to the recolonization of rock surfaces, and the rock-pool environment. *J. Anim. Ecol.*, 12, 82-108.

Raffaelli, D. & Hawkins, S. J. (1996) *Intertidal Ecology*. Chapman and Hall, London.

Reichert, K., Buchholz, F. & Giménez, L. (2008) Community composition of the rocky intertidal at Helgoland (German Bight, North Sea). *Helgoland Mar. Res.*, 62(4), 357-366.

Richier, S., Furla, P., Plantivaux, A., Merle, P.-L. & Allemand, D. (2005) Symbiosis-induced adaptation to oxidative stress. *J. Exp. Biol.*, 208, 277-285.

Richier, S., Sabourault, C., Courtiade, J., Zucchini, N., Allemand, D. & Furla, P. (2006) Oxidative stress and apoptotic events during thermal stress in the symbiotic sea anemone, *Anemonia viridis*. *FEBS J.*, 273, 4196-4198.

Rilov, G. & Schiel, D. R. (2011) Community regulation: the relative importance of recruitment and predation intensity of an intertidal community dominant in a seascape context. *PLoS One*, 6(8), e23958.

Rosa, C. E. D., Iurman, M. G., Abreu, P. C., Geracitano, L. A., & Monserrat, J. M. (2005). Antioxidant mechanisms of the Nereidid *Laeonereis acuta* (Anelida: Polychaeta) to cope with environmental hydrogen peroxide. *Physiological and Biochemical Zoology*, 78(4), 641-649.

Ross, C. & Alstyne, K. L. V. (2007) intraspecific variation in stress-induced hydrogen

- peroxide scavenging by the ulvoid macroalga *Ulva lactuca*. J. Phycol., 43, 466-474.
- Salovius, S., Nyqvist, M. & Bonsdorff, E. (2005) Life in the fast lane: macrobenthos use temporary drifting algal habitats. J. Sea Res., 53(3), 169-180.
- Sampath-Wiley, P., Neefus, C. D. & Jahnke, L. S. (2008) Seasonal effects of sun exposure and emersion on intertidal seaweed physiology: fluctuations in antioxidant contents, photosynthetic pigments and photosynthetic efficiency in the red alga *Porphyra umbilicalis* Kützing (Rhodophyta, Bangiales). J. Exp. Mar. Biol. Ecol., 361, 83-91.
- Saragosti, E., Tchernov, D., Katsir, A. & Shaked, Y. (2010) Extracellular production and degradation of superoxide in the coral *Stylophora pistillata* and cultured *Symbiodinium*. PLoS ONE, 5, e12508.
- Sawyer, S. J. & Muscatine, L. (2001) Cellular mechanisms underlying temperature-induced bleaching in the tropical sea anemone *Aiptasia pulchella*. J. Exp. Biol., 204, 3443-3456.
- Schoch, G. C., Menge, B. A., Allison, G., Kavanaugh, M., Thompson, S. A. & Wood, S. (2006) Fifteen degrees of separation: latitudinal gradients of rocky intertidal biota along the California Current. Limnol. Oceanogr., 51(6), 2564-2585.
- Sharma, P., Jha, A. B., Dubey, R. S. & Pessarakli, M. (2012) Reactive oxygen species, oxidative damage, and antioxidative defense mechanism in plants under stressful conditions. J. Bot., doi:10.1155/2012/217037
- Shick, J. M., Lesser, M.P. & Jokiel, P. L. (1996) Effects of ultraviolet radiation on corals and other coral reef organisms. Glob. Change Biol., 2, 527-545.
- Shigeoka, S., Ishikawa, T., Tamoi, M., Miyagawa, Y., Takeda, T., Yabuta, Y. & Yoshimura, K. (2002) Regulation and function of ascorbate peroxidase isoenzymes. J. Exp. Bot., 53, 1305-1319.
- Shikanai T. (2014) Central role of cyclic electron transport around photosystem I in the regulation of photosynthesis. Curr. Opin. Biotech., 26, 25-30.
- Shikanai, T. (2007) Cyclic electron transport around photosystem I: genetic approaches. Annu. Rev. Plant Biol. 58, 199–217.
- Sibaja-Cordero, J. A., & Cortés, J. (2008). Vertical zonation of rocky intertidal organisms

- in a seasonal upwelling area (Eastern Tropical Pacific). *Rev. Biol. Trop.*, 56(4), 91-104.
- Smith, D. (2013) Ecology of the New Zealand rocky shore community. Otago: New Zealand Marine Studies Centre, University of Otago.
- Smith, D. J., Suggett, D. J. & Baker, N. R. (2004) Is photoinhibition of zooxanthellae photosynthesis the primary cause of thermal bleaching in corals? *Glob. Change Biol.*, 11, 1-11.
- Smith, S. D. & Markic, A. (2013) Estimates of marine debris accumulation on beaches are strongly affected by the temporal scale of sampling. *PLoS One*, 8(12), e83694.
- Solymosi, K. (2012) Plastid structure, diversification and interconversions I. *Algae. Curr. Chem. Biol.*, 6, 167-186.
- Staniek, K. & Nohl, H. (1999) H₂O₂ detection from intact mitochondria as a measure for one-electron reduction of dioxygen requires a non-invasive assay system. *Biochim. Biophys. Acta*, 1413, 70-80.
- Steghens, J. P., Min, K. L., & Bernengo, J. C. (1998). Firefly luciferase has two nucleotide binding sites: effect of nucleoside monophosphate and CoA on the light-emission spectra. *Biochemical Journal*, 336(1), 109-113.
- Stephenson, T. A. & Stephenson, A. (1949) The universal features of zonation between tide-marks on rocky coasts. *J. Ecol.*, 37, 289-305.
- Stephenson, T., Zoond, A. & Eyre, J. (1934) The liberation and utilisation of oxygen by the population of rock-pools. *J. Exp. Biol.*, 11, 162-172.
- Suggett, D. J. & Smith, D. J. (2019) Coral bleaching patterns are the outcome of complex biological and environmental networking. *Glob. Change Biol.*, 26, 68-79.
- Sunagawa, S., Choi, J., Jay Forman, H. & Medina, M. (2008) Hyperthermic stress-induced increase in the expression of glutamate-cysteine ligase and glutathione levels in the symbiotic sea anemone *Aiptasia pallida*. *Comp. Biochem. Phys. B*, 151, 133-138.
- Takahashi, M.-A. & Asada, K. (1983) Superoxide anion permeability of phospholipid membranes and chloroplast thylakoids. *Arch. Biochem. Biophys.*, 226, 558-566.
- Takahashi, S. & Badger, M. R. (2011) Photoprotection in plants: a new light on

photosystem II damage. *Trends Plant Sci.*, 16(1), 53-60.

Tchernov, D., Gorbunov, M. Y., de Vargas, C., Narayan Yadav, S., Milligan, A. J., Häggblom, M. & Falkowski, F. G. (2004) Membrane lipids of symbiotic algae are diagnostic of sensitivity to thermal bleaching in corals. *PNAS USA*, 101, 13531-13535.

Thomas, M. L. H. (1994) Littoral communities and zonation on rocky shores in the Bay of Fundy, Canada: an area of high tidal range. *Biol. J. Linn. Soc.*, 51(1-2), 149-168.

Thornton, D. C. (2014). Dissolved organic matter (DOM) release by phytoplankton in the contemporary and future ocean. *Eur. J. Phycol.*, 49, 20-46.

Todgham, A. E. & Stillman, J. H. (2013) Physiological responses to shifts in multiple environmental stressors: Relevance in a changing world. *Integr. Comp. Biol.*, 53, 539-544.

Tomanek, L. & Helmuth, B. (2002) Physiological ecology of rocky intertidal organisms: a synergy of concepts. *Integr. Comp. Biol.*, 42(4), 771-775.

Travis, J. M. J., Brooker, R. W. & Dytham, C. (2005) The interplay of positive and negative species interactions across an environmental gradient: insights from an individual-based simulation model. *Biol. Lett.*, 1(1), 5-8.

Tripathy, B. C. & Oelmüller, R. (2012) Reactive oxygen species generation and signaling in plants. *Plant Signaling and Behavior*, 7, 1621-1633.

Truchot, J.-P. & Duhamel-Jouve, A. (1980) Oxygen and carbon dioxide in the marine intertidal environment: diurnal and tidal changes in rockpools. *Resp. Physiol.*, 39, 241-254.

Turner, A. (2010) Marine pollution from antifouling paint particles. *Mar. Poll. Bull.*, 60, 159-171.

Tuya, F. & Haroun, R. J. (2006) Spatial patterns and response to wave exposure of shallow water algal assemblages across the Canarian Archipelago: a multi-scaled approach. *Mar. Ecol. Prog. Ser.*, 311, 15-28.

Umanzor, S., Ladah, L., Calderon-Aguilera, L. E. & Zertuche-González, J. A. (2017) Intertidal macroalgae influence macroinvertebrate distribution across stress scenarios. *Mar. Ecol. Prog. Ser.*, 584, 67-77.

Underwood, A. J. & Jernakoff, P. (1981) Effects of interactions between algae and grazing gastropods on the structure of a low-shore intertidal algal community. *Oecologia*, 48(2), 221-233

Underwood A. J. (2000) Experimental ecology of rocky intertidal habitats: what are we learning? *J. Exp. Mar. Biol. Ecol.*, 250(1-2), 51-76

Underwood, A. & Jernakoff, P. (1984) The effects of tidal height, wave-exposure, seasonality and rock-pools on grazing and the distribution of intertidal macroalgae in New South Wales. *J. Exp. Mar. Biol. Ecol.*, 75, 71-96.

Underwood, A. & Skilleter, G. (1996) Effects of patch-size on the structure of assemblages in rock pools. *J. Exp. Mar. Biol. Ecol.*, 197, 63-90.

van Baalen, C. & Marler, J. (1966) Occurrence of hydrogen peroxide in sea water. *Nature*, 211, 951-951.

Veiga, P., Rubal, M., Vieira, R., Arenas, F. & Sousa-Pinto, I. (2013) Spatial variability in intertidal macroalgal assemblages on the North Portuguese coast: consistence between species and functional group approaches. *Helgoland Mar. Res.*, 67(1), 191-201.

Veiga, P., Torres, A. C., Aneiros, F., Sousa-Pinto, I., Troncoso, J. S. & Rubal, M. (2016) Consistent patterns of variation in macrobenthic assemblages and environmental variables over multiple spatial scales using taxonomic and functional approaches. *Mar. Environ. Res*, 120, 191-201.

Viarengo, A., Canesi, L., Martinez, P. G., Peters, L. & Livingstone, D. (1995) Pro-oxidant processes and antioxidant defence systems in the tissues of the Antarctic scallop (*Adamussium colbecki*) compared with the Mediterranean scallop (*Pecten jacobaeus*). *Comp. Biochem. Physiol. B*, 111, 119-126.

von Sonntag, C. & Schuchmann, H. P. (1991) The elucidation of peroxy radical reactions in aqueous solution with the help of radiation-chemical methods. *Angew. Chem. Int. Edit.*, 30, 1229-1253.

Whitelegge, J. P., Zhang, H., Aguilera, R., Taylor, R. M., & Cramer, W. A. (2002) Full subunit coverage liquid chromatography electrospray ionization mass spectrometry (LCMS+) of an oligomeric membrane protein: cytochrome *b₆f* complex from spinach and the cyanobacterium *Mastigocladus laminosus*. *Molecular and Cellular Proteomics*, 1,

816-827.

Widdows, J. & Brinsley, M. (2002) Impact of biotic and abiotic processes on sediment dynamics and the consequences to the structure and functioning of the intertidal zone. *J. Sea Res.*, 48(2), 143-156.

Willig, M. R., Kaufman, D. M. & Stevens, R. D. (2003) Latitudinal gradients of biodiversity: pattern, process, scale, and synthesis. *Annu. Rev. Ecol. Evol. System.*, 34(1), 273-309.

Wright, J. T., Byers, J. E., DeVore, J. L. & Sotka, E. E. (2014) Engineering or food? mechanisms of facilitation by a habitat-forming invasive seaweed. *Ecology*, 95(10), 2699-2706.

Xiao, C., Palmer, D. A., Wesolowski, D. J., Lovitz, S. B. & King, D. W. (2002) Carbon dioxide effects on luminol and 1,10-phenanthroline chemiluminescence. *Anal. Chem.*, 74, 2210-2216.

Yamamoto, H., Peng, L., Fukao, Y. & Shikanai, T. (2011) An Src homology 3 domain-like fold protein forms a ferredoxin binding site for the chloroplast NADH dehydrogenase-like complex in *Arabidopsis*. *Plant Cell*. 23, 1480-1493.

Yamashita, E., Zhang, H. & Cramer, W. A. (2007). Structure of the cytochrome *b₆f* complex: quinone analogue inhibitors as ligands of heme *c_n*. *J. Mol. Biol.* 370, 39-52.

Yocis, B. H., Kieber, D. J. & Mopper, K. (2000) Photochemical production of hydrogen peroxide in Antarctic waters. *Deep-Sea Res.*, 47, 1077-1099.

Yue, L., & Liu, Y. T. (2020). Mechanistic insight into pH-dependent luminol chemiluminescence in aqueous solution. *The Journal of Physical Chemistry B*, 124(35), 7682-7693.

Zander, C., Nieder, J. & Martin, K. (1999). Vertical distribution patterns. *Intertidal fishes: Life in Two Worlds*, 1, 26-54.

Zika, R. G., Moffett, J. W., Petasne, R. G., Cooper, W. J. & Saltzman, E. S. (1985a) Spatial and temporal variations of hydrogen peroxide in Gulf of Mexico waters. *Geochim. Cosmochim. Acta*, 49, 1173-1184.

Zika, R. G., Saltzman, E. S. & Cooper, W. J. (1985b) Hydrogen peroxide concentrations

in the Peru upwelling area. *Mar. Chem.*, 17, 265-275.